

AN ABSTRACT OF THE THESIS OF

Krysta J. Krippaehne for the degree of Master of Degree in Environmental Engineering presented on September 19, 2018.

Title: Cometabolism of 1,4-Dioxane and Chlorinated Aliphatic Hydrocarbons by Pure Cultures of *Rhodococcus rhodochrous* 21198 and *Mycobacterium* ELW1 and in Groundwater Microcosms Fed Isobutane and Isobutene as Growth Substrates.

Abstract approved: _____

Lewis Semprini

1,4-dioxane and chlorinated aliphatic hydrocarbons (CAHs) such as trichloroethylene (TCE) and 1,1-dichloroethene (1,1-DCE) are hazardous compounds commonly found in soil and groundwater. Bioremediation through aerobic cometabolism is a potential option for the remediation of these contaminated sites. The purpose of this study was to examine the use of different primary substrates to stimulate bacteria that can potentially perform concurrent aerobic cometabolism of 1,4-dioxane and chlorinated solvents. Batch pure-culture rate tests were conducted utilizing isobutane, ethane, and propane-grown *Rhodococcus rhodochrous* ATCC® 21198™ and isobutene-grown *Mycobacterium* sp. ELW1. In support of a field demonstration, microcosms containing a groundwater and sediment slurry from the Naval Air Station North Island in San Diego, California, were also performed using isobutane and isobutene as cometabolic growth substrates. This site is contaminated with CAHs (predominately TCE and 1,1-DCE) and 1,4-dioxane due to historical improper storage of chemical waste.

The effectiveness of the cometabolic transformation of CAHs and 1,4-dioxane was evaluated through the determination of zero order degradation rates of TCE, 1,1-DCE, cis-1,2-

dichloroethylene (c-DCE), 1,2-dichloroethane (1,2-DCA), 1,1,1-trichloroethane (1,1,1-TCA), and 1,4-dioxane and transformation capacities of c-DCE and 1,1-DCE by microorganisms grown on different substrates. The general trend in rates indicated isobutane-grown 21198 > ethane-grown 21198 > propane-grown 21198. The rates for TCE were comparable among all growth substrates with 21198. The TCE degradation rate of isobutene-grown ELW1 was double the rates observed for 21198 grown on all substrates. 1,4-dioxane, 1,2-DCA, and 1,1,1-TCA were not readily transformed by ELW1. Transformation of mixtures of CAHs and 1,4-dioxane were consistent with the single compound tests.

Isobutane and isobutene were selected as primary growth substrates to promote cometabolism in microcosm studies. After 52 days of isobutene exposure, isobutene uptake was observed in a native microcosm system in the presence of TCE, 1,1-DCE, and 1,4-dioxane. Once nearly complete uptake of isobutene was achieved, rapid 1,1-DCE transformation and slow TCE degradation were observed. After 130 days of isobutane exposure, no primary substrate uptake and minimal TCE and 1,1-DCE degradation were observed. It is hypothesized that the presence and transformation of 1,1-DCE is inhibitory to the stimulation of native microbes. This is due to the formation of a toxic epoxide resulting from the activation of a monooxygenase by the primary substrate and the observation that 1,1-DCE was transformed prior to isobutane utilization. In order to circumvent the toxic effects of 1,1-DCE, a variety of strategies were implemented, including sparging to remove the chlorinated compounds through air stripping, bioaugmentation with isobutane and isobutene-utilizing cultures, and isobutanol addition to cultivate an active isobutane-utilizing population without the activation of the monooxygenase enzyme responsible for 1,1-DCE transformation. Sparging and bioaugmentation were effective strategies in the stimulation of the microcosms to transform 1,4-dioxane, 1,1-DCE, and TCE.

©Copyright by Krysta J. Krippaehne
September 19, 2018
All Rights Reserved

Cometabolism of 1,4-Dioxane and Chlorinated Aliphatic Hydrocarbons by Pure Cultures of
Rhodococcus rhodochrous 21198 and *Mycobacterium* ELW1 and in Groundwater Microcosms Fed
Isobutane and Isobutene as Growth Substrates

by
Krysta J. Krippaehne

A THESIS

submitted to

Oregon State University

in partial fulfillment of
the requirements for the
degree of

Master of Science

Presented September 19, 2018
Commencement June 2019

Master of Science thesis of Krysta J. Krippaehne presented on September 19, 2018

APPROVED:

Major Professor, representing Environmental Engineering

Head of the School of Chemical, Biological, and Environmental Engineering

Dean of the Graduate School

I understand that my thesis will become part of the permanent collection of Oregon State University libraries. My signature below authorizes release of my thesis to any reader upon request.

Krysta J. Krippaehne, Author

ACKNOWLEDGEMENTS

First and foremost, I would like to thank my major professor, Dr. Lewis Semprini, for his mentorship over the last year and a half. Your patience and encouragement as I faced frustrations with the many roadblocks this project encountered were always so appreciated. I am thankful for everything you've taught me about environmental engineering, research, and perseverance. I feel very lucky to have had the opportunity to be a part of your lab group. You cultivate an environment of kindness, generosity, curiosity, and determination that made coming to work all the more enjoyable.

I would also like to thank my committee members, Dr. Mohammad Azizian, Dr. Mark Dolan, and Dr. Jack Istok, for taking the time to review my thesis, be present at my defense, and challenge my knowledge of my research. Special thanks are given to Dr. Azizian – your magic touch with all of the analytical equipment will be something I am forever grateful for. Your kindness and willingness to help and lend your expertise made a very positive impact on my long hours in the lab. I would also like to express my thanks to all of the CBEE faculty who have had a hand in my education these past six years. I feel fully prepared to take on the real world of engineering.

I will forever owe a huge debt of gratitude to Jon Laurance for his support with this project. This thesis would not have been completed without your help with microcosm babysitting duties through late nights and early mornings of data collection. Your kindness and generous spirit have meant so much to me. I cannot imagine leaving this project in any better hands than your own.

I would also like to thank the other members of the Semprini lab group: Hannah Rolston, Mitchell Rasmussen, Riley Murnane, and Alyssa Saito. Hannah, your mentorship and compassion will always be held dear to my heart. Mitchell and Riley, you guys made long and grueling days in the lab so much more fun. I will miss all of you greatly.

I am also sincerely grateful for the help of undergraduate researchers Eileen Lukens, Grant Kresge, and Gillian Williams. Eileen especially, thank you for teaching me all I know about working with pure cultures and for being a friend to encourage me through my microcosm mania and to share laughter about life's absurdities. You are going to do such great things in this world.

This project was funded by the Department of Defense Environmental Security Technology Certification Program, grant ER-201733. I would also like to thank Dave Lippicott for procurement of the groundwater used in this study from NAS North Island.

I would like to thank my family, especially my parents, Dick and Tammy Krippaehne, and my sister, Hillary Krippaehne. Your unwavering love and support over my 24 years of life have been the greatest blessing. God surely gifted me with your encouragement through my stresses and your celebration through my successes. I feel so lucky to share DNA with you three, even the crazy and weird bits – those are the parts that make us special.

And finally, this list of gratitude would not be complete without acknowledging my best friend, Grant Stein. I cannot imagine having endured these past two years without your support. Every day was made better through our shared laughter through the ups and downs of life. Thank you for making me dinners, doing the dishes, supplying me with chocolate, and making me smile during the stressful times. I am excited to continue adventuring through life with you.

TABLE OF CONTENTS

	<u>Page</u>
1.0 INTRODUCTION AND OBJECTIVES.....	1
2.0 LITERATURE REVIEW	3
2.1 Chlorinated Aliphatic Hydrocarbons	3
2.2 1,4-Dioxane	4
2.3 Bioremediation and Aerobic Cometabolism	5
2.3.1 Butane	5
2.3.2 Isobutane.....	7
2.3.3 Ethane	8
2.3.4 Propane	9
2.3.5 Isobutene	9
2.3.6 Methane.....	9
2.3.7 1,1-DCE Toxicity.....	10
2.4 Rhodococcus rhodochrous.....	11
2.5 ELW1.....	13
2.6 Naval Air Station North Island Site	14
3.0 MATERIALS AND METHODS	17
3.1 Chemicals	17
3.2 Analytical Methods	17
3.2.1 1,4-Dioxane	17
3.2.2 Chlorinated Aliphatic Hydrocarbons	18
3.2.3 Alkane and Alkene Hydrocarbons	18
3.2.4 Oxygen.....	18
3.2.5 Carbon Dioxide.....	18
3.2.6 Isobutanol	19
3.2.7 Biomass	19
3.2.8 Calculations	19
3.3 Pure Culture Studies.....	20

TABLE OF CONTENTS (Continued)

	<u>Page</u>
3.3.1 Inoculation	20
3.3.2 Harvesting	21
3.3.3 Rate Test Experimental Design	21
3.4 Microcosm Studies	24
3.4.1 Set 1: Native groundwater, isobutane.....	27
3.4.2 Set 2: Sparged groundwater, isobutane	27
3.4.3 Set 3: Bioaugmentation with 0.5 mg isobutane-grown 21198.....	28
3.4.4 Set 4: Bioaugmentation with 0.7 mg isobutane-grown 21198.....	28
3.4.5 Set 5: Isobutane data confirmation and isobutanol experimentation	29
3.4.6 Set 6: Native groundwater with isobutene.....	30
3.4.7 Set 7: Sparged groundwater with isobutane/isobutene and isobutanol experimentation	31
4.0 RESULTS AND DISCUSSION.....	33
4.1 Pure Culture Studies.....	33
4.1.1 Isobutane-grown 21198	33
4.1.2 Ethane-grown 21198.....	34
4.1.3 Propane-grown 21198.....	36
4.1.4 Isobutene-grown ELW1.....	37
4.1.5 Comparisons between growth substrates	39
4.2 Microcosm Studies	45
4.2.1 Isobutane in the presence in CAHs.....	45
4.2.2 Isobutane in the absence in CAHs	48
4.2.3 Isobutane bioaugmentation with 21198	54
4.2.4 Isobutane competitive inhibition	65
4.2.5 Isobutane and isobutanol	66
4.2.6 Isobutene in the presence of CAHs	69
4.2.7 Isobutene bioaugmentation with ELW1	72
4.2.8 Nutrient assessment.....	74
5.0 CONCLUSIONS	76
5.1 Rate Test Studies.....	76
5.2 Microcosm Studies	76

TABLE OF CONTENTS (Continued)

	<u>Page</u>
6.0 FUTURE WORK	79
7.0 REFERENCES	80
8.0 APPENDICES	85
A. Recipe for mineral salts media (growth media).....	86
B. Heterotrophic and minimal media plates.....	87
C. Pure Culture Rate Test Results.....	88
C.1 Isobutane-grown 21198 Pure Culture Rate Test Results.....	88
C.2 Ethane-grown 21198 Pure Culture Rate Test Results.....	89
C.3 Propane-grown 21198 Pure Culture Rate Test Results.....	91
C.4 Propane-grown 21198 Pure Culture Rate Test Results.....	94
D. Isobutene in the absence of CAHs.....	94

LIST OF TABLES

<u>Table</u>	<u>Page</u>
Table 2.1. <i>Physical and chemical properties, including molar mass, solubility (PUBCHEM), Henry's constant (Mackay and Shiu, 1981), and octanol-water partition coefficient (log KOW) (US EPA, 1992, 1995) of TCE, c-DCE, 1,1-DCE, 1,1,1-TCA, and 1,2-DCA.</i>	3
Table 2.2. <i>Summary of half saturation coefficients (K_s) and maximum degradation rates for butane-grown mixed culture.</i>	6
Table 2.3. <i>Liquid concentrations of key CAHs and 1,4-dioxane measured at monitoring wells SMW-08A and SMW-10A in December 2016 (Battelle and Accord Engineering, Inc., 2017).</i>	15
Table 3.1. Summary of chemical names, CAS numbers, manufactures, and purities used during experimentation.	17
Table 3.2. Henry's constants for select CAHs used during experimentation (Mackay and Shiu, 1981). ...	20
Table 3.3. Required volume of primary growth substrate and the typical number of days of incubation prior to refreshing.	21
Table 3.4. Summary of rate test experimental design parameters, including the volume of solution added, initial liquid concentration, mass of TSS, and biomass concentration for single-compound tests.	23
Table 3.5. Summary of rate test experimental design parameters, including the volume of solution added, initial liquid concentration, mass of TSS, and biomass concentration for mixture tests.	24
Table 3.6. Summary of days of the experiment additions or amendments were made to each microcosm.....	26
Table 3.7. Initial liquid concentrations and total masses of isobutane, 1,1-DCE, TCE, and 1,4-Dioxane in set 1, bottles 1 through 8.	27
Table 3.8. Initial liquid concentrations and total masses of isobutane, 1,1-DCE, TCE, and 1,4-Dioxane in set 2, bottles 1 through 6.	28
Table 3.9. Initial liquid concentrations and total masses of isobutane, 1,1-DCE, TCE, and 1,4-Dioxane in set 3, bottles 1 through 4.	28
Table 3.10. Initial liquid concentrations and total masses of isobutane, 1,1-DCE, TCE, and 1,4-Dioxane in set 4, bottles 1 through 4.	29
Table 3.11. Initial liquid concentrations and total masses of isobutane, 1,1-DCE, TCE, and 1,4-Dioxane in set 5, bottles 1 through 10.	30
Table 3.12. Initial liquid concentrations and total masses of isobutane, 1,1-DCE, TCE, and 1,4-Dioxane in set 6, bottles 1 through 8.	31
Table 3.13. Initial liquid concentrations of isobutane, 1,1-DCE, TCE, and 1,4-Dioxane in set 7, bottles 1 through 8.	32

LIST OF TABLES (Continued)

Table

Page

Table 4.1. *Summary of half-saturation constants (K_s), maximum transformation rates, and transformation capacities (T_c) for TCE, 1,1,1-TCA, 1,1-DCA, c-DCE, and 1,2-DCA by various mixed and pure cultures grown on butane, methane, and propane in previous studies. 42*

LIST OF FIGURES

<u>Figure</u>	<u>Page</u>
Figure 2.1. Chemical structure of TCE (A), c-DCE (B), 1,1-DCE (C), 1,1,1-TCA (D), and 1,2-DCA (E).....	3
Figure 2.2. Chemical structure of 1,4-dioxane.....	4
Figure 2.3. Depiction of primary metabolism of isobutane and cometabolism of 1,1-DCE to their respective transformation products.	11
Figure 2.4. ABPP using 1,7-octadiyne as a probe for detection of SCAM in dextrose, ethane, propane, n-butane, and isobutane-grown 21198 (Hyman).....	12
Figure 2.5. NAS North Island location map (Aptim Federal Services, LLC, 2018).	15
Figure 2.6. 1,4-dioxane isoconcentration contour map at NAS North Island, including monitoring well locations, from December 2015 (Aptim Federal Services, LLC, 2018).....	16
Figure 3.1. Microcosm schematic diagram.	25
Figure 4.1. Total mass of 1,1-DCE per mg TSS over time for isobutane-grown 21198. Approximately 4 mg of cells were used for experimentation.	34
Figure 4.2. Comparison of zero order degradation rates of 1,1-DCE, 1,2-DCA, 1,4-dioxane, c-DCE, 1,1,1-TCA, and TCE for isobutane-grown 21198. Error bars indicate the standard deviation of a two sample average.....	34
Figure 4.3. Total mass of 1,1-DCE per mg TSS over time for ethane-grown 21198. Approximately 4 mg of cells were used for experimentation.	35
Figure 4.4. Comparison of zero order degradation rates of 1,1-DCE, 1,2-DCA, 1,4-dioxane, c-DCE, 1,1,1-TCA, and TCE for ethane-grown 21198. Error bars indicate the standard deviation of a two sample average.....	35
Figure 4.5. Zero order primary substrate uptake rates of isobutane and ethane for ethane-grown 21198. Error bars indicate the standard deviation of a two sample average.	36
Figure 4.6. Total mass of 1,1-DCE per mg TSS over time for propane-grown 21198. Approximately 4 mg of cells were used for experimentation.	36
Figure 4.7. Comparison of zero order degradation rates of 1,1-DCE, 1,2-DCA, 1,4-dioxane, c-DCE, 1,1,1-TCA, and TCE for propane-grown 21198. Error bars indicate the standard deviation of a two sample average.....	37
Figure 4.8. Zero order primary substrate uptake rates of isobutane and propane for propane-grown 21198. Error bars indicate the standard deviation of a two sample average.	37
Figure 4.9. Total mass of 1,1-DCE per mg TSS over time for isobutene-grown ELW1. Approximately 4 mg of cells were used for experimentation.	38
Figure 4.10. Comparison of zero order degradation rates of 1,1-DCE, 1,4-dioxane, and TCE for isobutene-grown ELW1. Error bars indicate the standard deviation of a two sample average.....	38

LIST OF FIGURES (Continued)

<u>Figure</u>	<u>Page</u>
Figure 4.11. Total mass of 1,1-DCE, 1,1,1-TCA, TCE, 1,2-DCA, and 1,4-dioxane over time for isobutene-grown ELW1.	39
Figure 4.12. Total mass of 1,1-DCE, 1,1,1-TCA, TCE, 1,2-DCA, and isobutene over time for isobutene-grown ELW1 (1,4-dioxane data not shown).	39
Figure 4.13. Zero order degradation rates of 1,4-D (A), TCE (B), 1,1,1-TCA (C), 1,2-DCA (D), 1,1-DCE (E), and c-DCE (F) for isobutane-, ethane-, and propane-grown 21198 and isobutene-grown ELW1. Error bars indicate the standard deviation of a two sample average.	40
Figure 4.14. Transformation capacities of 1,1-DCE (A) and c-DCE (B) for isobutane, ethane, and propane-grown 21198 and isobutene-grown ELW1. Error bars indicate the standard deviation of a two sample average.....	41
Figure 4.15. Total mass of 1,1-DCE, 1,1,1-TCA, TCE, 1,2-DCA, and 1,4-dioxane in isobutane (A), ethane (B), and propane (C) grown 21198, and isobutene grown ELW1 (D) for COC mixtures. Approximately 5 mg of cells were used in each experiment.	44
Figure 4.16. Experimental microcosm road map indicating the general experimental process for long-term microcosm studies utilizing isobutane and isobutene as primary growth substrates.....	45
Figure 4.17. Total mass of isobutane (A), TCE (B), and 1,1-DCE (C) over time in native microcosms incubated with isobutane in the presence of CAHs (set 1). Bottles 1 and 2 do not have added nutrients; bottles 3 and 4 have added nutrients; bottles 5 and 6 are acetylene controls; and bottles 7 and 8 do not have isobutane added.....	47
Figure 4.18. Total mass of isobutane over time in native microcosms incubated with isobutane in the presence of CAHs (set 5). All bottles have nutrients added. Bottles 1 through 6 were constructed with groundwater from SMW-08A, and bottles 9 and 10 were constructed with groundwater from SMW-10A (with approximately two times the total mass of 1,1-DCE compared to SMW-08A).....	48
Figure 4.19. Total mass of isobutane (A), TCE (B), 1,1-DCE (C), and 1,4-dioxane (D) over time in native microcosms initially sparged to remove CAHs. Nutrients were added to bottles 1 and 2 on day 24. Bottles 3 through 6 had nutrients added on day 0. Bottles 5 and 6 were acetylene controls.....	49
Figure 4.20. Total mass of isobutane over time in native microcosms with added nutrients and initially sparged to remove CAHs (set 2, bottles 3 and 4).	50
Figure 4.21. Total mass of 1,4-dioxane and isobutane (A), and 1,1-DCE and TCE (B) over time in one native microcosm with added nutrients on day 0 and initially sparged to remove CAHs (set 2, bottle 3). This depicts an early spike of isobutane and COCs added to this microcosm on day 33.	51
Figure 4.22. Total mass of 1,4-dioxane and isobutane (A), and 1,1-DCE and TCE (B) over time in one native microcosm with added nutrients on day 0 and initially sparged to remove CAHs (set 2, bottle 3). This depicts the last spike of isobutane and COCs added to this microcosm on day 82.	52
Figure 4.23. Comparison of total mass of TCE over time in native active and acetylene control microcosms that were initially sparged to remove CAHs (set 2, bottles 3-6). TCE was added to the acetylene control bottles on day 102 in order to compare the change in total mass over time to the change observed in the active bottles.	53
Figure 4.24. Total mass of isobutane over time in native microcosms sparged to remove CAHs on day 0.	53

LIST OF FIGURES (Continued)

<u>Figure</u>	<u>Page</u>
Figure 4.25. Total mass of 1,1-DCE, TCE, and isobutane over time in native microcosms sparged to remove CAHs on days 23 and 51 (set 5, bottles 3 and 4). Complete isobutane uptake was observed in bottle 3 on day 69. Isobutane was added to bottle 3 on day 76, and subsequent uptake was observed within one day.	54
Figure 4.26. Total mass of isobutane (A), TCE (B), 1,1-DCE (C), and 1,4-dioxane (D) over time in microcosms bioaugmented with 0.5 mg of 21198 (set 3). Nutrients were added to all microcosms on day 0. Bottles 3 and 4 were acetylene controls. Bottles 1 and 2 were respiked with isobutane, 1,1-DCE, 1,4-dioxane, and gradually increasing concentrations of TCE over 120 days of incubation.	56
Figure 4.27. Total mass of isobutane, 1,1-DCE, and TCE over time set 3, bottles 1 (A) and 2 (B) bioaugmented with 0.5 mg 21198. The residual 1,1-DCE was hypothesized to be an unknown compound that coelutes with 1,1-DCE (further discussed below)	57
Figure 4.28. Total mass of 1,4-dioxane in set 3, bottles 1 and 2 bioaugmented with 0.5 mg 21198.	57
Figure 4.29. Total mass of 1,4-dioxane and isobutane (A), and 1,1-DCE and TCE (B) over time in one microcosm bioaugmented with 0.5 mg of isobutane-grown 21198 (set 3, bottle 1). This depicts an early spike of isobutane and COCs added to this microcosm on day 33.	58
Figure 4.30. Total mass of 1,4-dioxane and isobutane (A), and 1,1-DCE and TCE (B) over time in one microcosm bioaugmented with 0.5 mg of isobutane-grown 21198 (set 3, bottle 1). This depicts the final spike of isobutane and COCs added to this microcosm on day 75 after gradual increases in TCE concentration.	59
Figure 4.31. Comparison of total mass of TCE over time in microcosms bioaugmented with 0.5 mg of 21198. Active and acetylene control microcosms that were initially sparged to remove CAHs (set 3, bottles 3-6). TCE was added to the acetylene control bottles on day 102 in order to compare the change in total mass over time to the change observed in the active bottles.	60
Figure 4.32. Total mass of isobutane (A), TCE (B), 1,1-DCE (C), and 1,4-dioxane (D) over time in microcosms bioaugmented with 0.7 mg of 21198 (set 4). Nutrients were added to all microcosms on day 0. Bottles 3 and 4 were acetylene controls. Bottles 1 and 2 were respiked with isobutane, TCE, 1,4-dioxane, and gradually increasing concentrations of 1,1-DCE over 115 days of incubation.	61
Figure 4.33. Total mass of isobutane, 1,1-DCE, and TCE over time in set 4, bottles 1 (A) and 2 (B) bioaugmented with 0.7 mg 21198.	62
Figure 4.34. Total mass of 1,4-dioxane and isobutane (A), and 1,1-DCE and TCE (B) over time in one microcosm bioaugmented with 0.7 mg of isobutane-grown 21198 (set 4, bottle 1). This depicts an early spike of isobutane and COCs added to this microcosm on day 28.	63
Figure 4.35. Total mass of 1,4-dioxane and isobutane (A), and 1,1-DCE and TCE (B) over time in one microcosm bioaugmented with 0.7 mg of isobutane-grown 21198 (set 4, bottle 1). This depicts the final spike of isobutane and COCs added to this microcosm on day 70 after gradual increases in 1,1-DCE concentration. The presence of the unknown compound cannot be visualized due to the scale of the plot. 1,1-DCE was not able to be fully transformed.	64
Figure 4.36. Total mass of 1,4-dioxane and isobutane (A), and 1,1-DCE and TCE (B) over time in one microcosm bioaugmented with 0.7 mg of isobutane-grown 21198 (set 4, bottle 2). This depicts a spike of isobutane and COCs added to this microcosm on day 70 after gradual increases in 1,1-DCE concentration. The presence of the unknown compound cannot be visualized due to the scale of the plot.	65

LIST OF FIGURES (Continued)

<u>Figure</u>	<u>Page</u>
Figure 4.37. Total mass of isobutane over time in two native microcosms established in the presence of CAHS with approximately ten times greater starting mass of isobutane than other microcosms.	66
Figure 4.38. Total mass of isobutane and isobutanol (A), O ₂ and CO ₂ (B), and 1,1-DCE and TCE (C) in isobutanol-amended microcosms initially in the presence of isobutane. Isobutanol was initially added to microcosms on day 23.	67
Figure 4.39. Total mass of isobutane and isobutanol (A), O ₂ and CO ₂ (B), and 1,1-DCE and TCE (C) in isobutanol-amended microcosms initially in the absence of isobutane. Isobutanol was initially added to microcosms on day 0.	69
Figure 4.40. Total mass of isobutene over time in native isobutene microcosms established in the presence of CAHS (set 6, bottles 3 through 6). Microcosms 3 and 4 were sparged to remove CAHS on day 25, and microcosms 5 and 6 were bioaugmented with 0.9 mg of isobutene-grown ELW1 on day 33.	70
Figure 4.41. Total mass of isobutene, 1,1-DCE, and TCE over time in the native isobutene microcosm established in the presence of CAHS and 1,4-dioxane (set 6, bottle 1). The residual mass of 1,1-DCE remaining after the transformation is likely the unknown compound discussed in Section 4.2.3.	71
Figure 4.42. Comparison of degradation rates of isobutene (A), 1,1-DCE (B), and TCE (C) in the native isobutene microcosm established in the presence of CAHS over four spikes of primary substrate and CAHS (set 6, bottle 1).	71
Figure 4.43. Total mass of 1,4-dioxane over time in the native isobutene microcosm established in the presence of CAHS and 1,4-dioxane (set 6, bottle 1).	71
Figure 4.44. Total mass of isobutene, 1,1-DCE, and TCE over time in a second native isobutene microcosm established in the presence of CAHS (set 6, bottle 2).	72
Figure 4.45. Total mass of isobutene, 1,1-DCE, and TCE over time in ELW1 bioaugmented microcosm 5 (A). The first and second spikes spanning 16 days (A) and the third spike spanning 16 days (B) are shown to observe the inhibition of CAH transformations by the presence of isobutene.	73
Figure 4.46. Total mass of 1,4-dioxane over time in native isobutene microcosms established in the presence of CAHS and bioaugmented with 0.9 mg of isobutene-grown ELW1 on day 33 (set 6, bottles 5 and 6).	74
Figure 4.47. Comparison of degradation rates of isobutene (A), 1,1-DCE (B), and TCE (C) in ELW1 bioaugmented microcosms over three spikes of primary substrate and CAHS. Error bars indicate the standard deviation of a two sample average.	74
Figure 4.48. Liquid concentration of isobutane over time in microcosms initially sparged to remove CAHS (set 2). Microcosms 3 and 4 received nutrients on day zero, while microcosms 1 and 2 received nutrients on day 24.	75
Figure A.1. Total mass of TCE per mg TSS over time for isobutane-grown 21198.	88
Figure A.2. Total mass of 1,1,1-TCA per mg TSS over time for isobutane-grown 21198.	88
Figure A.3. Total mass of 1,2-DCA per mg TSS over time for isobutane-grown 21198.	88
Figure A.4. Total mass of c-DCE per mg TSS over time for isobutane-grown 21198.	89
Figure A.5. Total mass of 1,4-dioxane per mg TSS over time for ethane-grown 21198.	89

LIST OF FIGURES (Continued)

<u>Figure</u>	<u>Page</u>
Figure A.6. Total mass of TCE per mg TSS over time for ethane-grown 21198.	89
Figure A.7. Total mass of 1,1,1-TCA per mg TSS over time for ethane-grown 21198.	90
Figure A.8. Total mass of 1,2-DCA per mg TSS over time for ethane-grown 21198.	90
Figure A.9. Total mass of c-DCE per mg TSS over time for ethane-grown 21198.	90
Figure A.10. Total mass of ethane per mg TSS over time for ethane-grown 21198.	91
Figure A.11. Total mass of isobutane per mg TSS over time for ethane-grown 21198.	91
Figure A.12. Total mass of 1,4-dioxane per mg TSS over time for propane-grown 21198.	91
Figure A.13. Total mass of TCE per mg TSS over time for propane-grown 21198.	92
Figure A.14. Total mass of 1,1,1-TCA per mg TSS over time for propane-grown 21198.	92
Figure A.15. Total mass of 1,2-DCA per mg TSS over time for propane-grown 21198.	92
Figure A.16. Total mass of c-DCE per mg TSS over time for propane-grown 21198.	93
Figure A.17. Total mass of propane per mg TSS over time for propane-grown 21198.	93
Figure A.18. Total mass of isobutane per mg TSS over time for propane-grown 21198.	93
Figure A.19. Total mass of 1,4-dioxane per mg TSS over time for isobutene-grown ELW1.	94
Figure A.20. Total mass of TCE per mg TSS over time for isobutene-grown ELW1.	94
Figure A.21. Total mass of isobutene over time in native microcosms initially established in the presence of CAHs (set 6, bottles 3 and 4). CAHs were sparged from solution on day 25, and isobutene was re-added to the headspace.	95
Figure A.22. Total mass of isobutene over time in native microcosms established in the absence of CAHs (set 7, bottles 3 and 4). CAHs were sparged from solution on day 0 when isobutene was initially added to the headspace.	95

LIST OF ABBREVIATIONS

µg/L	micrograms per liter
µL	microliter(s)
ABPP	activity-based protein profiling
ATCC	American Type Culture Collection
BGS	below ground surface
°C	degrees Celsius
CAH	chlorinated aliphatic hydrocarbon
c-DCE	cis-1,2-dichloroethene
CAH(s)	chlorinated aliphatic hydrocarbon(s)
COC(s)	contaminant(s) of concern
CO ₂	carbon dioxide
1,4-D	1,4-dioxane
1,1-DCE	1,1-dichloroethene
1,2-DCE	1,2-dichloroethene
ECD	electron capture detector
FID	flame ionization detector
GC	gas chromatograph
GC-MS	gas chromatography-mass spectrometry
L	liter(s)
MCL	maximum contaminant level
mg	milligram(s)
mg/L	milligrams per liter
mL	milliliter(s)
MTBE	methyl tertiary butyl ether
m/z	mass-to-charge ratio
N	nitrogen
NAS	Naval Air Station
O ₂	oxygen
OHPHE	hydroxyphenanthrene
P	phosphorous
pMMO	particulate methane monooxygenase
PrMO	propane monooxygenase
RCF	relative centrifugal force
rpm	revolutions per minute
SCAM	short-chain alkane monooxygenase
sMMO	soluble methane monooxygenase
TBA	tert-butyl alcohol
1,1,1-TCA	1,1,1-trichloroethane
TCD	thermal conductivity detector
TCE	trichloroethylene
TSS	total suspended solids
USEPA/EPA	United States Environmental Protection Agency

1.0 INTRODUCTION AND OBJECTIVES

Historical use and improper storage and disposal of chlorinated solvents have resulted in widespread groundwater contamination with chlorinated aliphatic hydrocarbons (CAHs) such as trichloroethylene (TCE), 1,1-dichloroethylene (1,1-DCE), cis-1,2-dichloroethylene (c-DCE), 1,1,1-trichloroethane (1,1,1-TCA), and 1,2-dichloroethane (1,2-DCA), and the solvent stabilizer, 1,4-dioxane (1,4-D). These compounds often exist in as mixtures in the subsurface. While 1,4-dioxane contamination has most notably been connected to the use of 1,1,1-TCA, it has also been found to be a common co-contaminant with TCE (Anderson et al., 2012). This is likely due to the substitution of TCE with 1,1,1-TCA in the mid-1960s as a result of increased regulations restricting the use of TCE (Mohr et al., 2010).

These compounds are listed by the Environmental Protection Agency (EPA) as known or possible human carcinogens (US EPA, 2017a), and stringent drinking water standards have promoted a drive for the remediation of these sites. Due to the unique chemical and physical properties of these compounds, remediation can be difficult. Bioremediation, or the use of microbial metabolic processes to break down contaminants, has been shown to be an effective strategy for CAH and 1,4-dioxane remediation (Frasconi et al., 2015). Aerobic cometabolism is a specific bioremediation process by which microorganisms are fed a primary growth substrate for use as a carbon and energy source, while fortuitous transformation of contaminants of concern (COCs) is observed via the activation of monooxygenase enzymes by the primary growth substrate (Bradley, 2003).

Effective primary growth substrates for the promotion of aerobic cometabolism include compounds such as methane, ethane, propane, and butane (Dolinová et al., 2017). Many studies have reported successful transformations of 1,4-dioxane and a variety of chlorinated compounds including TCE, 1,1-DCE, c-DCE, 1,1,1-TCA, and 1,2-DCA via aerobic cometabolism (Alvarez-Cohen and Speitel, 2001; Mahendra and Alvarez-Cohen, 2006). An increasingly prevalent issue involves the implementation of aerobic cometabolism at sites contaminated with more complex mixtures of CAHs and 1,4-dioxane.

Multiple pure-cultures have been identified that are capable of performing cometabolism. Two such cultures include *Rhodococcus rhodochrous* American Type Culture Collection (ATCC) 21198 (hereby referred to as 21198) and *Mycobacterium* sp. ELW1 (hereby referred to as ELW1). 21198 has been shown to grow on a variety of gaseous short-chain alkanes including isobutane, ethane, propane, and n-butane (Babu and Brown, 1984; Hou et al., 1983; MacMichael and Brown, 1987). 21198 has been found to transform 1,4-dioxane and a variety of CAHs including 1,2-DCA, 1,1-DCA, 1,1,2-TCA, 1,1,1-TCA,

1,1-DCE via cometabolism (Bennett et al., 2018; Rich, 2015; Rolston, 2017; Thankitkul, 2016). ELW1 is an isobutene-utilizer that has been found to cometabolize phenanthrene, vinyl chloride, c-DCE, and TCE (Kottegoda et al., 2015; Rich, 2015; Schrlau et al., 2017).

A volatile organic compound plume was discovered at Naval Air Station (NAS) North Island in San Diego, California in 2005. Historical use and improper storage of chlorinated solvents resulted in contamination of groundwater with CAHs (predominately TCE and 1,1-DCE) and 1,4-dioxane. Due to the composition of the contaminant mixture located on NAS North Island, aerobic cometabolism and the implementation of a multiple primary substrate biosparging approach were proposed for the remediation of this site.

The objectives of this study were to:

1. Evaluate the cometabolic abilities of isobutane, ethane, and propane-grown 21198 and isobutene-grown ELW1 to transform single-compounds and mixtures of CAHs and 1,4-dioxane;
2. Use microcosms with groundwater and aquifer solids from NAS North Island in San Diego, California to evaluate the use of isobutane and isobutene as primary growth substrates to promote cometabolism of mixtures of 1,4-dioxane and CAHs by native microbial communities;
3. Evaluate the effectiveness of bioaugmentation to native microcosms containing mixtures of COCs with isobutane-grown 21198 and isobutene-grown ELW1;
4. Evaluate the long-term effectiveness of cometabolism in microcosms containing 1,4-dioxane and exposed to increasing concentrations of 1,1-DCE and TCE.

2.0 LITERATURE REVIEW

2.1 Chlorinated Aliphatic Hydrocarbons

Chlorinated aliphatic hydrocarbons (CAHs), including TCE, c-DCE, 1,1-DCE, 1,1,1-TCA, and 1,2-DCA are common groundwater contaminants existing from the improper disposal of chlorinated solvents. Chlorinated solvents have been used most often in degreasing and dry-cleaning operations (Mohr et al., 2010). Other industrial applications have included use in adhesives, pharmaceuticals, textile processing, and coating solvents (Ward and Stroo, 2010). These solvents gained popularity due to their effectiveness, noncorrosivity, nonflammability, and ease of recycling (Doherty, 2000). The physical structures of primary CAHs are shown in Figure 2.1, and key physical and chemical properties for TCE, c-DCE, 1,1-DCE, 1,1,1-TCA, and 1,2-DCA are shown in Table 2.1.

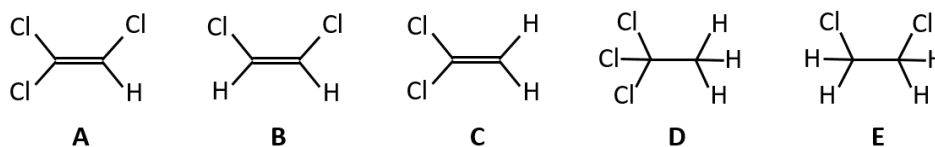


Figure 2.1. Chemical structure of TCE (A), c-DCE (B), 1,1-DCE (C), 1,1,1-TCA (D), and 1,2-DCA (E).

Table 2.1. Physical and chemical properties, including molar mass, solubility (PUBCHEM), Henry's constant (Mackay and Shiu, 1981), and octanol-water partition coefficient (log K_{OW}) (US EPA, 1992, 1995) of TCE, c-DCE, 1,1-DCE, 1,1,1-TCA, and 1,2-DCA.

	TCE	c-DCE	1,1-DCE	1,1,1-TCA	1,2-DCA
Molar mass (g/mol)	131.38	96.94	96.94	133.40	98.95
Solubility @ 25 °C (mg/L)	1,280	3,500	2,420	1,290	8,600
Henry's constant @ 20°C (dimensionless)	0.296	0.122	0.857	0.548	0.179
Log K_{OW}	2.53	1.86	1.48	2.47	1.45

While the physical and chemical properties of CAHs made them ideal for industrial applications, they have also contributed to their proliferation throughout the environment and impacted their fate and transport in aquifers. Most chlorinated solvents have densities greater than that of water, promoting their downward movement through the subsurface (Ward and Stroo, 2010). When groundwater encounters a CAH source, solvents dissolve into solution up to their solubility limits and proceed to travel along the downward gradient of groundwater flow. The hydrogeological features of the subsurface can also greatly impact the fate and transport of CAHs through aquifers. Chlorinated solvent plumes have been found to travel great distances beyond their source.

Many CAHs have been found to have adverse effects on human health and/or have been identified as known or possible human carcinogens. As such, the USEPA has established drinking water maximum

contaminant levels (MCLs) for a variety of compounds, including TCE (5 µg/L), c-DCE (70 µg/L), 1,1-DCE (7 µg/L), 1,1,1-TCA (200 µg/L), and 1,2-DCA (5 µg/L).

2.2 1,4-Dioxane

As shown in Figure 2.2, 1,4-dioxane is a cyclic ether with a highly stable structure (Mohr et al., 2010). The commercial sale of 1,4-dioxane began in 1929. 1,4-dioxane has many industrial uses including the application as a constituent in pharmaceuticals and pesticides and as a solvent in paints, stains, resins, oils, and adhesives (US EPA, 2006). Production and use of 1,4-dioxane increased in the 1950s and early 1960s due to its use as a stabilizer in 1,1,1-TCA (Agency for Toxic Substances and Disease Registry, 2012). 1,1,1-TCA actively reacts with aluminum. To counteract this reaction, 1,4-dioxane was added at approximately 4% (Ward and Stroo, 2010).

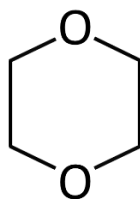


Figure 2.2. Chemical structure of 1,4-dioxane.

1,4-dioxane is hydrophilic, fully miscible in water and has a low octanol-water partition coefficient (0.27), which makes sorption to organic matter unlikely (US EPA, 2006). Due to these physical and chemical properties, 1,4-dioxane contaminant plumes have the ability to travel great distances with the flow of groundwater. The low Henry's constant (3×10^{-6} atm·m³/mol) and vapor pressure of 1,4-dioxane (37 mm Hg at 25°C) also prevent volatilization into the vapor phase, complicating remediation via air stripping (Mohr, 2001).

While 1,4-dioxane contamination has most notably been connected to the use of 1,1,1-TCA, it has also been found to be a common co-contaminant with TCE (Anderson et al., 2012). This is likely due to the substitution of TCE with 1,1,1-TCA in the mid-1960s due to increased regulations restricting the use of TCE (Mohr et al., 2010). Anderson et al. studied the co-occurrence of 1,4-dioxane and TCE at U.S. Air Force installations (Anderson et al., 2012). They found that 93.7% of all 1,4-dioxane detections were concurrently detected with 1,1,1-TCA and/or TCE, and 64.4% of all 1,4-dioxane detections were independently connected to TCE detections.

1,1-DCE is often also present at 1,4-dioxane contaminated sites due to its formation during the abiotic transformation of 1,1,1-TCA (Vogel, 1987). A survey conducted by Adamson et al. found that 1,4-

dioxane was present at 68% of 1,1-DCE contaminated sites, and 97% of surveyed sites with 1,1-DCE contamination and no 1,1,1-TCA or TCE detection were not analyzed for 1,4-dioxane (Adamson et al., 2014). This finding suggests that the absence of 1,1,1-TCA and TCE should not be accepted as proof that 1,4-dioxane contamination is not present.

1,4-dioxane has been classified by the US EPA as a probable human carcinogen (US EPA, 2006). While there is currently no established federal drinking water MCL for 1,4-dioxane, it is included in the US EPA's Third Unregulated Contaminant Monitoring Rule (US EPA, 2016). In addition, numerous states have established drinking water and groundwater guidelines (US EPA, 2017b).

2.3 Bioremediation and Aerobic Cometabolism

Bioremediation is the practice of applying microbiological processes to the clean-up of contaminated soil and groundwater through engineered systems (Mandelbaum et al., 1997). Biostimulation, the modification of a natural aquifer through the addition of limiting nutrients, oxygen, and/or primary substrates, and bioaugmentation, the addition of a known COC-degrading microorganism to a natural aquifer, are common forms of bioremediation (Adams et al.). Bioremediation can be applied through direct metabolism wherein microbes utilize a particular COC as the sole carbon and energy source, or through cometabolism wherein microbes utilize a separate primary substrate as a carbon and energy source, while COCs are fortuitous transformed via enzymes induced by the primary substrate (Frasconi et al., 2015). A variety of compounds can be employed as primary growth substrates to induce cometabolism, including butane, isobutane, propane, methane, ethane, ethene, isobutene, n-pentane, n-hexane, propene, toluene, and ammonia (CITATION). Specific studies conducted with the use of butane, isobutane, ethane, propane, isobutene, and methane as primary growth substrates are summarized in Sections 2.4.2 through 2.4.7.

2.3.1 *Butane*

Numerous studies have been conducted utilizing butane as a primary growth substrate for aerobic cometabolism (Doughty et al., 2005; Hamamura et al., 1997; Jitnuyanont et al., 2001; Kim et al., 1997, 2000, 2002; Semprini et al., 2007a, 2007b, 2009; Tovanabootr and Semprini, 1998). Tovanabootr and Semprini researched the use of butane to stimulate the cometabolism of TCE in batch aquifer microcosms (Tovanabootr and Semprini, 1998). A substrate utilization lag time of 20 days was observed, and an average of 3 days were required for complete utilization. The stimulated butane-utilizers were not able to transform TCE. Kim et al. studied the cometabolism of a variety of CAHs by a butane-grown

mixed culture (Kim et al., 2000). Chloromethane, dichloromethane, chloroform, chloroethane, 1,1-DCA, 1,2-DCA, 1,1,1-TCA, 1,1,2-TCA, vinyl chloride, 1,1-DCE, and c-DCE were all capable of transformation via cometabolism. TCE was not readily transformed by the butane enrichment culture. CAH transformations were inactivated by the presence of acetylene, suggesting a monooxygenase is likely responsible for the lack of transformations.

Kim et al. further conducted kinetic and inhibition studies for the cometabolism of 1,1,1-TCA, 1,1-DCE, and 1,1-DCA by a butane-grown mixed culture (Kim et al., 2002). They determined the maximum degradation rates and half-saturation coefficients via single compound kinetic tests (Table 2.2). Direct linear plots were used to identify the types of inhibition. Competitive and mixed inhibition were found to be the prominent inhibition types at work in the system. CAHs were found to be weak inhibitors of butane utilization, while butane was found to be a strong inhibitor of CAH transformation. The results also suggested that 1,1-DCE was a stronger inhibitor than 1,1,1-TCA and 1,1-DCA.

Table 2.2. Summary of half saturation coefficients (K_s) and maximum degradation rates for butane-grown mixed culture.

Compound	K_s ($\mu\text{mol/L}$)	Max Rate ($\mu\text{mol S/mg TSS/h}$)
1,1,1-TCA	12	0.19
1,1-DCE	1.5	1.3
1,1-DCA	19	0.49
Butane	19	2.6

Jitnuyanont et al. studied the bioaugmentation of butane-utilizing microorganisms to promote cometabolism of 1,1,1-TCA in groundwater microcosms (Jitnuyanont et al., 2001). Two microcosms containing groundwater and aquifer solids from Moffett Field, Sunnyvale, California, were established with butane as the primary substrate. No butane uptake was observed in either microcosm after 57 days of incubation. Bioaugmentation potential was tested via inoculation of one microcosm with a butane-utilizing enrichment from the Hanford DOE site. Butane uptake was observed three days after the inoculation. The bioaugmented microcosm initially demonstrated effective 1,1,1-TCA transformation, but the transformation ability decreased after prolonged exposure. After 80 days of incubation, the non-bioaugmented microcosm began to uptake butane. The transformation of 1,1,1-TCA was initially limited but improved with time. The transformation yields (0.04 mg 1,1,1-TCA/mg butane) and the microbial compositions of the bioaugmented and non-bioaugmented systems were found to be similar after 440 days of incubation.

Semprini et al. have researched the bioaugmentation of butane-utilizing microorganisms for the transformation of 1,1-DCE, 1,1-DCA, and 1,1,1-TCA (Semprini et al., 2007a). A butane-enriched culture consisting primarily of *Rhodococcus* sp.-type microorganisms was used to bioaugment laboratory microcosms containing aquifer solids and groundwater from the Moffett Field Test Facility. 1,1-DCE was most quickly transformed, followed by 1,1-DCA and then 1,1,1-TCA. The transformation of 1,1,1-TCA appeared to be the strongest inhibitor of butane uptake. Accelerated removal rates with subsequent butane and CAH additions were observed over 100 days of incubation. Butane uptake was not observed in non-bioaugmented microcosms over 83 days of incubation.

Semprini et al. conducted further studies into the bioaugmentation of butane-utilizing microorganisms for the transformation of 1,1-DCE, 1,1-DCA, and 1,1,1-TCA (Semprini et al., 2007b). Rapid 1,1-DCE transformation with high product toxicity and poor inhibition by butane were demonstrated in microcosm experiments and modeling studies. Model simulations of laboratory data determined a 1,1-DCE transformation capacity 0.175 $\mu\text{mol}/\text{mg}$ cells. 1,1,1-TCA transformation was much slower and strongly inhibited by butane.

2.3.2 Isobutane

Studies have been conducted that demonstrate the successful use of isobutane as the sole carbon and energy source for the growth microorganism *Rhodococcus rhodochrous* (Babu and Brown, 1984; MacMichael and Brown, 1987). Bennett et al. quantified 1,4-dioxane biodegradation in isobutane-grown *Rhodococcus rhodochrous* strain 21198 (Further discussed in Section 2.5) (Bennett et al., 2018). Resting isobutane-grown cells were able to transform $\geq 95\%$ of the initial 1,4-dioxane within 80 to 220 hours. The inhibition of 1,4-dioxane degradation by the presence of 1-butyne, a known monooxygenase blocker, suggests monooxygenase enzymes are responsible for the transformation.

Rich conducted a kinetic analysis of the aerobic degradation of chlorinated ethanes and ethenes by isobutane-grown 21198 (Rich, 2015). This research was conducted via pure cultures studies in batch reactors. 21198 was able to cometabolize a variety of CAHs. The rates of transformation were ordered as follows: vinyl chloride > 1,1-DCE > c-DCE > TCE, and 1,2-DCA > 1,1,2-TCA > 1,1,1-TCA > 1,2,3-TCP. Thankitkul further studied the kinetics of cometabolic transformations of CAHs by isobutane-grown 21198 (Thankitkul, 2016). The transformation capacities were ranked as follows: 1,2-DCA > 1,1-DCA > 1,1,2-TCA > 1,1,1-TCA > 1,1-DCE. The zero order transformation rates were ranked as follow: 1,1-DCA > 1,2-DCA > 1,1-DCE > 1,1,2-TCA > 1,1,1-TCA.

Rolston researched the use of isobutane to promote the aerobic cometabolism of 1,4-dioxane in native microbial aquifer communities and by 21198 (Rolston, 2017). Rolston also investigated the potential inhibition of 1,4-dioxane transformation by the presence of TCE and the importance of inorganic nutrients. Isobutane was found to successfully stimulate native microbes after a lag time of approximately one week, with subsequent 1,4-dioxane transformation. Bioaugmentation with 21198 was also effective, with 1,4-dioxane transformation observed after the concentration of isobutane reached below 0.15 mg/L. Primary substrate inhibition was observed in both biostimulated and bioaugmented microcosms.

TCE was minimally transformed relative to 1,4-dioxane in both the native and bioaugmented microcosms. Results found that neither the rates of isobutane and 1,4-dioxane transformation nor the length of the biostimulation lag period were inhibited by the presence of TCE at a liquid concentration of 200 µg/L. The importance of inorganic nutrients was assessed through the addition of spent growth media with the bioaugmentation inoculum. Higher 1,4-dioxane degradation rates were maintained when compared to microcosms devoid of spent media, suggesting nutrient addition is important for sustained 1,4-dioxane transformation.

2.3.3 Ethane

Few studies have been conducted regarding the use of ethane as a primary growth substrate for aerobic cometabolism of 1,4-dioxane and chlorinated solvents. Freedman and Herz evaluated the use of ethane as a primary substrate for aerobic cometabolism of vinyl chloride (Freedman and Herz, 1996). An ethane-grown enrichment culture was capable of utilizing vinyl chloride as a primary substrate and was able to transform it below 2 µg/L. Verce and Freedman modeled the kinetics of vinyl chloride cometabolism by novel ethane-grown *Pseudomonas* sp. Strain EA1 (Verce and Freedman, 2000). EA1 was isolated from an enrichment culture that had been fed ethane and vinyl chloride over two years. A yield of 0.99 mg TSS per mg ethane was determined. EA1 cometabolized vinyl chloride at a maximum rate of 0.35 µmol/mg VSS/d when ethane was utilized as the primary substrate. Primary substrate inhibition was not observed, though the presence of ethane reduced the total mass of vinyl chloride transformed. Hatzinger et al. researched the use of ethane to promote aerobic cometabolism of 1,4-dioxane in aquifers (Hatzinger et al., 2017). Through natural aquifer microcosms, aquifer enrichment cultures, and pure cultures, ethane was found to promote cometabolism of 1,4-dioxane. 1,4-dioxane concentrations within aquifer microcosms decreased from 370 µg/L to 32 µg/L over 49 days.

2.3.4 Propane

Deng et al. examined the cometabolism of 1,4-dioxane and 1,1-DCE by novel propane-utilizing *Azoarcus* sp. DD4 (Deng et al., 2018). Field sample microcosms containing approximately 10 mg/L 1,4-dioxane and 3.3 mg/L 1,1-DCE were bioaugmented with 0.024 mg of DD4 protein and 8 mg/L propane. 12.6% of propane was consumed over the first 7 days, with minimal 1,4-dioxane and 1,1-DCE degradation. Accelerated propane uptake and 1,1-DCE transformation were observed until propane was completely consumed on day 18, while only 23% of the 1,4-dioxane had been degraded. The concentration of 1,1-DCE decreased from 0.92 mg/L to below the detection limit of 0.02 mg/L by day 23, after a second addition of propane. The 1,4-dioxane concentration rapidly decreased to 0.17 mg/L on day 32 following complete 1,1-DCE transformation. In summary, high concentrations of 1,1-DCE significantly inhibited primary growth substrate uptake and delayed the removal of 1,4-dioxane and 1,1-DCE.

2.3.5 Isobutene

Rich conducted a kinetic analysis of the aerobic degradation of chlorinated ethenes by novel isobutene-grown ELW1 (further described in Section 2.6) (Rich, 2015). ELW1 was able to cometabolize a number of CAHs. The rates of transformation were ordered as follows: vinyl chloride > c-DCE > TCE. Rich also found that the addition of formate increased the transformation capacities of ELW1.

Schrlau et al. researched the capabilities of isobutene-grown ELW1 to cometabolize phenanthrene, a polycyclic aromatic hydrocarbon (Schrlau et al., 2017). ELW1 was found to fully transform phenanthrene. Transformation products included 1-hydroxyphenanthrene (OHPHE), 3-OHPHE, 4-OHPHE, 9-OHPHE, 1,9-OHPHE, and trans-9,10-OHPHE. Minor metabolites, including 1-OHPHE, 3-OHPHE, 4-OHPHE, 9-OHPHE, 1,9-OHPHE, were found to be toxic to embryonic zebrafish. Phenanthrene transformation was moderately inhibited by 1-octyne, suggesting that an alkene monooxygenase is likely the responsible transformation enzyme.

2.3.6 Methane

Methanotroph metabolism is supported by the production of methane monooxygenase enzymes (MMO) (Balasubramanian and Rosenzweig, 2007). These enzymes can either be expressed in the soluble (sMMO) or particulate form (pMMO) (Ayala and Torres, 2004). When grown in the presence of copper, particulate methane monooxygenase is expressed, while the soluble methane monooxygenase is expressed in copper-deficient environments. Burrows et al. found that raising the concentration of

Cu^{2+} from 1 $\mu\text{mol/L}$ to 5 $\mu\text{mol/L}$ promoted a transition from the production of sMMO to pMMO (Burrows et al., 1984).

The specific expression of the MMO enzymes can affect the capabilities of methane-grown microorganisms to transform compounds of interest. Jahng and Wood found that methane-grown *Methylosinus trichosporium* OB3b was able to degrade TCE and chloroform when sMMO was expressed (Jahng and Wood, 1994). TCE transformation was found by Tsien et al. to be significantly less in cultures grown with greater than 0.25 $\mu\text{mol/L}$ of copper added (Tsien et al., 1989).

Chang and Alvarez-Cohen studied the biodegradation of a variety of CAHs by methane-oxidizing cultures (Chang and Alvarez-Cohen, 1996). Methane-grown cultures were able to degrade chloroform, dichloromethane, 1,1,1-TCA, TCE, 1,1-DCE, c-DCE, t-DCE, and vinyl chloride. The maximum transformation rates of TCE and c-DCE for a chemostat-grown mixed methane-oxidizing culture were estimated to be 73 and 86 μmol per mg TSS per day, respectively. The half saturation coefficients for TCE and c-DCE were 47 and 31 $\mu\text{mol/L}$, respectively.

Mahendra and Alvarez-Cohen researched the kinetics of 1,4-dioxane biodegradation by a variety of monooxygenase-expressing bacteria, including the methane-grown OB3b (Mahendra and Alvarez-Cohen, 2006). OB3b was found to only degrade 1,4-dioxane when the soluble methane monooxygenase was expressed. With an initial 1,4-dioxane concentration of 50 mg/L, the degradation rate was 0.38 mg 1,4-dioxane per mg protein per hour.

2.3.7 1,1-DCE Toxicity

As shown in Figure 2.3, an epoxide is formed via the transformation of 1,1-DCE by the monooxygenase enzyme activated by isobutane. Epoxides are electrophilic and have the ability to modify cellular components including DNA, RNA, lipids, proteins, and other small molecules, often resulting in cellular inactivation (Rui et al., 2004). This epoxide has been found to exhibit strong toxicity to microorganisms grown on a variety of substrates.

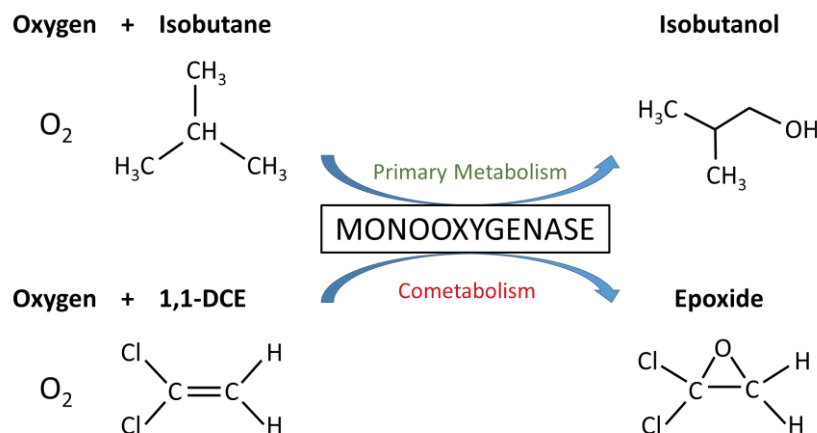


Figure 2.3. Depiction of primary metabolism of isobutane and cometabolism of 1,1-DCE to their respective transformation products.

1,1-DCE toxicity has been observed in various cometabolism systems established for laboratory and field-scale implementation. Anderson and McCarty reported on the effect of chlorinated ethenes on growth rates for a mixed methanotrophic culture (Anderson and McCarty, 1996). They found that growth rates were reduced by approximately 20% in the presence of 0.05 mg/L 1,1-DCE, 1 mg/L t-DCE, or 1 mg/L TCE. Growth rate data were modeled, and transformation product toxicity was shown to have the greatest impact on the growth rate reduction. Dolan and McCarty investigated 1,1-DCE transformation product toxicity in a mixed methanotrophic culture (Dolan and McCarty, 1995). Results indicated that cell inactivation was caused by 1,1-DCE transformation products rather than 1,1-DCE itself.

Kim et al. studied the transformation of CAH mixtures, including 1,1-DCE, by a butane-grown mixed culture (Kim et al., 2002). The transformation capacity of 1,1-DCE was found to be 0.52 $\mu\text{mol}/\text{mg}$ TSS. Semprini et al. further examined the transformation capacity of butane-grown microorganisms through modeling of microcosm data. Model simulations of laboratory data determined a 1,1-DCE transformation capacity 0.175 $\mu\text{mol}/\text{mg}$ cells (Semprini et al., 2007b). These results show greater product toxicity of 1,1-DCE than reported by Kim et al. Chang and Alvarez-Cohen reported a transformation capacity of 0.36 $\mu\text{mol}/\text{mg}$ TSS for methane-grown pure culture *Methylosinus tricosproium* OB3b (Chang and Alvarez-Cohen, 1996).

2.4 Rhodococcus rhodochrous

Rhodococci are prolific in natural systems and have been isolated from numerous environmental sources including soil, groundwater, and marine sediments (Bell et al., 1998). The metabolic diversity

and distinctive enzymatic abilities of *Rhodococci* have permitted an array of applications in the environmental, pharmaceutical, energy, and chemical industries (van der Geize and Dijkhuizen, 2004). The hydrophobic nature of their cell walls contributes to their ability to uptake hydrophobic substrates (Bell et al., 1998). *Rhodococcus* cells also have the ability to survive in starvation conditions (Martinkova et al., 2009).

Rhodococcus rhodochrous strain ATCC 21198, formally known as *Nocardia paraffinica*, was isolated from soil (Tanaka et al., 1973). This is a gram-positive, aerobic microorganism that experiences optimum growth between 25 to 37°C at a pH between 6.0 and 9.0. 21198 has been shown to grown on a variety of gaseous short-chain alkanes including isobutane, ethane, propane, and n-butane (Babu and Brown, 1984; Hou et al., 1983; MacMichael and Brown, 1987). Rolston estimated the growth yield for isobutane-grown 21198 to be 0.8 mg TSS per mg isobutane (Rolston, 2017). Figure 2.4 shows the results of activity-based protein profiling (ABPP) for the detection of the short chain alkane monooxygenase (SCAM) and the propane monooxygenase (PrMO) in dextrose, ethane, propane, n-butane, and isobutane-grown 21198. The expression of these enzymes is suggested to be the cause of the fortuitous transformations of CAHs and 1,4-dioxane. The expression of 59 kDa is greatest for isobutane-grown 21198, followed by ethane and butane-grown 21198. Propane-grown 21198 minimally expresses this enzyme. PrMO is only expressed by propane-grown 21198 and minimally expressed by isobutane-grown 21198.

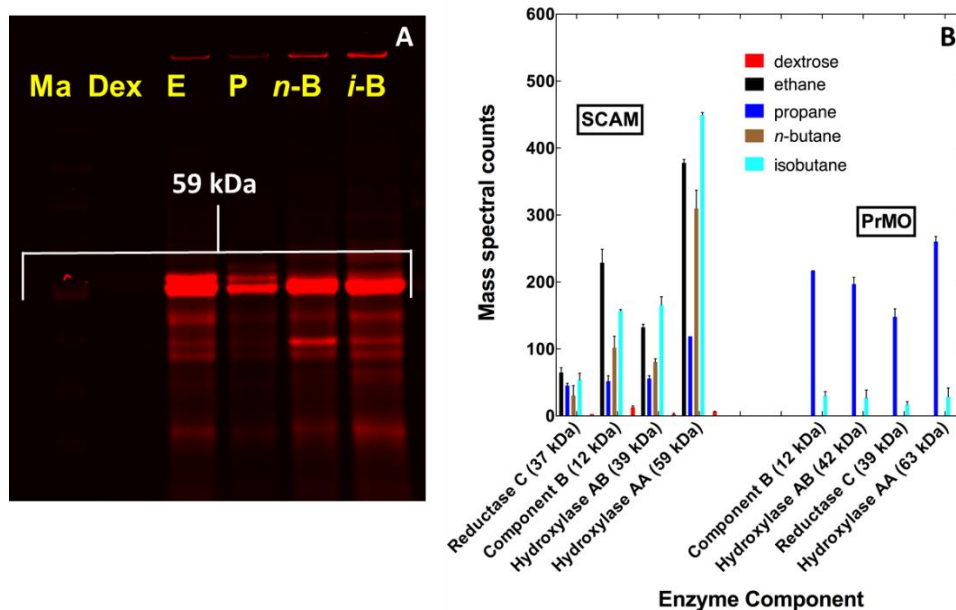


Figure 2.4. ABPP using 1,7-octadiyne as a probe for detection of SCAM in dextrose, ethane, propane, n-butane, and isobutane-grown 21198 (Hyman).

Rhodococci have been found to be capable of degrading polychlorinated biphenyls, benzene, toluene, naphthalene, 1,4-dioxane and a range of CAHs including TCE, vinyl chloride, chloroform, 1,1-DCE, and 1,1,1-TCA (van der Geize and Dijkhuizen, 2004; Mahendra and Alvarez-Cohen, 2006; Malachowsky et al., 1994). As discussed in Section 2.3.2, isobutane-grown 21198 has been found to transform 1,4-dioxane and a variety of CAHs including 1,2-DCA, 1,1-DCA, 1,1,2-TCA, 1,1,1-TCA, 1,1-DCE via cometabolism (Bennett et al., 2018; Rich, 2015; Rolston, 2017; Thankitkul, 2016).

2.5 ELW1

ELW1 was isolated from stream sediment collected from the campus of North Carolina State University by Dr. Michael Hyman of North Carolina State University (Kottegoda et al., 2015). The sample was cultured using isobutene as the singular source of carbon and energy. Results from PCR amplification and 16S rRNA sequencing were compared with the Ribosomal Database Project database. ELW1 was found to be most closely related to several strains of *Mycobacterium*, including *Mycobacterium sphagni*, *Mycobacterium* sp. Strain CP-2, and numerous strains of *Mycobacterium* with recognized hydrocarbon-oxidizing capabilities such as *Mycobacterium petroleophilum* ATCC 21497, *Mycobacterium petroleophilum* ATCC 21498, and *Mycobacterium* sp. Strain TA27.

The growth yield was estimated to be 0.38 mg (dry weight) per mg isobutene consumed. ELW1 was unable to grow on smaller branched alkanes, such as isobutane and isopentane, or any of the aromatic compounds, C₁ to C₆ n-alkanes, or C₂ to C₅ straight-chain, branched, or chlorinated alkenes tested. Various alkynes were tested to determine their capabilities for monooxygenase inhibition. Propyne and 1-butyne showed strong initial inhibition with decreased effectiveness over time. 1-octyne was an effective inhibitor during long term testing.

Previous studies emphasized the importance of cobalt or cobalamin in the metabolism of methyl tertiary butyl ether (MTBE) and tert-butyl alcohol (TBA) by MTBE and TBA-oxidizing microorganisms (Hyman, 2013). Kottegoda et al. conducted studies of ELW1 growth in both cobalt supplemented and cobalt deficient medium (Kottegoda et al., 2015). It was hypothesized that the degradation pathway of isobutene would be similar to that of MTBE and TBA and thus also exhibit a dependence on the presence of cobalt. ELW1 growth on isobutene was severely impacted by the absence of cobalt ions. These results suggest the metabolism pathway of isobutene by ELW1 involves a cobalt/cobalamin-dependent transformation of the end metabolite product.

The ability of ELW1 to transform environmental COCs has been minimally studied. As discussed in Section 2.4.6, Schrlau et al. researched the capabilities of ELW1 to cometabolize phenanthrene, a polycyclic aromatic hydrocarbon (Schrlau et al., 2017). ELW1 was found to fully transform phenanthrene. Transformation products included 1-hydroxyphenanthrene (OHPHE), 3-OHPHE, 4-OHPHE, 9-OHPHE, 1,9-OHPHE, and trans-9,10-OHPHE. Phenanthrene transformation was moderately inhibited by 1-octyne, suggesting that an alkene monooxygenase is likely the responsible transformation enzyme. Rich conducted a kinetic analysis of the aerobic degradation of chlorinated ethenes by ELW2 (Rich, 2015). ELW1 was able to cometabolize a number of CAHs. The rates of transformation were ordered as follows: vinyl chloride > c-DCE > TCE.

2.6 Naval Air Station North Island Site

The NAS North Island was commissioned in 1917 and has since been used by as a naval hub for the United States Navy (Commander, Navy Installations Command). A volatile organic compound groundwater plume was discovered in the central portion of the island in 2005 (Figure 2.5). Former sludge basins and settling ponds that were located near the NAS North Island Industrial Waste Treatment Plant were identified as the source of the plume (Aptim Federal Services, LLC, 2018). The site hydrogeology consists of approximately 41 feet of unconfined sand/silty sand underlain by a four- to five-foot thick low permeability silt deposit that acts as a semi-confining layer. The depth to groundwater resides at approximately 25 feet below ground surface (BGS). The proposed treatment zone for this project is within the saturated zone between 25 to 41 BGS. Chlorinated volatile organic compounds and 1,4-dioxane concentrations within the proposed treatment zone range from approximately 1,000 µg/L to 5,000 µg/L. Table 2.3 includes concentration details for specific CAHs and 1,4-dioxane measured in two monitoring wells (SMW-08A and SMW-10A) near the proposed treatment zone. Figure 2.6 identifies the specific locations of the groundwater monitoring wells, SMW-08A and SMW-10A, used in this study.

Table 2.3. Liquid concentrations of key CAHs and 1,4-dioxane measured at monitoring wells SMW-08A and SMW-10A in December 2016 (Battelle and Accord Engineering, Inc., 2017).

Compound	Liquid Concentration ($\mu\text{g/L}$)	
	SMW-08A	SMW-10A
PCE	2.1	12
TCE	720	1,400
1,1,1-TCA	ND	ND
1,1-DCA	46	310
1,2-DCA	1.3	16
c-DCE	37	3,200
t-DCE	1.1	4.5
1,1-DCE	510	3,100
Chloroform	3.2	9.9
Vinyl Chloride	0.75	13
1,4-dioxane	130	3,300

ND: not detected

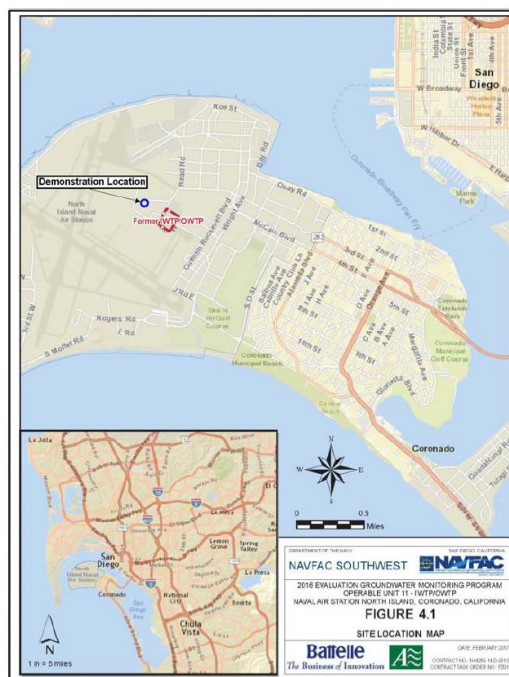


Figure 2.5. NAS North Island location map (Aptim Federal Services, LLC, 2018).

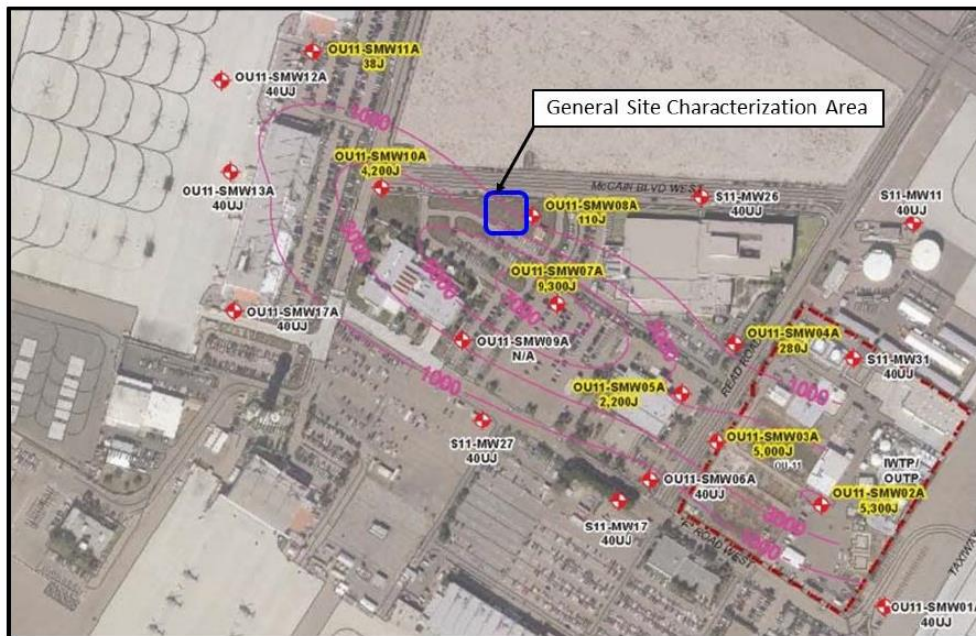


Figure 2.6. 1,4-dioxane isoconcentration contour map at NAS North Island, including monitoring well locations, from December 2015 (Aptim Federal Services, LLC, 2018).

Due to the composition of the contaminant mixture located on the NAS North Island, aerobic cometabolism has been proposed for the remediation of this site. As described in Sections 2.3.1 through 2.3.6, a variety of primary substrates have been studied for the remediation of CAHs and 1,4-dioxane via cometabolism. The implementation of a multiple primary substrate biosparging approach could be beneficial at NAS North Island due to the mixture of contaminants present. For instance, methane and/or propane could be better utilized to remediate CAHs, while isobutane could be used to transform 1,4-dioxane.

3.0 MATERIALS AND METHODS

3.1 Chemicals

All chemicals used for experimentation are listed in Table 3.1.

Table 3.1. Summary of chemical names, CAS numbers, manufactures, and purities used during experimentation.

Name	CAS No.	Manufacturer	Purity
Ethane	74-84-0	Adlrich Chemical Company	99+%
Isobutane	75-28-5	Gas Innovations	99.99%
Isobutanol	78-83-1	Mallinckrodt AR	99.9%
Isobutene	115-11-7	Aldrich	99%
Propane	74-98-6	Airgas	99%
Propyne	74-99-7	Aldrich Chemical Company	97%
1,4-Dioxane	123-91-1	Baker Analytical	100%
1,1-DCA	75-34-3	Acros	99+%
1,2-DCA	107-06-2	TCI America	>99.5% (GC)
1,1-DCE	75-34-4	Aldrich	99%
cis-DCE	156-59-2	TCI	min. 99.0%
trans-DCE	156-60-5	TCI America	98% (GC)
1,1,1-TCA	71-55-6	Baker Analytical	95.5%
TCE	79-01-6	Macron Fine Chemicals	AR/ACS

3.2 Analytical Methods

All headspace measurements were analyzed via 100 μ L headspace samples taken by Hamilton 1700 Series gas-tight syringes to be run through gas chromatographic (GC) analysis. Liquid samples for the analysis of 1,4-dioxane and/or isobutanol were extracted from microcosm bottles or rate test sample vials. Microcosm liquid samples (0.5 mL) were first run on an Eppendorf 5415C Centrifuge at 9,500 revolutions per minute (rpm) for two minutes to separate larger suspended solids. All liquid samples were filtered through 0.2 μ m polyvinylidene fluoride syringe tip filters (Phenomenex AF6-5205-12) and stored at 4°C. Liquid isobutanol samples for GC analysis were analyzed using a 25 μ L Hamilton 1700 Series gas-tight syringe.

3.2.1 1,4-Dioxane

1,4-dioxane was measured using liquid samples run on a Hewlett Packard 6890 Series GC containing a Restk 30 mx 0.2 mm Rtx-VMS capillary column and a Hewlett Packard 5973 Mass Selective Detector. The gas chromatography-mass spectrometry (GC-MS) was preceded by a Tekmar Dohrmann 3100 sample purge and trap concentrator and an AQUA Tek 70 Liquid Autosampler. Samples were diluted in 40 mL VOA vials to below 50 ppb using 25 to 40 mL of nano-pure water. An internal standard of 5 μ g/L

of deuterated 1,4-dioxane (m/z 96) was added to each sample to compare peak areas with 1,4-dioxane (m/z 88). A single ion scan was used to detect low concentrations of 1,4-dioxane. The GC-MS was calibrated by creating a standard curve of varying 1,4-dioxane (m/z 88) concentrations with a constant internal standard of 5 $\mu\text{g/L}$ deuterated 1,4-dioxane (m/z 96).

3.2.2 Chlorinated Aliphatic Hydrocarbons

Chlorinated aliphatic hydrocarbons, including TCE, 1,1-DCE, 1,2-DCA, 1,1,1-TCA, were measured using a Hewlett Packard 6890 Series GC with an electron capture detector (ECD) and an Agilent DB-624 UI 30 mx 0.53 mm capillary column. The carrier gas was helium and ran at a flow rate of either 10 or 15 mL/min, with a constant oven temperature of 50°C. Cis-DCE was measured using a Hewlett Packard 6890 Series GC with a flame ionization detector (FID) and an Agilent 30 mx 0.53 mm capillary column. The carrier gas was helium and ran at a flow rate of 15 mL/min, with a constant oven temperature of 150°C. The GC was calibrated using external standards made from saturated solutions of CAHs.

3.2.3 Alkane and Alkene Hydrocarbons

Alkane and alkene hydrocarbons, including isobutane, propane, ethane, and isobutene, were measured using a Hewlett Packard 6890 Series GC with a FID and an Agilent 30 mx 0.53 mm capillary column. The carrier gas was helium and ran at a flow rate of 15 mL/min, with a constant oven temperature of 150°C. The GC was calibrated by creating a standard curve with varying concentrations of hydrocarbons.

3.2.4 Oxygen

Oxygen (O_2) was measured using a Hewlett Packard 5890 Series II GC with a thermal conductivity detector (TCD) and a Supelco 60/80 Carboxen 1000 capillary column. The carrier gas was helium and ran at a flow rate of 30 mL/min, with a constant oven temperature of 40°C. The GC was calibrated by creating an external standard via the injection of varying volumes of air, assuming 21% O_2 in atmospheric air.

3.2.5 Carbon Dioxide

Carbon dioxide (CO_2) was measured using a Hewlett Packard 5890 Series II GC with a TCD and a Supelco 60/80 Carboxen 1000 stainless steel capillary column. The carrier gas was argon and ran at a flow rate of 30 mL/min, with a constant oven temperature of 220°C. The GC was calibrated by creating an external standard via the injection of varying volumes of 10% CO_2 .

3.2.6 Isobutanol

Isobutanol was measured using 5 μ L liquid injections on a Hewlett Packard 5890 Series II GC with a FID and a Supelco 80/100 Carbopack-C packed column (6ft x 1/8 in.). The carrier gas was nitrogen at a constant column pressure of 40 pounds per square inch, with a constant oven temperature of 105°C. Before samples were run, the oven temperature was set to 150°C for approximately 10 minutes in order to clear the column. The GC was calibrated using an external standard made from a stock solution of isobutanol.

3.2.7 Biomass

Biomass was quantified using total suspended solids (TSS) analysis. A 0.45 μ m mixed cellulose ester membrane (Advantec A045A047A) and a glass filtration apparatus were used to filter 0.5 or 0.8 mL of concentrated cell solution. The membrane was then placed into a 103°C drying oven for 15 minutes to obtain the dry weight of cells present in the cell solution.

3.2.8 Calculations

The total masses (M_T) of CAHs were calculated assuming equilibrium between liquid and gas phase partitioning. The dimensionless Henry's constant (H_{cc}) was evaluated using Equation 1 and specifies the ratio of the gas concentration (C_g) to the liquid concentration (C_l). The total mass was calculated using Equation 2, where V_l is the liquid volume of the reactor, and V_g is the gas volume of the reactor. The Henry's constants used for experimentation are reported in Table 3.2.

$$H_{cc} = \frac{C_g}{C_l} \quad (1)$$

$$M_T = (C_l \cdot V_l) + (C_g \cdot V_g) \quad (2)$$

Table 3.2. Henry's constants for select CAHs used during experimentation (Mackay and Shiu, 1981).

Compound	Henry's constant @ 20°C (dimensionless)
TCE	0.296
c-DCE	0.122
1,1-DCE	0.857
1,1,1-TCA	0.548
1,2-DCA	0.179

Zero order degradation rates (r) were calculated by taking the slope of the first three to four points on a plot of the total mass of a compound per initial quantity of biomass (X_0 , in mg TSS) over time (t), as shown in Equation 3.

$$r = \frac{M_T/X_0}{t} \quad (3)$$

The transformation capacity (T_c) of a compound was calculated using Equation 4, where M_i is the initial total mass (μmol) and M_f is the final total mass (μmol). Compounds that exhibited higher transformation capacities required multiple additions of the CAH of interest over time until the biomass was exhausted and transformation was no longer observed.

$$T_c = \frac{\sum M_i - M_f}{X_0} \quad (4)$$

3.3 Pure Culture Studies

3.3.1 Inoculation

Autoclaved 720 mL glass Wheaton bottles containing 300 mL of autoclaved media solution (1X MV media - recipe shown in Appendix A) were used to grow 21198 and ELW1 in batch pure cultures. Both 21198 and ELW1 were obtained from Michael Hyman at North Carolina State University. 21198 and ELW1 were incubated on minimal salts media growth plates (recipe shown in Appendix B) at 30°C in 3.5 L canisters with 1-2% v/v isobutane/air and isobutene/air, respectively. All work with pure cultures was performed under a laminar flow hood to prevent contamination. A colony of 21198 or ELW1 were aseptically removed from a media plate to inoculate the growth reactor bottles. The bottles were then sealed with autoclaved butyl septa and plastic caps, injected with the primary growth substrate of choice, and stored at 30°C on a shaker table at 200 rpm until significant growth was observed (Table 3.3). The specified volume of primary growth substrate was chosen to keep the levels above the upper explosive limit (UEL).

Table 3.3. Required volume of primary growth substrate and the typical number of days of incubation prior to refreshing.

	21198			ELW1
	Isobutane	Propane	Ethane	Isobutene
Volume of Gas Added (mL)	45	45	60	50
Days of Incubation Before Refreshing	4-5	5-6	6-10	6-7

After significant growth was observed, the bottles were opened for approximately 15 minutes in a laminar flow hood to allow for oxygen replenishment, and the required volume of primary growth substrate was re-injected into the headspace. The bottles were returned to the shaker table for an additional 24 hours of growth time to allow the cells to reach late exponential growth phase. At the time of refreshing, heterotrophic growth plates (recipe shown in Appendix B) were streaked with cell solution to determine the purity of the culture prior to use.

3.3.2 Harvesting

The growth reactor cell solution was centrifuged in 50 mL centrifuge tubes using a Beckman Coulter Allegra 21 Centrifuge for 15 minutes at 4,000 relative centrifugal force (RCF) in order to concentrate the cells. The cells were then rinsed in the centrifuge for 15 minutes at 4,000 RCF with 50 mmol/L monosodium phosphate buffer (pH 7). The cells were then resuspended in five to ten mL of buffer to reach the desired biomass concentration (between 7 and 20 mg TSS/L) and stored at 4°C prior to use. The cells were typically stored for no longer than one to two days prior to experimental use.

3.3.3 Rate Test Experimental Design

10 mL of 1X MV media were added to autoclaved 27 mL glass vials. The vials were sealed with autoclaved butyl rubber septa and metal crimp tops. Typical tests were comprised of four vials, including one with 2 mL of acetylene or propyne added to the headspace to act as a monooxygenase blocker, one without cells (abiotic), and two duplicate 'active' vials. Based on the results of the TSS test, the required volume of concentrated cell solution was calculated in order to obtain a desired cell mass. Between 4 and 14 mg of TSS were added to the active and acetylene or propyne control vials. The acetylene or propyne was allowed to interact with the cells for approximately one hour prior to adding the contaminant interest to ensure the monooxygenase enzymes were effectively blocked. CAHs were added to the vials via injection of a saturated solution of the compound of interest. 1,4-dioxane was added to the vials via injection of a 1,000 mg/L stock solution. CAHs were added to the vials and allowed to equilibrate on a shaker table at 200 rpm for approximately 15 minutes prior to initial

headspace measurements on the GC-ECD. The cells were added to the active bottles after equilibration of the CAHs had been achieved.

Table 3.4 provides a summary of rate test experimental design parameters for single-compound tests. Table 3.5 provides a summary of rate test experimental design parameters for mixture tests. The tables describe the compound tested, the growth substrate and culture used, the volume of compound added, the initial liquid concentration of the compound, the mass of TSS added, and the resulting biomass concentration. Tests were performed at different biomass concentrations depending on the anticipated rate of contaminant transformation.

Table 3.4. Summary of rate test experimental design parameters, including the volume of solution added, initial liquid concentration, mass of TSS, and biomass concentration for single-compound tests.

Compound	Growth Substrate/ Culture	Volume of Soln. Added (μL)	Initial Liq. Conc. ($\mu\text{mol/L}$)		Mass of TSS Added (mg)	Biomass Conc. (mg/L)
			Avg.	SD		
1,4-D	Isobutane-grown 21198	175 μL of 1,000 ppm stock	168	24.2	5.0	~ 500
	Ethane-grown 21198		244	16.7	5.0	467
	Propane-grown 21198		235	10.4	5.0	467
	Isobutene-grown ELW1		176	1.1	5.1	496
TCE	Isobutane-grown 21198	10	10.2	0.5	12.9	1,212
	Ethane-grown 21198		10.3	0.6	11.8	1,050
	Propane-grown 21198		12.7	0.5	12.8	1,146
	Isobutene-grown ELW1		9.3	0.2	13.0	1,200
1,1-DCE	Isobutane-grown 21198	20	24.4	0.8	4.0	393
		60	69.8	1.4		
	Ethane-grown 21198	20	25.3	0.1	3.9	391
		60	70.3	2.4		
	Propane-grown 21198	20	27.3	0.6	4.2	405
		60	71.8	0.8		
Isobutene-grown ELW1	20	27.2	0.6	4.0	389	
	60	76.3	2.0			
c-DCE	Isobutane-grown 21198	80	292	1.1	11.8	1,073
	Ethane-grown 21198		293	7.2	10.8	982
	Propane-grown 21198		269	4.6	9.5	881
1,2-DCA	Isobutane-grown 21198	40	242	0.5	11.8	1,073
	Ethane-grown 21198		241	3.7	12.8	1,193
	Propane-grown 21198		237	4.8	12.9	1,173
1,1,1-TCA	Isobutane-grown 21198	100	39.1	1.2	13.1	1,197
	Ethane-grown 21198		41.0	0.2	12.8	1,193
	Propane-grown 21198		38.9	1.7	13.1	1,179

Table 3.5. Summary of rate test experimental design parameters, including the volume of solution added, initial liquid concentration, mass of TSS, and biomass concentration for mixture tests.

Growth Substrate/ Culture	Compound	Volume of Soln. Added (μL)	Initial Liq. Conc. ($\mu\text{mol/L}$)		Mass of TSS Added (mg)	Biomass Conc. (mg/L)
			Avg.	SD		
Isobutane-grown 21198	1,4-D	50 μL 1,000 ppm stock	51.4	0.2	5.0	476
	TCE	5	4.71	0.14		
	1,1-DCE	5	2.98	0.13		
	1,1,1-TCA	5*	0.51	0.027		
	1,2-DCA	5	8.78	0.57		
Ethane-grown 21198	1,4-D	50 μL 1,000 ppm stock	66.1	0.8	5.1	487
	TCE	5	4.27	0.05		
	1,1-DCE	5	2.77	0.05		
	1,1,1-TCA	5	4.71	0.04		
	1,2-DCA	5	5.77	0.02		
Propane-grown 21198	1,4-D	50 μL 1,000 ppm stock	49.7	1.0	5.0	478
	TCE	5	4.59	0.16		
	1,1-DCE	5	2.79	0.05		
	1,1,1-TCA	5*	0.014	0.001		
	1,2-DCA	5	8.25	0.03		
Isobutene-grown ELW1	1,4-D	50 μL 1,000 ppm stock	60.3	7.7	4.9	484
	TCE	5	4.17	0.003		
	1,1-DCE	5	2.58	0.10		
	1,1,1-TCA	5	5.21	0.29		
	1,2-DCA	5	6.18	0.07		
Isobutene-grown ELW1	1,4-D	50 μL 1,000 ppm stock	71.8	4.3	5.5	536
	TCE	5	4.74	0.02		
	1,1-DCE	5	3.56	0.02		
	1,1,1-TCA	5	6.58	0.10		
	1,2-DCA	5	6.98	0.16		
	Isobutene	~1000	258	0.2		

*Likely less than 5 μL added to solution; inaccurate syringe needle

3.4 Microcosm Studies

Groundwater used for microcosm construction was obtained from monitoring wells SMW-08A and SMW-10A located on the NAS North Island in San Diego, California. The groundwater was stored at 4°C in one liter plastic bottles. Aquifer cores were not available for experimentation; therefore, groundwater sampling was conducted to include trace amounts of aquifer sediments. The minor amount of aquifer solids present in the groundwater appeared to consist of sand and silt. Analyses for particle size, nutrient content, and organic matter were not conducted. Groundwater was shaken to

suspend the aquifer solids, and 50 mL were measured into autoclaved 155 mL glass Wheaton bottles (Figure 3.1). The bottles were sealed with autoclaved butyl septa and plastic caps, and the caps were wrapped with parafilm. All microcosms were incubated at 20°C on a 200 rpm shaker table.

Table 3.6 shows a summary of the days of the experiment additions or amendments were made to each microcosm. Seven sets of microcosms were operated and will be further described in the following sections. Sets 1 through 4 utilized isobutane as a primary growth substrate and incorporated experimentation with nitrogen sparging to remove CAHs and with bioaugmentation with isobutane-grown 21198. Sets 5 and 7 examined the use of isobutanol as a primary growth substrate. As shown in Figure 2.3, isobutanol is the product of isobutane transformation by SCAM. The purpose of this approach was to determine if isobutane-utilizers could be stimulated in the presence of isobutane and CAHs via the direct addition of the isobutane metabolite, isobutanol. Set 6 explored the use of isobutene as a primary growth substrate and incorporated bioaugmentation with isobutene-grown ELW1. Each microcosm set is further described in Sections 3.4.1 through 3.4.7.

Microcosms were analyzed for oxygen content prior to re-spikes of primary substrate and COCs. Pure oxygen was added to the headspace if oxygen content was low (less than $\sim 3,000$ $\mu\text{mol/L}$ gas concentration). Microcosms received nutrients via the addition of 200 μL of 1X MV media. This quantity of media corresponds to a concentration of approximately 620 $\mu\text{mol N/L}$ and 240 $\mu\text{mol P/L}$. Monooxygenase inhibitors acetylene (for isobutane microcosms) or propyne (for isobutene microcosms) were added to control microcosms at 2% headspace concentration.

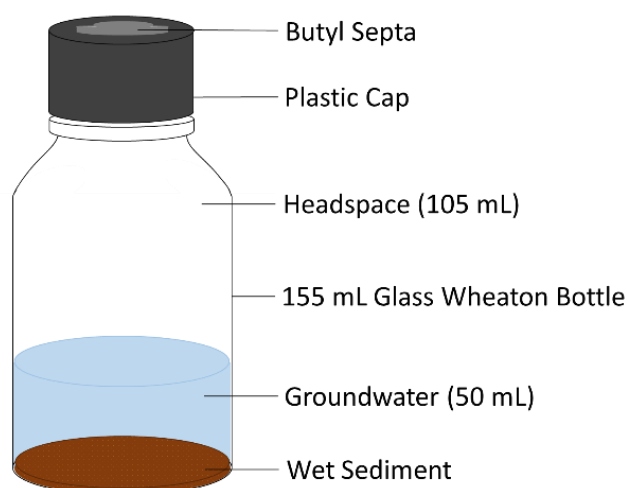


Figure 3.1. *Microcosm schematic diagram.*

Table 3.6. Summary of days of the experiment additions or amendments were made to each microcosm.

	MW ¹	Sparged ²	Media ³	Isobutane ⁴	Isobutene ⁵	Isobutanol ⁶	Acetylene ⁷	Propyne ⁸	21198 Bioaug. ⁹	ELW1 Bioaug. ¹⁰
Set 1 - Native Groundwater and Isobutane										
B 1/2	SMW-08A	--	--	0	--	--	--	--	--	--
B 3/4	SMW-08A	--	0	0	--	--	--	--	--	--
B 5/6	SMW-08A	--	0	0	--	--	0	--	--	--
B 7/8	SMW-08A	--	--	--	--	--	--	--	--	--
Set 2 - Sparged Groundwater and Isobutane										
B 1	SMW-08A	0	24	0	--	--	--	--	--	--
B 2	SMW-08A	0	24	0,32	--	--	--	--	--	--
B 3	SMW-08A	0	0,65	0,19,20,25,33, 40,47,61,82	--	--	--	--	--	--
B 4	SMW-08A	0	0,65	0,19,20,25,33, 40,47,61,82	--	--	--	--	--	--
B 5/6	SMW-08A	0	0	0	--	--	0	--	--	--
Set 3 - Bioaugmentation with 0.5 mg of Isobutane-Grown 21198										
B 1	SMW-08A	--	0,58	0,5,12,13,14, 26,33,40,54,75	--	--	--	--	0	--
B 2	SMW-08A	--	0,58	0,12,14,18,26, 33,40,54,75	--	--	--	--	0	--
B 3/4	SMW-08A	--	0	0	--	--	0	--	0	--
Set 4 - Bioaugmentation with 0.7 mg of Isobutane-Grown 21198										
B 1	SMW-08A	--	0,53	0,7,9,21,28, 35,49,70	--	--	--	--	0	--
B 2	SMW-08A	--	0,53	0,7,9,21,28, 35,49,70,103	--	--	--	--	0	--
B 3/4	SMW-08A	--	0	0	--	--	0	--	0	--
Set 5 - Isobutane Data Confirmation and Isobutanol Experimentation										
B 1/2	SMW-08A	--	0	0	--	--	--	--	--	--
B 3	SMW-08A	23,51	0	0*,23,51, 76	--	--	--	--	--	--
B 4	SMW-08A	23,51	0	0*,23,51	--	--	--	--	--	--
B 5/6	SMW-08A	--	0	0	--	23,43,55, 58,63, 70	--	--	--	--
B 7/8	SMW-08A	--	0	0	--	--	0	--	--	--
B 9/10	SMW-10A	--	0	0	--	--	--	--	--	--
Set 6 - Native Groundwater with Isobutene										
B 1	SMW-08A	--	0	--	0, 67, 74, 83	--	--	--	--	--
B 2	SMW-08A	--	0	--	0	--	--	--	--	--
B 3/4	SMW-08A	25,29	0	--	0,25,29	--	--	--	--	--
B 5/6	SMW-08A	--	0	--	0,40, 67	--	--	--	--	33
B 7/8	SMW-08A	--	0	--	0	--	0	20	--	--
Set 7 - Sparged Groundwater with Isobutane/Isobutene and Isobutanol Experimentation										
B 1/2	SMW-08A	0	0	0	--	--	--	--	--	--
B 3/4	SMW-08A	0	0	--	0	--	--	--	--	--
B 5-8	SMW-08A	--	0	17	--	0,10,12, 30, 37, 39	--	--	--	--

Notes:

1. Indicates the monitoring well from which groundwater was used
 2. Indicates the day of experiment that groundwater was sparged with nitrogen
 3. Indicates the day of experiment that 0.2 mL of 1X MV media was added to the microcosm
 4. Indicates the day of experiment that 1.26 mL of isobutane was added to the microcosm
 5. Indicates the day of experiment that 1.26 mL of isobutene was added to the microcosm
 6. Indicates the day of experiment that 0.3 mL of 8,333.3 ppm isobutanol was added to the microcosm
 7. Indicates the day of experiment that 2.1 mL of acetylene were added to the microcosm
 8. Indicates the day of experiment that 2.1 mL of propyne were added to the microcosm
 9. Indicates the day of experiment that the microcosm was bioaugmented with 0.5 mg (set 3) or 0.7 mg (set 4) of 21198
 10. Indicates the day of experiment that the microcosm was bioaugmented with 0.9 g of ELW1
- : not applicable for the listed microcosm
* : 15 mL of isobutane were added added to the microcosm

3.4.1 Set 1: Native groundwater, isobutane

Table 3.7 indicates the initial liquid concentrations of isobutane, 1,1-DCE, TCE, and 1,4-D in bottles 1 through 8 in microcosm set 1. The initial liquid concentration of 1,1-DCE is variable for each bottle due to the volatilization of 1,1-DCE during the open-system transfer of groundwater from the plastic 1 L storage bottle to the microcosm bottles. Media addition was omitted from bottles 1 and 2 to determine if nutrients were required for the system.

Table 3.7. Initial liquid concentrations and total masses of isobutane, 1,1-DCE, TCE, and 1,4-Dioxane in set 1, bottles 1 through 8.

Bottle #	Isobutane		1,1-DCE		TCE		1,4-Dioxane	
	Initial Liq. Conc. (ug/L)	Total Mass (μmol)	Initial Liq. Conc. (ug/L)	Total Mass (μmol)	Initial Liq. Conc. (ug/L)	Total Mass (μmol)	Initial Liq. Conc. (ug/L)	Total Mass (μmol)
1	563	51	93	0.13	292	0.18	190	0.11
2	575	52	222	0.32	451	0.28	177	0.10
3	539	49	220	0.32	417	0.26	161	0.09
4	578	52	137	0.20	380	0.23	275	0.16
5	537	48	148	0.21	365	0.23	301	0.17
6	567	51	76	0.11	315	0.19	247	0.14
7	0	0	202	0.29	398	0.25	295	0.17
8	0	0	68	0.10	295	0.18	173	0.10

3.4.2 Set 2: Sparged groundwater, isobutane

In order to determine if native isobutane-utilizers could be stimulated in the absence of CAHs, groundwater was sparged with nitrogen to remove CAHs from solution. Table 3.8 indicates the initial liquid concentrations of isobutane, 1,1-DCE, TCE, and 1,4-D in bottles 1 through 6 in microcosm set 2. Media addition was initially omitted from bottles 1 and 2 to determine if nutrients were required for the system. Media was later added to bottles 1 and 2 on day 24 of incubation. On day 25, TCE was reintroduced to bottles 3 through 6 to a liquid concentration of approximately 300 μg/L after three to four additions of isobutane to bottles 3 and 4. 1,4-dioxane was also added at a concentration of approximately 3,500 μg/L on day 25. On day 33, 1,1-DCE was reintroduced to bottles 3 through 6 to a liquid concentration of approximately 150 μg/L. The concentration of TCE was gradually increased over five subsequent additions, culminating in a liquid concentration of approximately 4.5 mg/L.

Table 3.8. Initial liquid concentrations and total masses of isobutane, 1,1-DCE, TCE, and 1,4-Dioxane in set 2, bottles 1 through 6.

Bottle #	Isobutane		1,1-DCE		TCE		1,4-Dioxane	
	Initial Liq.	Total Mass	Initial Liq.	Total Mass	Initial Liq.	Total Mass	Initial Liq.	Total Mass
	Conc. (ug/L)	(μ mol)	Conc. (ug/L)	(μ mol)	Conc. (ug/L)	(μ mol)	Conc. (ug/L)	(μ mol)
1	572	51	0	0	0.9	0.001	137	0.08
2	589	53	0	0	2.6	0.002	105	0.06
3	559	50	0	0	1.1	0.001	111	0.06
4	538	48	0	0	1.3	0.001	116	0.07
5	570	51	0	0	1.4	0.001	114	0.06
6	551	50	0	0	1.8	0.001	129	0.07

3.4.3 Set 3: Bioaugmentation with 0.5 mg isobutane-grown 21198

Table 3.9 indicates the initial liquid concentrations of isobutane, 1,1-DCE, TCE, and 1,4-D in bottles 1 through 4 in microcosm set 3. Media was added to all bottles to supply nutrients. 0.5 mg of isobutane-grown 21198 (cultured as described in Sections 3.3.1 and 3.3.2) was added to all bottles. Five to six additions of isobutane were made to bottles 1 and 2 over the first 18 days of incubation. The concentration of TCE was gradually increased over the course of 75 days with five subsequent additions, culminating in a liquid concentration of approximately 4.5 mg/L. On day 18, 0.2 mL of 1,000 mg/L 1,4-dioxane was added to bottles 1 through 4, for an initial liquid concentration of 3,000 to 4,000 μ g/L. The concentrations of 1,1-DCE and 1,4-dioxane were kept constant with subsequent re-spikes.

Table 3.9. Initial liquid concentrations and total masses of isobutane, 1,1-DCE, TCE, and 1,4-Dioxane in set 3, bottles 1 through 4.

Bottle #	Isobutane		1,1-DCE		TCE		1,4-Dioxane	
	Initial Liq.	Total Mass	Initial Liq.	Total Mass	Initial Liq.	Total Mass	Initial Liq.	Total Mass
	Conc. (μ g/L)	(μ mol)	Conc. (μ g/L)	(μ mol)	Conc. (μ g/L)	(μ mol)	Conc. (μ g/L)	(μ mol)
1	595	54	145	0.21	265	0.16	113	0.06
2	608	55	176	0.25	300	0.19	138	0.08
3	600	54	191	0.28	293	0.18	115	0.07
4	604	54	235	0.34	329	0.20	119	0.07

3.4.4 Set 4: Bioaugmentation with 0.7 mg isobutane-grown 21198

Table 3.10 indicates the initial liquid concentrations of isobutane, 1,1-DCE, TCE, and 1,4-D in bottles 1 through 4 in microcosm set 3. Media was added to all bottles to supply nutrients. 0.7 mg of isobutane-grown 21198 (cultured as described in Sections 3.3.1 and 3.3.2) was added to all bottles. Four additions of isobutane were made to bottles 1 and 2 over the first 20 days of incubation. The concentration of 1,1-DCE was gradually increased over the course of 103 days with four subsequent additions to bottle 1 and five additions to bottle 2, culminating in a liquid concentration of approximately 1530 μ g/L and 830 μ g/L, respectively. On day 21, 0.2 mL of 1,000 mg/L 1,4-dioxane was added to bottles 1 through 4, for an initial liquid concentration of 3,000 to 4,000 μ g/L. The concentration of 1,4-dioxane were kept

constant with subsequent re-spikes. The concentration of TCE in bottles 1 and 2 was increased from approximately 230 $\mu\text{g/L}$ to approximately on day 950 $\mu\text{g/L}$ on day 35.

Table 3.10. Initial liquid concentrations and total masses of isobutane, 1,1-DCE, TCE, and 1,4-Dioxane in set 4, bottles 1 through 4.

Bottle #	Isobutane		1,1-DCE		TCE		1,4-Dioxane	
	Initial Liq. Conc. ($\mu\text{g/L}$)	Total Mass (μmol)	Initial Liq. Conc. ($\mu\text{g/L}$)	Total Mass (μmol)	Initial Liq. Conc. ($\mu\text{g/L}$)	Total Mass (μmol)	Initial Liq. Conc. ($\mu\text{g/L}$)	Total Mass (μmol)
1	613	55	66	0.10	228	0.14	132	0.07
2	622	56	76	0.11	228	0.14	115	0.07
3	592	53	81	0.12	233	0.14	87	0.05
4	619	56	110	0.16	276	0.17	134	0.08

3.4.5 Set 5: Isobutane data confirmation and isobutanol experimentation

The microcosms in set 5 were established to confirm the results from sets 1 and 2, as well as study the addition of isobutanol as a primary growth substrate. As shown in Figure 2.3, isobutanol is the product of isobutane transformation by SCAM. The purpose of this approach was to determine if isobutane-utilizers could be stimulated in the presence of isobutane and CAHs via the direct addition of the isobutane metabolite, isobutanol.

Table 3.11 indicates the initial liquid concentrations of isobutane, 1,1-DCE, TCE, and 1,4-D in bottles 1 through 10 in microcosm set 5. Media was added to all bottles to supply nutrients. 0.2 mL of 1,000 mg/L 1,4-dioxane was also added to bottles 1 through 8, for an initial liquid concentration of 3,000 to 4,000 $\mu\text{g/L}$. Bottles 3 and 4 were sparged with nitrogen on day 23 to remove CAHs and again on day 51 to further remove CAHs that had desorbed back into solution. Isobutane was re-added to the headspace of bottles 3 and 4 following the sparging events. Isobutanol was added to bottles 5 and 6 on day 23 at an initial liquid concentration of approximately 45 mg/L. Five additional re-spikes of isobutanol were added to these bottles between days 43 and 70. Oxygen and carbon dioxide were subsequently monitored in these bottles.

Table 3.11. Initial liquid concentrations and total masses of isobutane, 1,1-DCE, TCE, and 1,4-Dioxane in set 5, bottles 1 through 10.

Bottle #	Isobutane		1,1-DCE		TCE		1,4-Dioxane	
	Initial Liq. Conc. (µg/L)	Total Mass (µmol)	Initial Liq. Conc. (µg/L)	Total Mass (µmol)	Initial Liq. Conc. (µg/L)	Total Mass (µmol)	Initial Liq. Conc. (µg/L)	Total Mass (µmol)
1	580	59	160	0.23	319	0.17	3,282	1.86
2	616	63	151	0.21	333	0.18	3,648	2.07
3	6,609	686	163	0.23	346	0.19	3,764	2.14
4	6,724	689	149	0.21	337	0.18	3,706	2.10
5	590	60	150	0.21	364	0.20	3,900	2.21
6	619	63	180	0.26	346	0.19	3,423	1.94
7	624	64	145	0.21	322	0.17	3,523	2.00
8	610	62	155	0.22	332	0.18	3,352	1.90
9	598	61	385	0.55	338	0.18	2,495	1.42
10	642	66	429	0.61	326	0.18	2,339	1.33

3.4.6 Set 6: Native groundwater with isobutene

The microcosms in set 6 were established to determine if native isobutene-utilizers could be stimulated in the presence of CAHs and to evaluate the use of bioaugmentation with isobutene-grown ELW1

Table 3.12 indicates the initial liquid concentrations of isobutene, 1,1-DCE, TCE, and 1,4-D in bottles 1 through 8 in microcosm set 6. Media was added to all bottles to supply nutrients. 0.2 mL of 1,000 mg/L 1,4-dioxane was also added to bottles 1 through 8, for an initial liquid concentration of 3,000 to 4,000 µg/L. Bottles 3 and 4 were sparged with nitrogen on day 25 to remove CAHs and again on day 29 to further remove CAHs that had desorbed back into solution. Isobutene was re-added to the headspace of bottles 3 and 4 following the sparging events. 0.9 mg of isobutene-grown ELW1 (cultured as described in Sections 3.3.1 and 3.3.2) was added to bottles 5 and 6 on day 33 of incubation. On day 40, bottles 5 and 6 were re-spiked with isobutene, TCE, and 1,1-DCE to liquid concentrations of approximately 3,100 µg/L, 530 µg/L and 270 µg/L, respectively.

Table 3.12. Initial liquid concentrations and total masses of isobutane, 1,1-DCE, TCE, and 1,4-Dioxane in set 6, bottles 1 through 8.

Bottle #	Isobutene		1,1-DCE		TCE		1,4-Dioxane	
	Initial Liq. Conc. ($\mu\text{g/L}$)	Total Mass (μmol)	Initial Liq. Conc. ($\mu\text{g/L}$)	Total Mass (μmol)	Initial Liq. Conc. ($\mu\text{g/L}$)	Total Mass (μmol)	Initial Liq. Conc. ($\mu\text{g/L}$)	Total Mass (μmol)
1	2,905	50	225	0.33	373	0.23	3,469	1.97
2	3,025	52	234	0.34	347	0.21	3,229	1.83
3	2,987	51	240	0.35	381	0.23	3,596	2.04
4	3,021	52	205	0.30	404	0.25	3,432	1.95
5	3,174	54	224	0.32	390	0.24	3,433	1.95
6	3,109	53	222	0.32	396	0.24	3,423	1.94
7	2,979	51	218	0.32	395	0.24	3,770	2.14
8	3,101	53	228	0.33	393	0.24	3,460	1.96

3.4.7 Set 7: Sparged groundwater with isobutane/isobutene and isobutanol experimentation

The microcosms in set 7 were established to confirm the results from sets 2 and 5. As shown in Figure 2.3, isobutanol is the product of isobutane transformation by SCAM. The purpose of this approach was to determine if isobutane-utilizers could be stimulated in the initial absence of isobutane and in the presence of CAHs via the direct addition of the isobutane metabolite, isobutanol.

Table 3.13 indicates the initial liquid concentrations of isobutane, 1,1-DCE, TCE, and 1,4-D in bottles 1 through 8 in microcosm set 7. Media was added to all bottles to supply nutrients. Isobutane was added to the headspaces of bottles 1 and 2 at an initial liquid concentration of approximately 580 $\mu\text{g/L}$, and isobutene was added to headspaces of bottles 3 and 4 at an initial liquid concentration of approximately 2,800 $\mu\text{g/L}$. Isobutanol was added to bottles 5 through 8 at an initial liquid concentration of approximately 45 mg/L . 0.2 mL of 1,000 mg/L 1,4-dioxane was also added to bottles 5 through 8, for an initial liquid concentration of 3,000 to 4,000 $\mu\text{g/L}$. Two subsequent additions of approximately 45 mg/L isobutanol were added to bottles 5 through 8 on days 10 and 13 before isobutane was added to the headspace on day 17 at an initial liquid concentration of approximately 600 $\mu\text{g/L}$. Three additional re-spikes of isobutanol were added to these bottles between days 30 and 45. Oxygen and carbon dioxide were subsequently monitored in these bottles.

Table 3.13. Initial liquid concentrations of isobutane, 1,1-DCE, TCE, and 1,4-Dioxane in set 7, bottles 1 through 8.

Bottle #	Isobutane		Isobutene		1,1-DCE		TCE		1,4-Dioxane	
	Initial Liq. Conc. (µg/L)	Total Mass (µmol)	Initial Liq. Conc. (µg/L)	Total Mass (µmol)	Initial Liq. Conc. (µg/L)	Total Mass (µmol)	Initial Liq. Conc. (µg/L)	Total Mass (µmol)	Initial Liq. Conc. (µg/L)	Total Mass (µmol)
1	580	52	0	0	0	0	3.1	0.002	278	0.16
2	587	53	0	0	0	0	0.9	0.001	303	0.17
3	0	0	2,867	49	0	0	0.7	0.000	213	0.12
4	0	0	2,913	50	0	0	0.7	0.000	264	0.15
5	0	0	0	0	175	0.25	384	0.24	3,000-4,000	1.7-2.2
6	0	0	0	0	196	0.28	432	0.27	3,000-4,000	1.7-2.2
7	0	0	0	0	208	0.30	404	0.25	3,000-4,000	1.7-2.2
8	0	0	0	0	188	0.27	400	0.25	3,000-4,000	1.7-2.2

4.0 RESULTS AND DISCUSSION

4.1 Pure Culture Studies

Resting cell rate tests were performed with isobutane, ethane, and propane-grown 21198 and isobutene-grown ELW1 in order to identify potential effective primary substrates to promote the cometabolic transformation of COCs. As previously shown in Figure 2.4, the relative quantity of monooxygenase expression of 21198 has been found to vary based on the primary growth substrate. The results indicate that the isobutane-grown 21198 produces the greatest quantity of SCAM expression, followed by ethane and then propane-grown 21198. It was hypothesized that isobutane-grown 21198 would demonstrate the most effective transformation of COCs (i.e. fastest zero order degradation rate and highest transformation capacity), followed by ethane and then propane-grown 21198. As noted in section 2.5, minimal studies have been conducted to investigate the abilities of isobutene-grown ELW1 to cometabolize CAHs and 1,4-dioxane. ELW1 was employed in this study as a model isobutene-utilizer to determine its potential effectiveness for CAH and 1,4-dioxane cometabolism.

Resting cell rate tests included single-compound analyses for TCE, 1,1,1-TCA, 1,1-DCE, c-DCE, 1,2-DCA, and 1,4-dioxane as well as mixtures of the afore listed COCs. The results from these experiments are presented in Sections 4.1.1 to 4.1.5. Data plots for all conducted rate tests are included in Appendix C.

4.1.1 Isobutane-grown 21198

Figure 4.1 depicts the results from a typical rate test, showing the total mass of 1,1-DCE per mg TSS over time for isobutane-grown 21198. The transformation of 1,1-DCE occurs rapidly. The degradation rate moderately changes between high and low initial 1,1-DCE concentrations ($30.5 \pm 4.4 \mu\text{mol/mg TSS/d}$ at an initial concentration of approximately $25 \mu\text{mol/L}$ versus $39.3 \pm 5.8 \mu\text{mol/mg TSS/d}$ at an initial concentration of approximately $70 \mu\text{mol/L}$). The transformation capacity for 1,1-DCE was determined to be $0.66 \mu\text{mol/mg TSS}$ at a high initial concentration and $0.51 \mu\text{mol/mg TSS}$ at a low initial concentration. Acetylene actively blocked the degradation of all COCs tested, suggesting monooxygenase enzymes are involved in the transformations of these compounds.

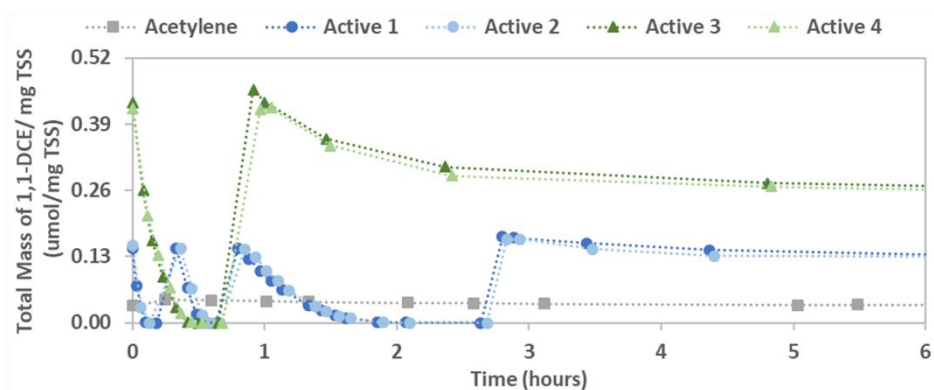


Figure 4.1. Total mass of 1,1-DCE per mg TSS over time for isobutane-grown 21198. Approximately 4 mg of cells were used for experimentation.

As shown in Figure 4.2, the zero order degradation rates of CAHs and 1,4-dioxane by isobutane-grown 21198 were ordered in the following rank: 1,1-DCE > 1,2-DCA > 1,4-dioxane > c-DCE > 1,1,1-TCA > and TCE. These results are consistent with the findings of Thankitkul (Thankitkul, 2016). These results are also fairly similar to those of Kim et al. in that more chlorinated compounds (TCE and 1,1,1-TCA) exhibited slower rates of transformation than less chlorinated compounds (1,1-DCE, c-DCE, and 1,2-DCA) in a butane-grown mixed culture (Kim et al., 2000).

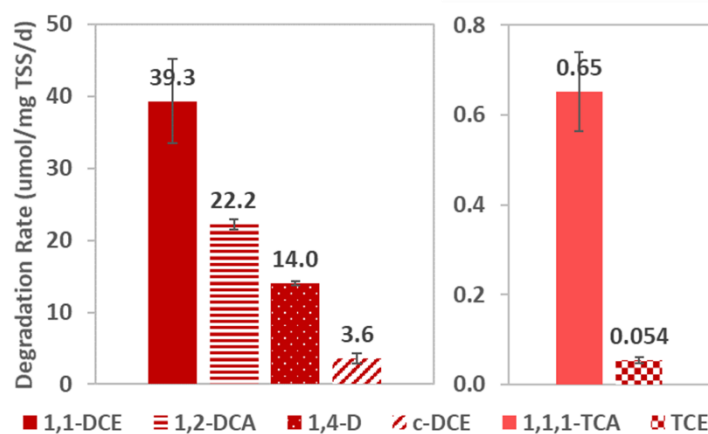


Figure 4.2. Comparison of zero order degradation rates of 1,1-DCE, 1,2-DCA, 1,4-dioxane, c-DCE, 1,1,1-TCA, and TCE for isobutane-grown 21198. Error bars indicate the standard deviation of a two sample average.

4.1.2 Ethane-grown 21198

Figure 4.3 depicts the results from a typical rate test, showing the total mass of 1,1-DCE per mg TSS over time for ethane-grown 21198. The transformation of 1,1-DCE occurs rapidly. The degradation rate is similar between high and low initial 1,1-DCE concentrations ($25.2 \pm 0.3 \mu\text{mol/mg TSS/d}$ at an initial concentration of approximately $25 \mu\text{mol/L}$ versus $26.7 \pm 0.7 \mu\text{mol/mg TSS/d}$ at an initial concentration of approximately $70 \mu\text{mol/L}$). The transformation capacity for 1,1-DCE was determined to be 0.78

$\mu\text{mol}/\text{mg TSS}$ at a high initial concentration and $0.58 \mu\text{mol}/\text{mg TSS}$ at a low initial concentration. Acetylene actively blocked the degradation of all COCs tested, suggesting monooxygenase enzymes are involved in the transformations of these compounds.

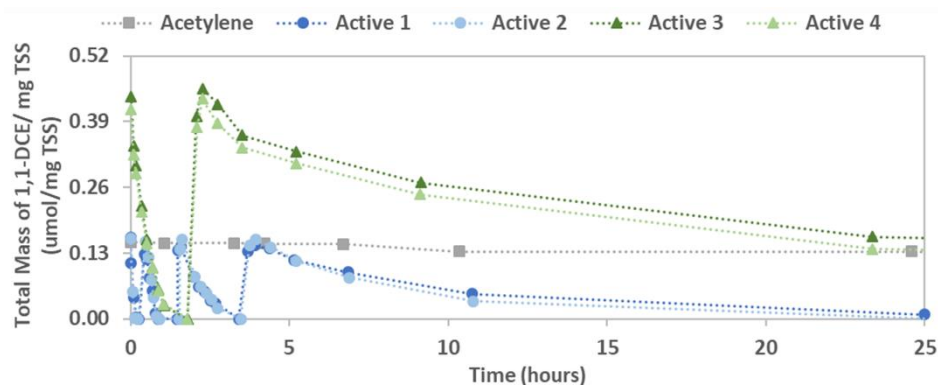


Figure 4.3. Total mass of 1,1-DCE per mg TSS over time for ethane-grown 21198. Approximately 4 mg of cells were used for experimentation.

As shown in Figure 4.4, the zero order degradation rates of CAHs and 1,4-dioxane by ethane-grown 21198 were ordered in the following rank: 1,1-DCE > 1,4-dioxane > 1,2-DCA > c-DCE > 1,1,1-TCA > and TCE.

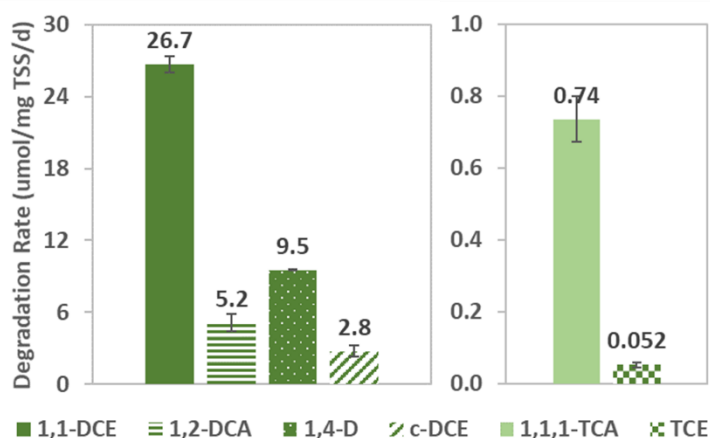


Figure 4.4. Comparison of zero order degradation rates of 1,1-DCE, 1,2-DCA, 1,4-dioxane, c-DCE, 1,1,1-TCA, and TCE for ethane-grown 21198. Error bars indicate the standard deviation of a two sample average.

Figure 4.5 depicts the zero order primary substrate uptake rates of isobutane and ethane for ethane-grown 21198. The rate of isobutane uptake was greater than the rate of ethane uptake. The rates of primary substrate uptake were on similar orders of magnitude to the transformation rates of less chlorinated compounds, 1,1-DCE and 1,2-DCA, but were much greater than the transformation rates of more chlorinated compounds, TCE and 1,1,1-TCA.

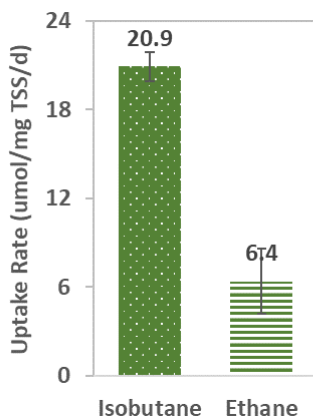


Figure 4.5. Zero order primary substrate uptake rates of isobutane and ethane for ethane-grown 21198. Error bars indicate the standard deviation of a two sample average.

4.1.3 Propane-grown 21198

Figure 4.6 depicts the results from a typical rate test, showing the total mass of 1,1-DCE per mg TSS over time for propane-grown 21198. The transformation of 1,1-DCE occurs moderately quickly. The degradation rate is similar between high and low initial 1,1-DCE concentrations ($9.3 \pm 0.9 \mu\text{mol/mg TSS/d}$ at an initial concentration of approximately $27 \mu\text{mol/L}$ versus $11.9 \pm 1.6 \mu\text{mol/mg TSS/d}$ at an initial concentration of approximately $72 \mu\text{mol/L}$). The transformation capacity for 1,1-DCE was determined to be $0.32 \mu\text{mol/mg TSS}$ at a high initial concentration and $0.30 \mu\text{mol/mg TSS}$ at a low initial concentration. Acetylene actively blocked the degradation of all COCs tested, suggesting monooxygenase enzymes are involved in the transformations of these compounds.

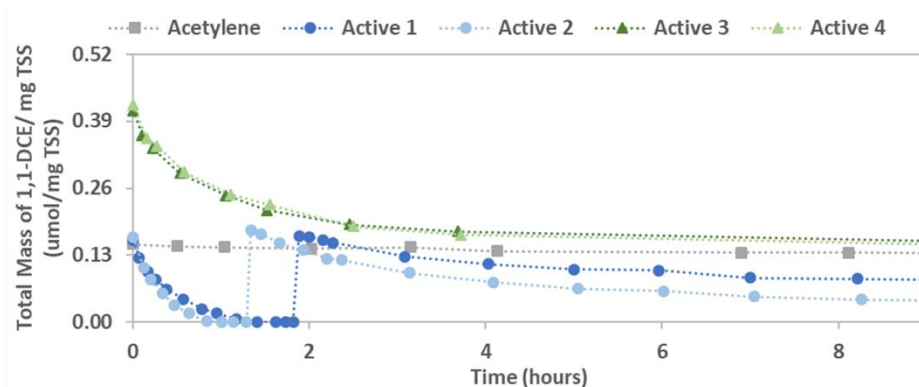


Figure 4.6. Total mass of 1,1-DCE per mg TSS over time for propane-grown 21198. Approximately 4 mg of cells were used for experimentation.

As shown in Figure 4.7, the zero order degradation rates of CAHs and 1,4-dioxane by propane-grown 21198 were ordered in the following rank: 1,1-DCE > 1,4-dioxane > 1,2-DCA > c-DCE > 1,1,1-TCA > and TCE.

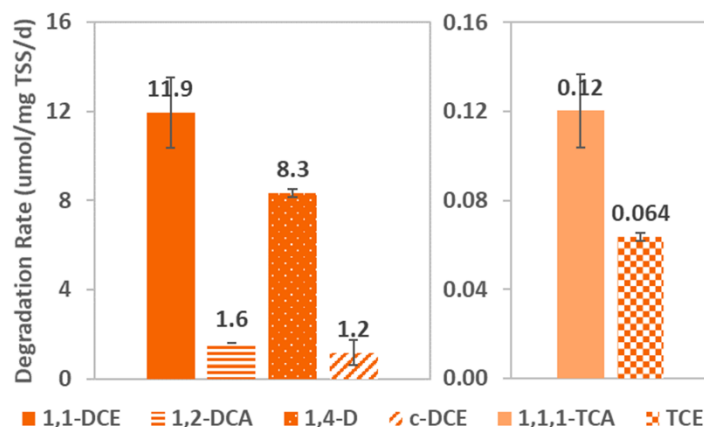


Figure 4.7. Comparison of zero order degradation rates of 1,1-DCE, 1,2-DCA, 1,4-dioxane, c-DCE, 1,1,1-TCA, and TCE for propane-grown 21198. Error bars indicate the standard deviation of a two sample average.

Figure 4.8 depicts the zero order primary substrate uptake rates of isobutane and propane for propane-grown 21198. The rate of isobutane uptake was greater than the rate of propane uptake. The rates of primary substrate uptake were on similar orders of magnitude to the transformation rates of less chlorinated compounds, 1,1-DCE and 1,2-DCA, but were much greater than the transformation rates of more chlorinated compounds, TCE and 1,1,1-TCA.

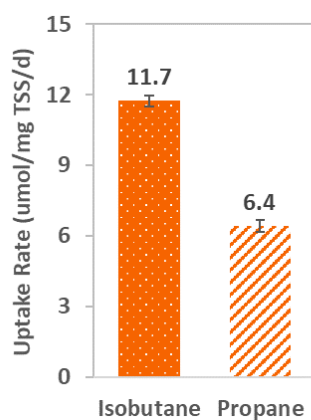


Figure 4.8. Zero order primary substrate uptake rates of isobutane and propane for propane-grown 21198. Error bars indicate the standard deviation of a two sample average.

4.1.4 Isobutene-grown ELW1

Figure 4.9 depicts the results from a typical rate test, showing the total mass of 1,1-DCE per mg TSS over time for isobutene-grown ELW1. The transformation of 1,1-DCE occurs moderately quickly. The degradation rate is similar between high and low initial 1,1-DCE concentrations (9.7 ± 0.4 μmol/mg TSS/d at an initial concentration of approximately 27 μmol/L versus 6.2 ± 1.0 μmol/mg TSS/d at an initial concentration of approximately 76 μmol/L). The transformation capacity for 1,1-DCE was determined to

be $0.30 \mu\text{mol}/\text{mg TSS}$ at a high initial concentration and $0.33 \mu\text{mol}/\text{mg TSS}$ at a low initial concentration. Acetylene was only moderately effective at blocking the degradation of 1,1-DCE. Propyne was used for later experimentation with TCE and 1,4-dioxane in order to provide improved monooxygenase inhibition.

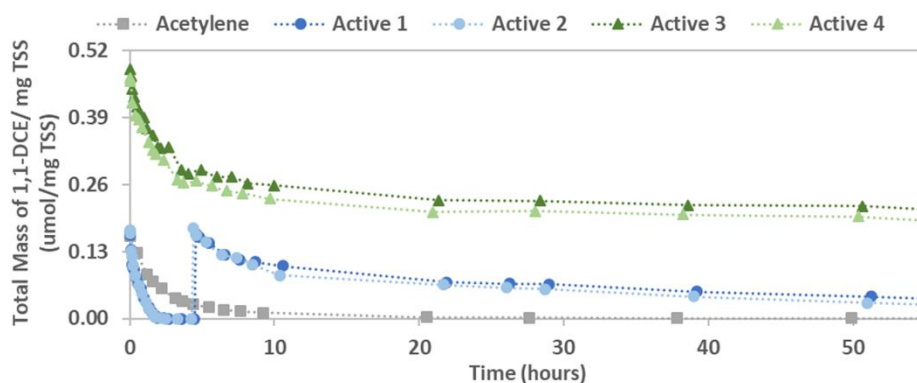


Figure 4.9. Total mass of 1,1-DCE per mg TSS over time for isobutene-grown ELW1. Approximately 4 mg of cells were used for experimentation.

As shown in Figure 4.10, the zero order degradation rates of CAHs and 1,4-dioxane by isobutene-grown ELW1 were ordered in the following rank: 1,1-DCE > 1,4-dioxane > and TCE. The transformation of 1,1-DCE was much faster than that of both 1,4-dioxane and TCE. These rates are similar to those observed in other systems, in that more chlorinated compounds (TCE) are more slowly transformed than less chlorinated compounds (1,1-DCE).

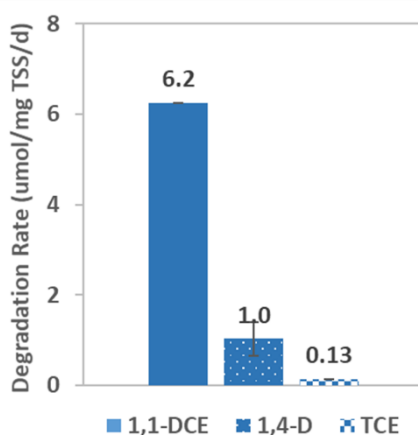


Figure 4.10. Comparison of zero order degradation rates of 1,1-DCE, 1,4-dioxane, and TCE for isobutene-grown ELW1. Error bars indicate the standard deviation of a two sample average.

Individual rate tests with 1,1,1-TCA, 1,2-DCA, and c-DCE were not performed with ELW1. Two mixture tests were conducted; one with TCE, 1,1,1-TCA, 1,1-DCE, 1,2-DCA, and 1,4-dioxane and one with TCE, 1,1,1-TCA, 1,1-DCE, 1,2-DCA, 1,4-dioxane, and isobutene. As shown in Figure 4.11, 1,1-DCE was rapidly

transformed in the absence of isobutene, while TCE was more slowly degraded. 1,1,1-TCA, 1,2-DCA, and 1,4-dioxane were not readily transformed by ELW1. Figure 4.12 demonstrates metabolism in the presence of the primary substrate, isobutene. Isobutene significantly inhibited the transformation of CAHs. Rapid 1,1-DCE transformation did not begin until the total mass of isobutene reached below 1.5 μmol (approximately 10 $\mu\text{mol/L}$ or 560 $\mu\text{g/L}$). These results were also observed in microcosm studies further discussed in Section 4.2.8 in which microcosms were bioaugmented with 0.9 mg of ELW1. As with the mixture in the absence of isobutene, 1,1,1-TCA, 1,2-DCA, and 1,4-dioxane were not readily transformed by ELW1 (1,4-dioxane data not shown).

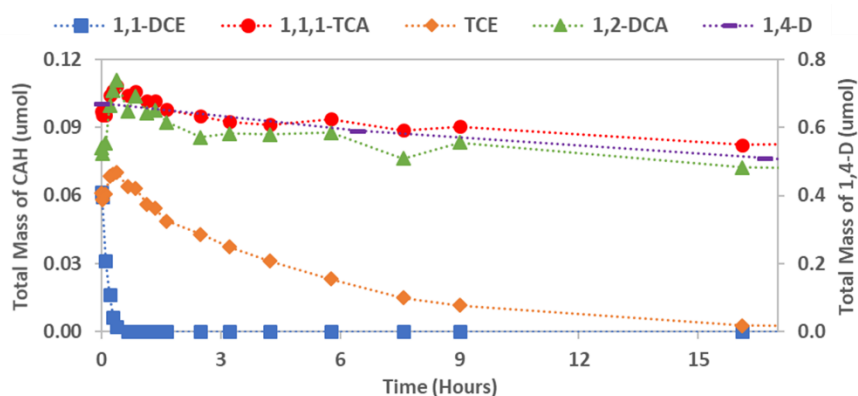


Figure 4.11. Total mass of 1,1-DCE, 1,1,1-TCA, TCE, 1,2-DCA, and 1,4-dioxane over time for isobutene-grown ELW1.

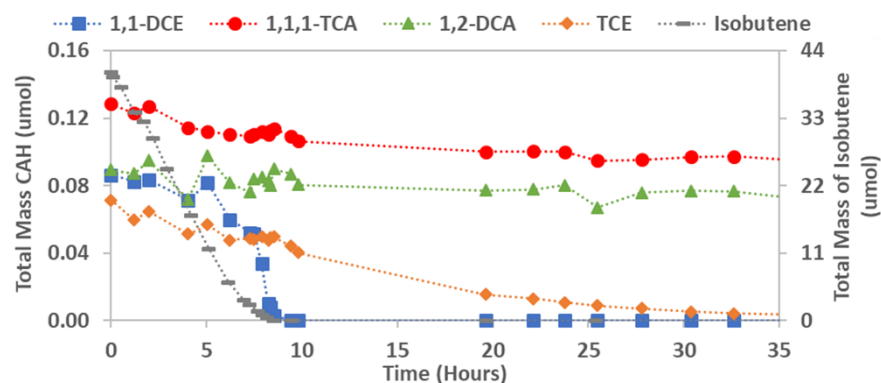


Figure 4.12. Total mass of 1,1-DCE, 1,1,1-TCA, TCE, 1,2-DCA, and isobutene over time for isobutene-grown ELW1 (1,4-dioxane data not shown).

4.1.5 Comparisons between growth substrates

A comparison of zero order degradation rates of 1,4-dioxane, TCE, 1,1,1-TCA, 1,2-DCA, 1,1-DCE, and c-DCE for isobutane, ethane, and propane-grown 21198 and isobutene-grown ELW1 is shown in Figure 4.13. The general trend in rates for 1,4-dioxane, 1,2-DCA, 1,1-DCE, and c-DCE shows isobutane-grown 21198 > ethane-grown 21198 > propane-grown 21198. The rates for TCE are comparable among all growth substrates with 21198. The TCE degradation rate of isobutene-grown ELW1 is double the rates

observed for 21198 grown on all substrates. The 1,4-dioxane transformation rate by ELW1 was eight to 14 times less than that of 21198 grown on all substrates. 1,1,1-TCA rates were comparable for isobutane and ethane-grown 21198, but the rate of transformation with propane-grown 21198 was much lower.

As shown in Figure 2.4, the results CAH and 1,4-dioxane transformation rates by 21198 generally reflect the relative quantity of SCAM detected in isobutane, ethane, and propane-grown culture. The highest quantity of SCAM was detected in isobutane-grown cultures (approximately 450 mass spectral counts for 59 kDa), followed by ethane-grown (approximately 375 mass spectral counts for 59 kDa) and then propane-grown (approximately 110 mass spectral counts for 59 kDa) cultures. The rates of CAH transformations were generally highest for isobutane-grown 21198, followed by ethane and then propane-grown cultures.

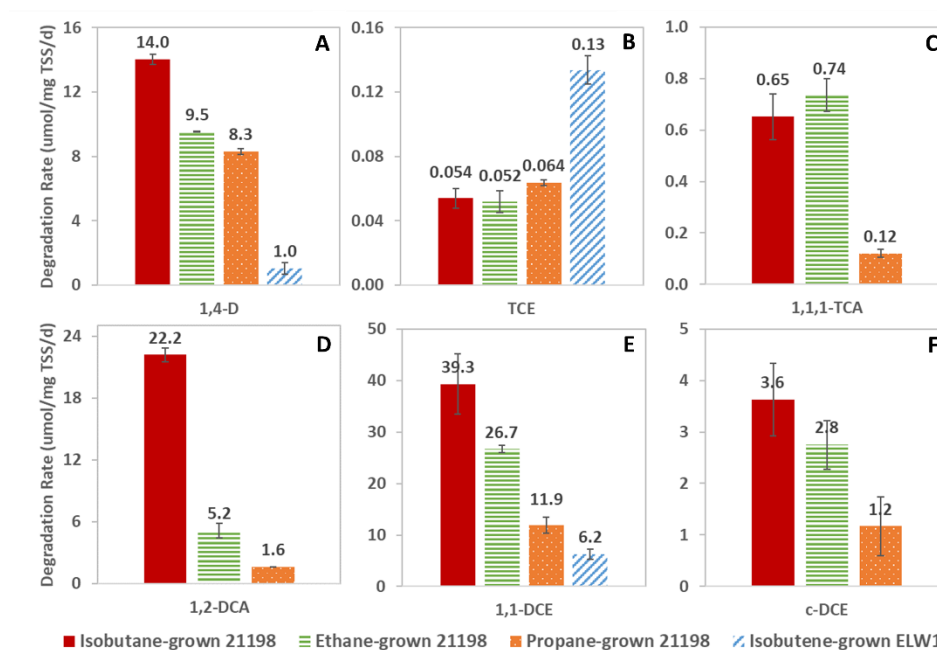


Figure 4.13. Zero order degradation rates of 1,4-D (A), TCE (B), 1,1,1-TCA (C), 1,2-DCA (D), 1,1-DCE (E), and c-DCE (F) for isobutane-, ethane-, and propane-grown 21198 and isobutene-grown ELW1. Error bars indicate the standard deviation of a two sample average.

Figure 4.14 shows the transformation capacities of 1,1-DCE and c-DCE for isobutane, ethane, and propane-grown 21198 and the transformation capacity of 1,1-DCE for isobutene-grown ELW1. The transformation capacities for isobutane and ethane-grown 21198 are comparable for both 1,1-DCE and c-DCE and greater than those for propane-grown 21198. Isobutene-grown ELW1 had the lowest transformation capacity for 1,1-DCE but was comparable with propane-grown 21198. Transformation

capacities for 1,2-DCA were attempted to be obtained. Minimum transformation capacities were 1.7 $\mu\text{mol}/\text{mg TSS}$, 0.95 $\mu\text{mol}/\text{mg TSS}$, and 1.8 $\mu\text{mol}/\text{mg TSS}$ for isobutane, ethane, and propane-grown 21198, respectively. These are greater than those obtained for 1,1-DCE. These results could be explained by the likely formation of an epoxide intermediate in the transformation of chlorinated ethenes. The transformations of chlorinated ethanes, like 1,2-DCA, likely do not involve a toxic epoxide intermediate, which could allow microbial communities to be capable of transforming a greater quantity of these compounds.

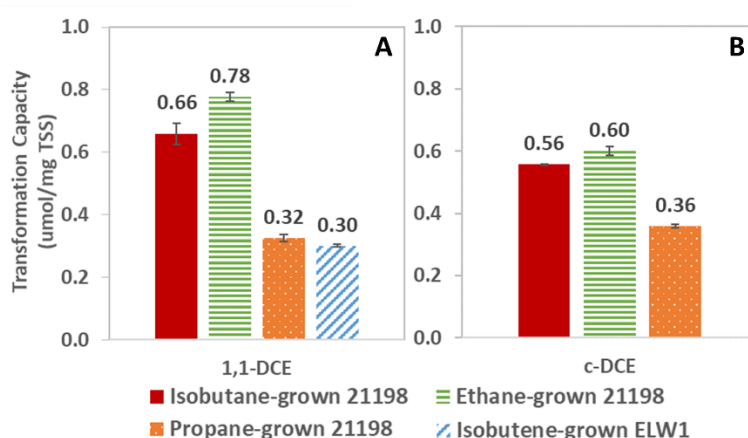


Figure 4.14. Transformation capacities of 1,1-DCE (A) and c-DCE (B) for isobutane, ethane, and propane-grown 21198 and isobutene-grown ELW1. Error bars indicate the standard deviation of a two sample average.

These results can be compared to previous studies conducted with mixed and pure cultures of butane, methane, and propane grown cultures (summarized in Table 4.1). The general trend of more chlorinated compounds exhibiting slower transformation rates can be observed from cultures grown on nearly all of these primary substrates. Butane-grown cultures also exhibited similar trends to the results from isobutane-grown 21198 presented in this thesis.

Table 4.1. Summary of half-saturation constants (K_s), maximum transformation rates, and transformation capacities (T_c) for TCE, 1,1,1-TCA, 1,1-DCE, c-DCE, and 1,2-DCA by various mixed and pure cultures grown on butane, methane, and propane in previous studies.

Compound	Organism/Condition	Growth Substrate	Temp. (°C)	Initial Conc. (μmol/L)	K_s (μmol/L)	Max Rate (μmol S/mg TSS/d)	T_c (μmol/mg TSS)	Source
TCE	Mixed culture	Butane	--	19	--	0.24		Kim et al. 2000
TCE	<i>M. trichosporium</i> OB3b PP358	Methane/Formate	22	0.46-60.9	82.2	158.3		Aziz et al., 1999
TCE	<i>M. trichosporium</i> OB3b	Methane	30	30.4-685	145	418		Oldenhuis et al., 1991
TCE	Mixed culture, chemostat	Methane	20		47	73	4.1	Chang and Alvarez-Cohen, 1996
TCE	Mixed culture, chemostat	Methane	20		29.2	7.8	0.381	Chang and Alvarez-Cohen, 1995
TCE	Mixed culture, chemostat	Methane/Formate	20		52.9	31.7	0.761	Chang and Alvarez-Cohen, 1995
TCE	<i>Mycobacterium vaccae</i> JOB5	Propane	30		4.4	0.43		Alvarez & Speitel, 2001
TCE	Mixed culture, chemostat	Propane	20		39.7	3.4	0.049	Chang and Alvarez-Cohen, 1995
1,1,1-TCA	Mixed culture	Butane	--	25	--	0.72		Kim et al. 2000
1,1,1-TCA	Mixed culture	Butane	20		12	4.56		Kim et al. 2002
1,1,1-TCA	<i>M. trichosporium</i> OB3b	Methane	30		214	35		Oldenhuis et al., 1991
1,1-DCE	Mixed culture	Butane	--	37	--	8.16		Kim et al. 2000
1,1-DCE	Mixed culture	Butane	20		1.5	31.2	0.52	Kim et al. 2002
1,1-DCE	<i>M. trichosporium</i> OB3b PP358	Methane/Formate	22	0.10-35.1	>35.1	>77.4		Aziz et al., 1999
1,1-DCE	<i>M. trichosporium</i> OB3b	Methane	30		5	9		Oldenhuis et al., 1991
c-DCE	Mixed culture	Butane	--	87	--	4.8		Kim et al. 2000
c-DCE	Mixed culture, chemostat	Methane	20		31	86	5.9	Chang and Alvarez-Cohen, 1996
c-DCE	<i>M. trichosporium</i> OB3b PP358	Methane/Formate	22	0.52-57.8	11.3	98.0		Aziz et al., 1999
c-DCE	<i>M. trichosporium</i> OB3b	Methane	30		30	262		Oldenhuis et al., 1991
1,2-DCA	Mixed culture	Butane	--	52	--	0.24		Kim et al. 2000
1,2-DCA	<i>M. trichosporium</i> OB3b	Methane	30		77	94		Oldenhuis et al., 1991

Figure 4.15 shows the total mass of 1,1-DCE, 1,1,1-TCA, TCE, 1,2-DCA, and 1,4-dioxane over time for isobutane, ethane, and propane-grown 21198 and isobutene-grown ELW1 for a mixture of COCs. The observed rates between each compound for each substrate are consistent with those observed in single compound studies. 1,1-DCE and 1,2-DCA are most rapidly transformed, followed by slower 1,4-dioxane, and 1,1,1-TCA transformation and minimal TCE degradation for 21198 grown on all substrates. The transformations by propane-grown 21198 were slower than those for isobutane and ethane-grown 21198. 1,1-DCE was transformed rapidly for isobutene-grown ELW1. TCE was more readily transformed by ELW1 than 21198 grown on any substrate. 1,4-dioxane, 1,1,1-TCA, and 1,2-DCA were not readily degraded by ELW1 compared to 21198.

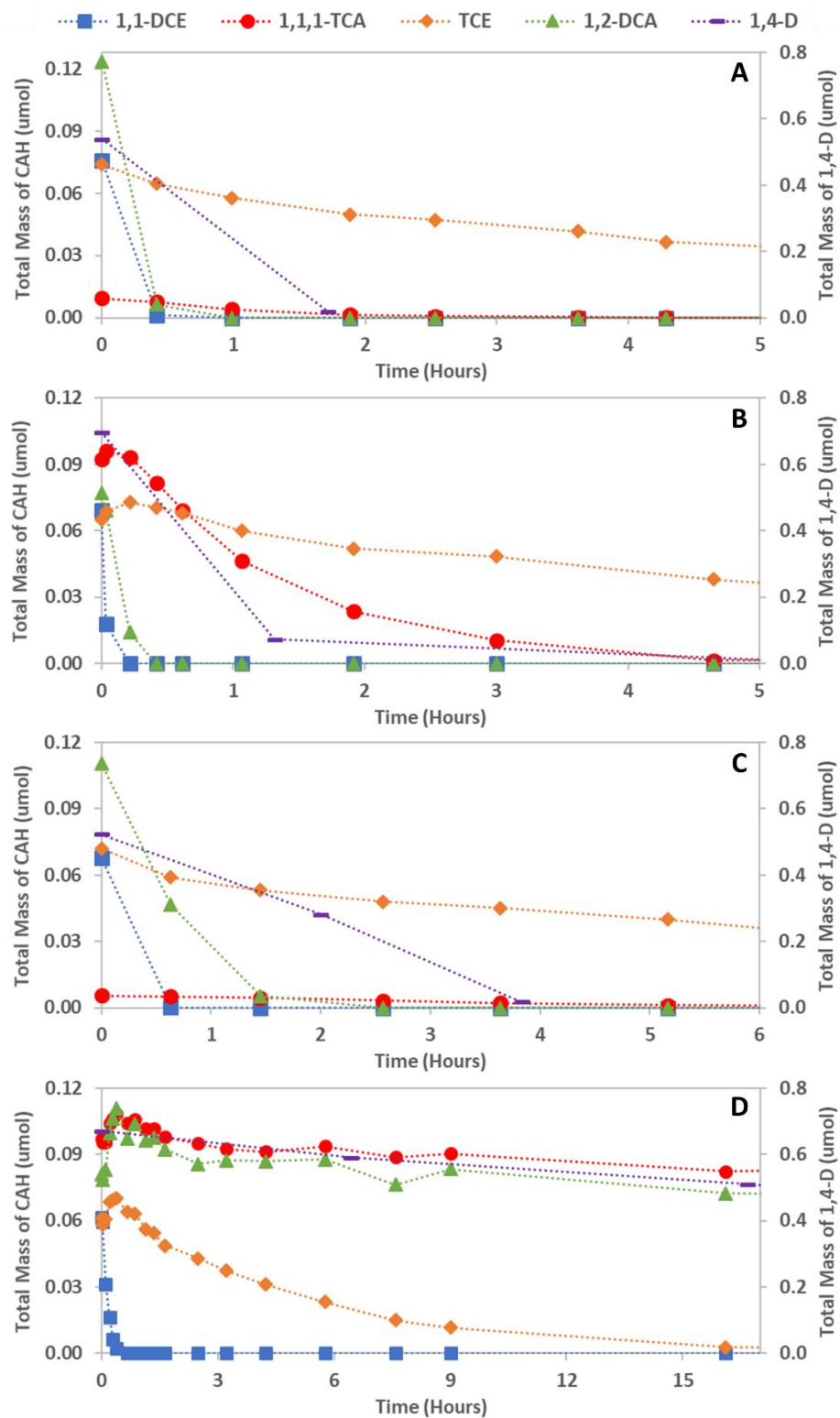


Figure 4.15. Total mass of 1,1-DCE, 1,1,1-TCA, TCE, 1,2-DCA, and 1,4-dioxane in isobutane (A), ethane (B), and propane (C) grown 21198, and isobutene grown ELW1 (D) for COC mixtures. Approximately 5 mg of cells were used in each experiment.

4.2 Microcosm Studies

Microcosm studies were conducted using groundwater and sediment from NAS North Island in San Diego, California. As discussed in Section 2.8, this site is contaminated with CAHs (predominately TCE and 1,1-DCE) and 1,4-dioxane due to historical improper storage of chemical waste. Aerobic cometabolism has been proposed for the remediation of this site due to the composition of the contaminant mixture. The purpose of this section was to identify an effective primary substrate, or combination of multiple primary substrates, that was capable of performing concurrent transformations of CAHs and 1,4-dioxane.

Figure 4.16 depicts the microcosm experimental process for long-term microcosm studies utilizing isobutane and isobutene as primary growth substrates. Early isobutane experimentation (further discussed in Section 4.2.1) demonstrated the difficulty of achieving stimulation of native microbial communities in the presence of CAHs, particularly 1,1-DCE. In order to circumvent this challenge, three main strategies were employed, including the removal of CAHs via sparging (Section 4.2.2), the bioaugmentation with isobutane-grown 21198 (Section 4.2.3), and the addition of isobutanol (Section 4.2.4). Isobutene ultimately demonstrated successful stimulation of the native microbial community in the presence of CAHs (Section 4.2.6), though the removal of CAHs via sparging (Appendix D) and bioaugmentation with isobutene-grown ELW1 (Section 4.2.8) were also employed.

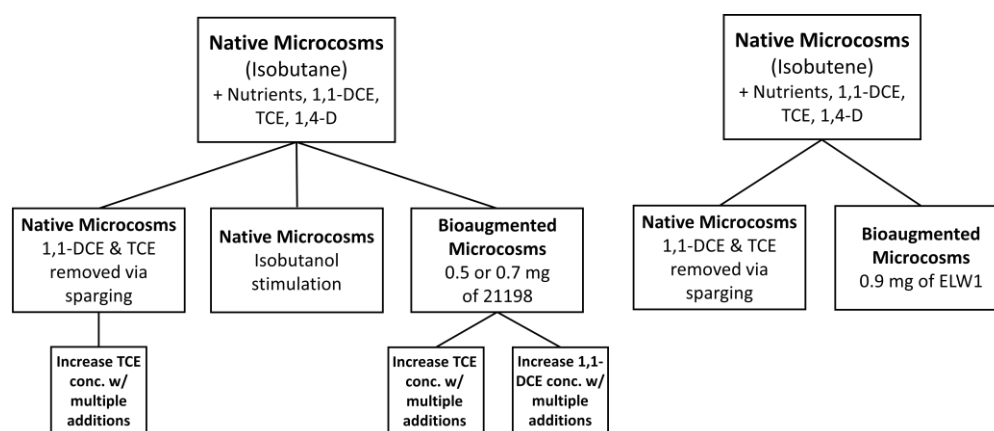


Figure 4.16. Experimental microcosm road map indicating the general experimental process for long-term microcosm studies utilizing isobutane and isobutene as primary growth substrates.

4.2.1 Isobutane in the presence in CAHs

Eight microcosms were initially established with isobutane in the presence of CAHs. Bottles 1 and 2 did not have nutrients added; bottles 3 and 4 had nutrients added; bottles 5 and 6 were acetylene controls; and bottles 7 and 8 did not have isobutane added to the headspace. As shown in Figure 4.17A,

isobutane uptake was not observed in any of the microcosms over 130 days of incubation in the presence of CAHs.

The total mass of TCE decreased by 60 to 70 percent over the span of the incubation (Figure 4.17B). Because this phenomenon occurred in the acetylene controls, the observed decrease in TCE was likely due to abiotic transformations or due to sorption to sediment and/or the rubber septa rather than biological activity. Jeffers et al. reported an abiotic hydrolysis half-life of 1.0×10^6 years for TCE (Jeffers et al., 1989). Due to this slow rate, it is unlikely that the loss of TCE can be accounted for by abiotic transformations. As noted in Table 2.1, the octanol-water partition coefficient ($\log K_{ow}$) for TCE is 2.53. The $\log K_{ow}$ represents the partitioning of a compound into water and octanol phases and is often used to signify the hydrophobicity of the compound and describe the partitioning of the compound between water and organic solids. Compounds with a higher $\log K_{ow}$ are more apt to partition into organic or solid phases rather than the aqueous phase, as demonstrated by TCE. The loss in total mass of TCE over time can likely be attributed to sorption to sediment and/or the rubber septa.

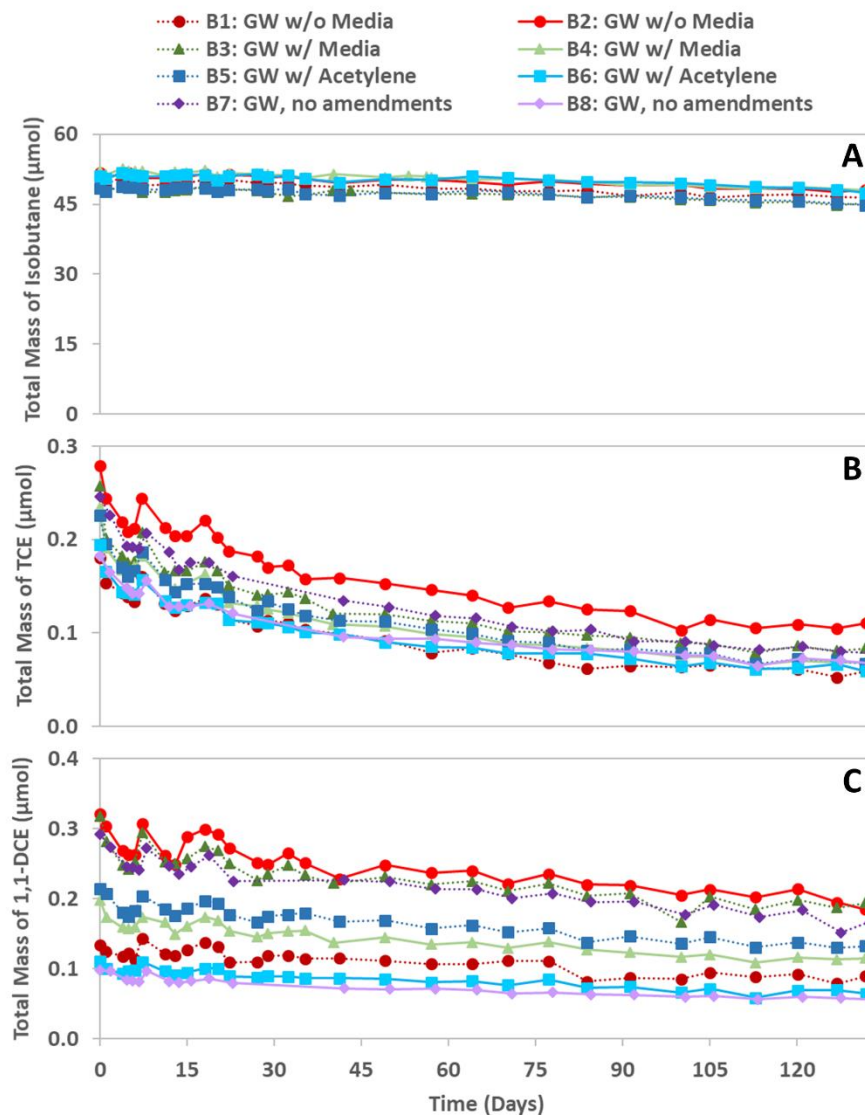


Figure 4.17. Total mass of isobutane (A), TCE (B), and 1,1-DCE (C) over time in native microcosms incubated with isobutane in the presence of CAHs (set 1). Bottles 1 and 2 do not have added nutrients; bottles 3 and 4 have added nutrients; bottles 5 and 6 are acetylene controls; and bottles 7 and 8 do not have isobutane added.

These results were confirmed in subsequent microcosms wherein isobutane uptake was not observed after 22 to 105 days of incubation in the presence of CAHs (Figure 4.18). The lack of activity is hypothesized to be due to the toxicity of the 1,1-DCE epoxide formed from the activation of the monooxygenase enzyme. Minimal isobutane may have been utilized, but the microbial population was not able to grow due to immediate toxicity exposure from concurrent 1,1-DCE transformation.

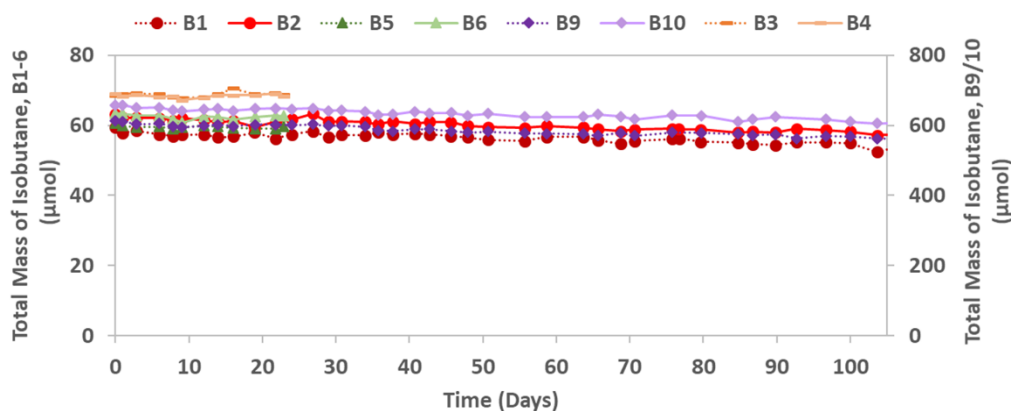


Figure 4.18. Total mass of isobutane over time in native microcosms incubated with isobutane in the presence of CAHs (set 5). All bottles have nutrients added. Bottles 1 through 6 were constructed with groundwater from SMW-08A, and bottles 9 and 10 were constructed with groundwater from SMW-10A (with approximately two times the total mass of 1,1-DCE compared to SMW-08A).

4.2.2 Isobutane in the absence in CAHs

Based on the results described in Section 4.2.1, it was hypothesized that the presence of 1,1-DCE was inhibitory to the stimulation of native isobutane-utilizers due to the toxicity of the 1,1-DCE epoxide. In order to test this hypothesis, the groundwater used for experimentation described in this section was sparged with nitrogen to remove CAHs from solution prior to the addition of isobutane to the headspace of the microcosm. Six microcosms were established with isobutane in the absence of CAHs from day 0 (set 2). Microcosms 1 and 2 did not have added nutrients; microcosms 3 and 4 had added nutrients; and microcosms 5 and 6 were acetylene controls. Figure 4.19 depicts data from the long-term incubation of groundwater with isobutane in the initial absence of CAHs. As described in greater detail later in this section, isobutane uptake was observed after 12 days of incubation in the absence of CAHs. 1,1-DCE and TCE were reintroduced to the system, and subsequent respikes of isobutane, 1,4-dioxane, and CAHs were performed over 125 days of incubation, with gradually increasing concentrations of TCE.

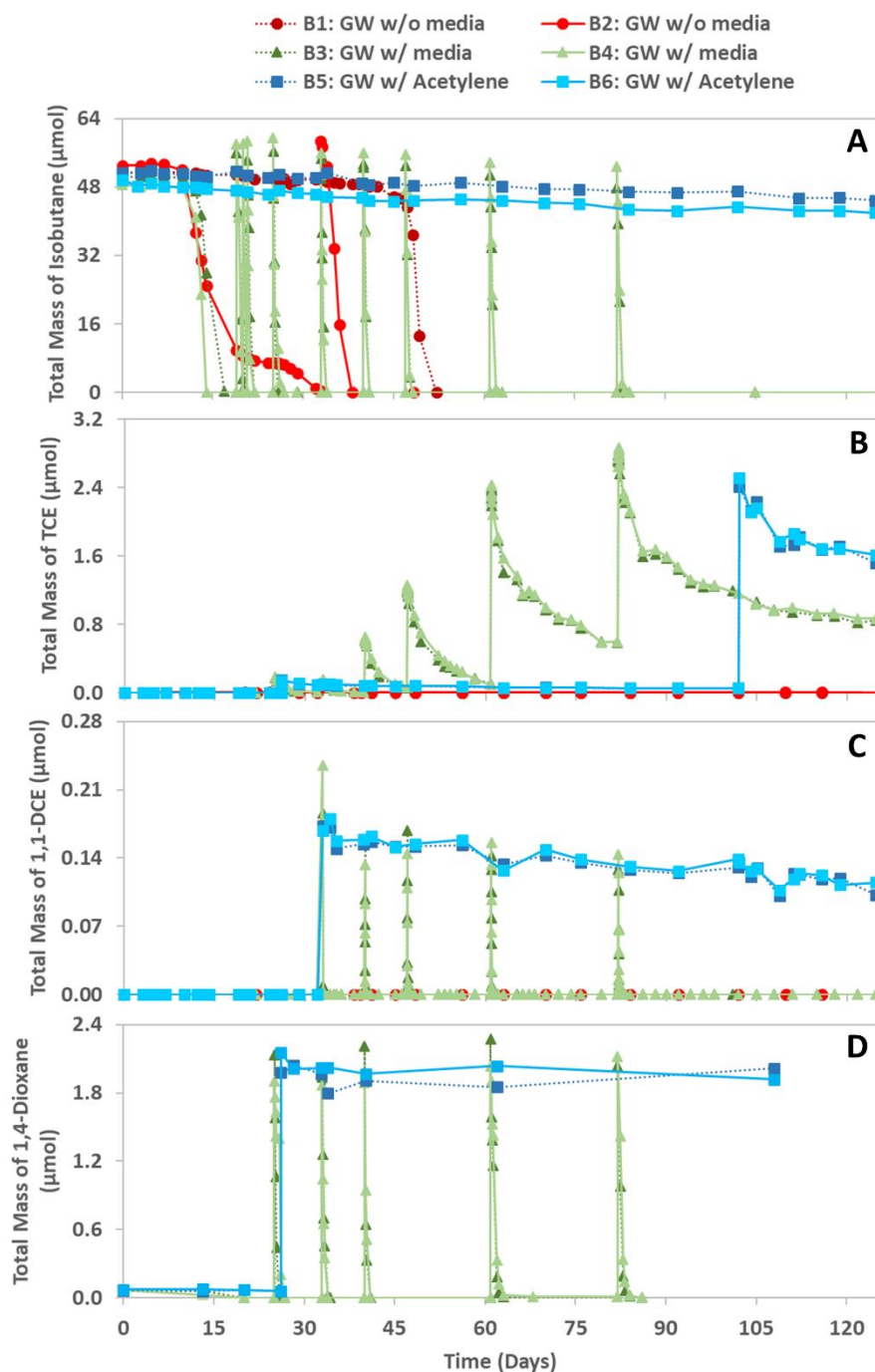


Figure 4.19. Total mass of isobutane (A), TCE (B), 1,1-DCE (C), and 1,4-dioxane (D) over time in native microcosms initially sparged to remove CAHs. Nutrients were added to bottles 1 and 2 on day 24. Bottles 3 through 6 had nutrients added on day 0. Bottles 5 and 6 were acetylene controls.

As shown in Figure 4.20, isobutane uptake was observed in microcosms 3 and 4 (those with nutrients added) after approximately 12 days of incubation. Isobutane uptake observed in microcosms 1 and 2 (without added nutrients) is further discussed in Section 4.2.8. Microcosms 3 and 4 continued to

support repeated isobutane additions and demonstrated an increase in uptake rate with subsequent additions of isobutane.

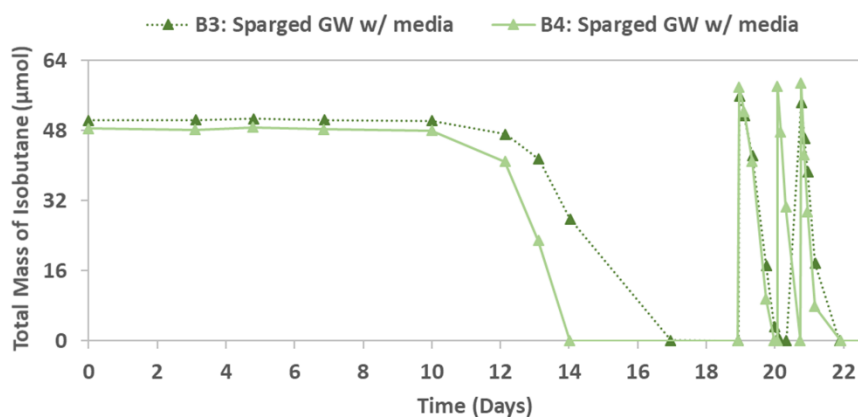


Figure 4.20. Total mass of isobutane over time in native microcosms with added nutrients and initially sparged to remove CAHs (set 2, bottles 3 and 4).

Isobutane, TCE, and 1,4-dioxane were added to microcosms 3 and 4 on day 25 (data not shown).

Isobutane and 1,4-dioxane were transformed within one day, while TCE was more slowly degraded over four days. As shown in Figure 4.21, 1,1-DCE was introduced into the system on day 33, along with another spike of isobutane, TCE, and 1,4-dioxane. 1,1-DCE was transformed very rapidly (within 2 hours), followed by isobutane uptake and 1,4-dioxane degradation within one day. TCE was more slowly transformed over five days.

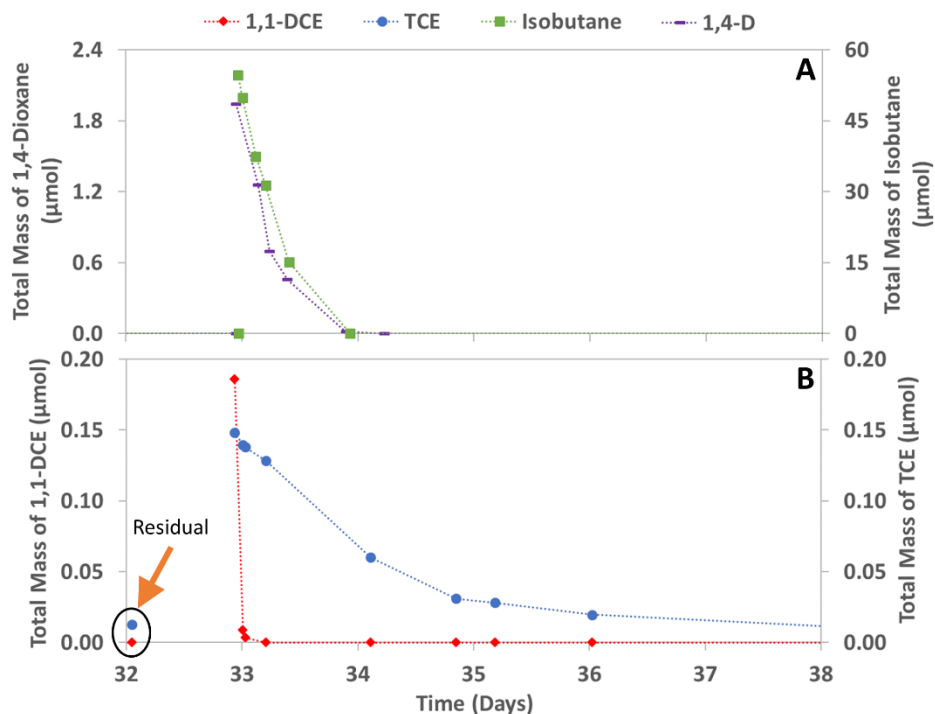


Figure 4.21. Total mass of 1,4-dioxane and isobutane (A), and 1,1-DCE and TCE (B) over time in one native microcosm with added nutrients on day 0 and initially sparged to remove CAHs (set 2, bottle 3). This depicts an early spike of isobutane and COCs added to this microcosm on day 33.

Four subsequent additions of isobutane, TCE, 1,1-DCE, and 1,4-dioxane were made between days 40 and 82, with gradual increases in TCE concentrations, culminating in a liquid concentration of 4.5 mg/L. The final spike of primary substrate and COCs on day 82 is depicted in Figure 4.22. Rapid 1,1-DCE transformation continued to be observed, followed by concurrent isobutane uptake and 1,4-dioxane degradation. TCE was slowly degraded by the native microbial community. The final measured concentration of TCE was approximately 1.3 mg/L (an approximately 70% overall reduction).

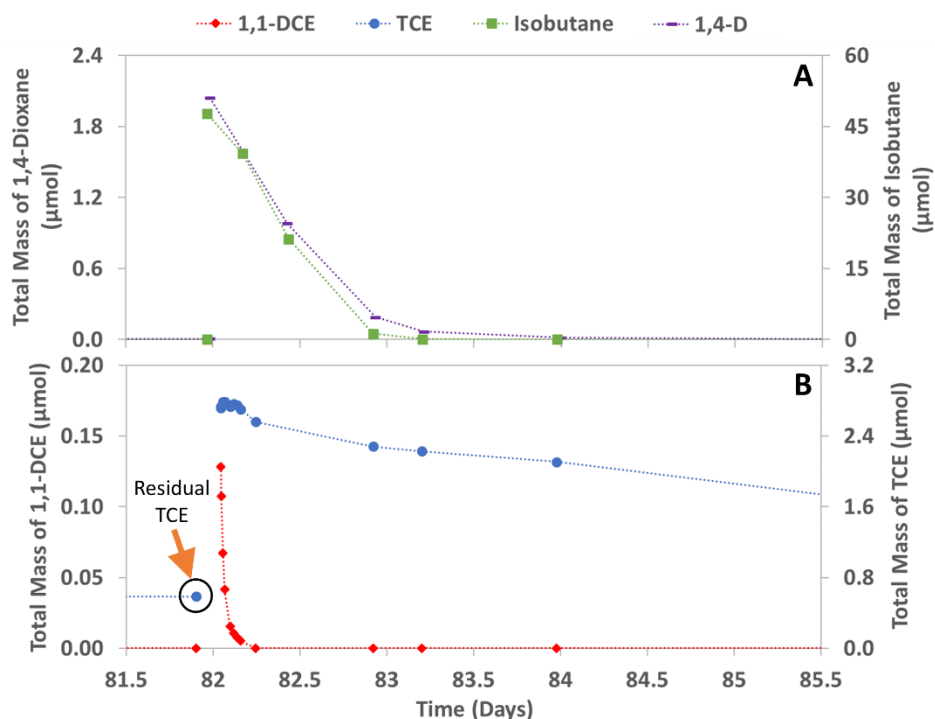


Figure 4.22. Total mass of 1,4-dioxane and isobutane (A), and 1,1-DCE and TCE (B) over time in one native microcosm with added nutrients on day 0 and initially sparged to remove CAHs (set 2, bottle 3). This depicts the last spike of isobutane and COCs added to this microcosm on day 82.

To verify that the observed decrease in TCE concentration in microcosms 3 and 4 was due to biological activity, TCE was added to the acetylene control bottles 5 and 6 at a comparable concentration to the last two TCE spikes in microcosms 3 and 4 (Figure 4.23). Over the span of 10 days, the TCE concentrations in microcosms 5 and 6 decreased by approximately 25%, while the concentrations in microcosms 3 and 4 decreased by approximately 45%. This suggests that while there is some TCE concentration decrease likely due to sorption to sediment and/or the rubber septa, there is also a biological component to the decrease.

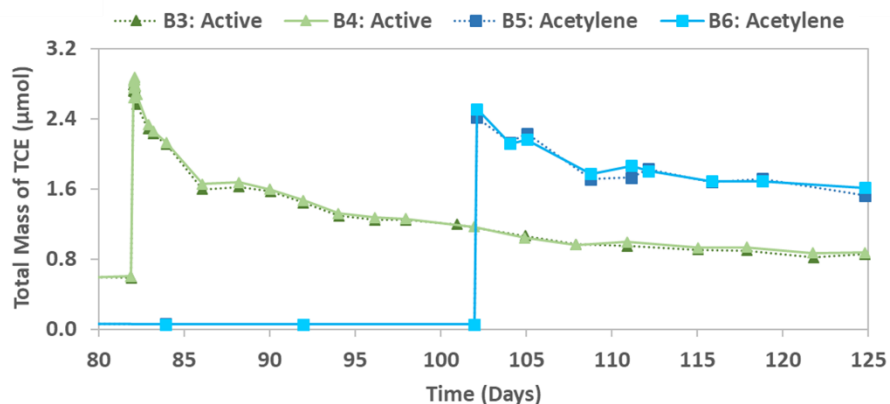


Figure 4.23. Comparison of total mass of TCE over time in native active and acetylene control microcosms that were initially sparged to remove CAHs (set 2, bottles 3-6). TCE was added to the acetylene control bottles on day 102 in order to compare the change in total mass over time to the change observed in the active bottles.

To verify the results from the initially sparged microcosms with added nutrients (set 2, bottles 3 and 4), two additional microcosms were established with isobutane in the absence of CAHs (set 7, bottles 1 and 2). As shown in Figure 4.24, isobutane uptake was not observed over 60 days of incubation. The lack of activity could be explained by a very small initial biomass, either from a lack of native isobutane-utilizers present at NAS North Island and/or due to the minimal quantity of aquifer solids present in the microcosm, or due to slow growth rates. There is also the possibility that the set 2 microcosms were contaminated with 21198 over the course of the experimentation and that native isobutane-utilizers were not responsible for the observed activity.

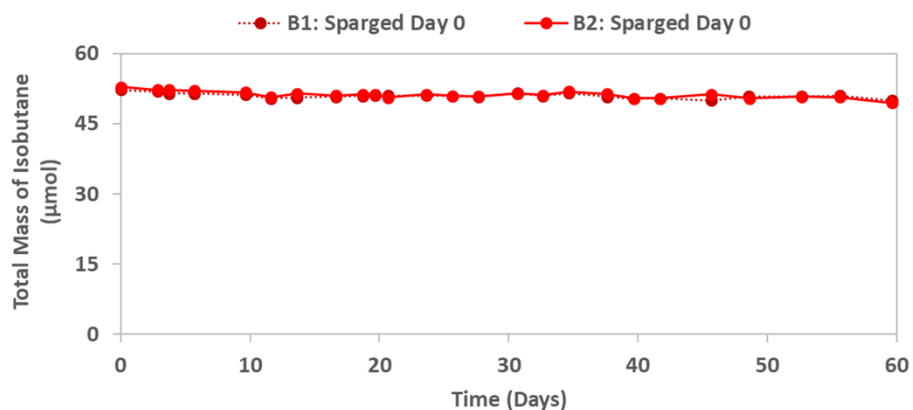


Figure 4.24. Total mass of isobutane over time in native microcosms sparged to remove CAHs on day 0.

To further confirm the results from the active native microcosms with added nutrients initially sparged to remove CAHs (set 2, bottles 3 and 4), two additional microcosms were established with isobutane initially in the presence of CAHs (set 5, bottles 3 and 4). These microcosms were sparged with nitrogen on day 23 to remove CAHs from solution. They were again sparged on day 51 to further remove CAHs

that had desorbed from the aquifer solids. After the second sparging event, the liquid concentrations of 1,1-DCE and TCE were approximately 1 to 5 $\mu\text{g/L}$ and approximately 20 to 30 $\mu\text{g/L}$, respectively.

As shown in Figure 4.25, isobutane uptake was observed in set 5, bottle 3 46 days after the initial sparging event and after 69 days of isobutane incubation. This microcosm consumed a second addition of isobutane at a faster rate. The 1,1-DCE concentration dropped to below detection levels, and the TCE concentration was 9 $\mu\text{g/L}$ on day 106. The 1,4-dioxane concentration also decreased from 3.8 mg/L to 49 $\mu\text{g/L}$ (data not shown). These results support the assertion that native isobutane-utilizers can be stimulated in the absence of CAHs following initial concurrent exposure to isobutane, CAHs, and 1,4-dioxane.

Isobutane uptake has not been observed in bottle 4 after 106 days of incubation. As with bottles 1 and 2 from set 7 that were sparged to remove CAHs on day 0, these results could be explained by a very small initial biomass, either from a lack of native isobutane-utilizers present at NAS North Island and/or due to the minimal quantity of aquifer solids present in the microcosm, or due to slow growth rates.

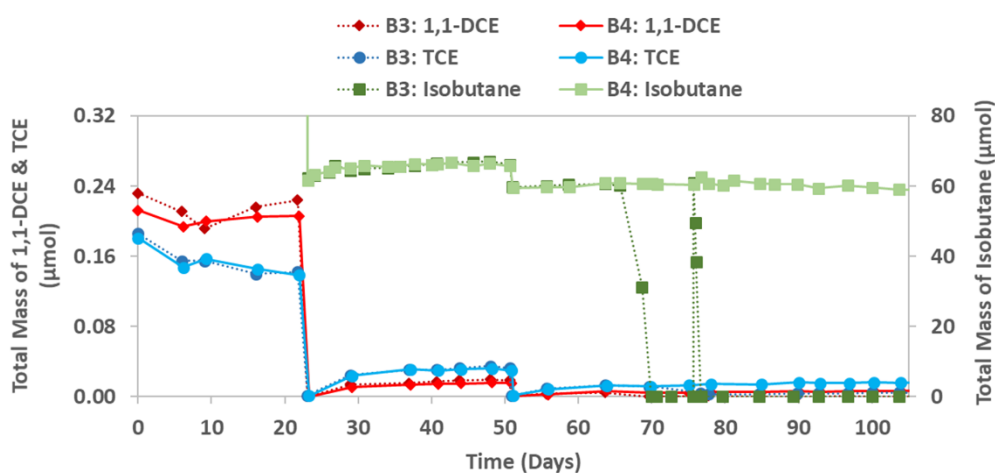


Figure 4.25. Total mass of 1,1-DCE, TCE, and isobutane over time in native microcosms sparged to remove CAHs on days 23 and 51 (set 5, bottles 3 and 4). Complete isobutane uptake was observed in bottle 3 on day 69. Isobutane was added to bottle 3 on day 76, and subsequent uptake was observed within one day.

4.2.3 Isobutane bioaugmentation with 21198

Another proposed method to circumvent to toxic effects of the 1,1-DCE epoxide was the implementation of bioaugmentation with isobutane-grown 21198. As discussed in Section 4.1.1, isobutane-grown 21198 is capable of transforming 1,1-DCE at a fast rate but with a low transformation capacity (0.66 $\mu\text{mol/mg TSS}$). The purpose of the approach described in this section was to add a sufficient quantity of 21198 biomass to fully transform the amount of 1,1-DCE present in the system.

Set 3 was comprised of four microcosms that were bioaugmented with 0.5 mg of 21198, and set 4 was comprised of four microcosms that were bioaugmented with 0.7 mg of 21198. Microcosms 1 and 2 were described as “active”, while microcosms 3 and 4 were acetylene controls. All microcosms had nutrients added to the system. Figure 4.26 depicts data from the long-term incubation of groundwater with isobutane in the presence of CAHs and bioaugmented with 0.5 mg of isobutane-grown 21198. As described in greater detail later in this section, 1,1-DCE transformation was observed immediately and rapidly, followed by isobutane uptake, 1,4-dioxane transformation, and slow TCE transformation. Subsequent respikes of isobutane, 1,4-dioxane, and CAHs were performed over 120 days of incubation, with gradually increasing concentrations of TCE.

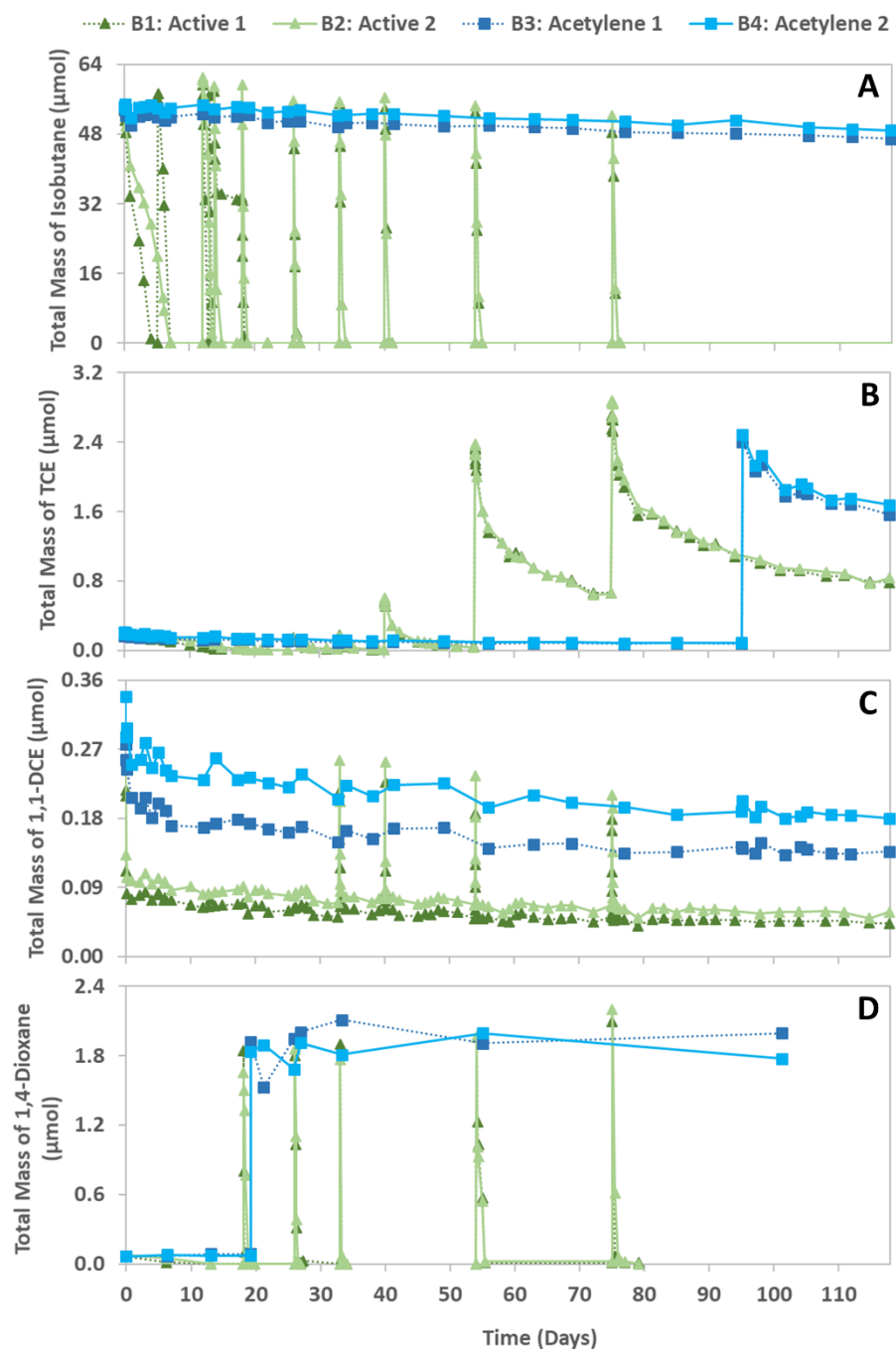


Figure 4.26. Total mass of isobutane (A), TCE (B), 1,1-DCE (C), and 1,4-dioxane (D) over time in microcosms bioaugmented with 0.5 mg of 21198 (set 3). Nutrients were added to all microcosms on day 0. Bottles 3 and 4 were acetylene controls. Bottles 1 and 2 were respiked with isobutane, 1,1-DCE, 1,4-dioxane, and gradually increasing concentrations of TCE over 120 days of incubation.

As shown in Figure 4.27, 1,1-DCE was immediately transformed over two to four hours, and isobutane was consumed within four to seven days. The rate of isobutane uptake increased with subsequent additions. Isobutane uptake in bottle 3 stalled around day 15 due to lack of oxygen and resumed on day 18 after oxygen was added to the headspace. TCE was slowly transformed over 19 days with the

addition of four to five spikes of isobutane. Though minimal 1,4-dioxane was initially present in the groundwater, the concentration decreased from approximately 110 to 140 $\mu\text{g/L}$ to below the detection limit over the first 1 to 2 spikes of isobutane (Figure 4.28). 1,4-dioxane was added at a concentration of approximately 3 mg/L on day 18 and was transformed to below the detection limit within one day.

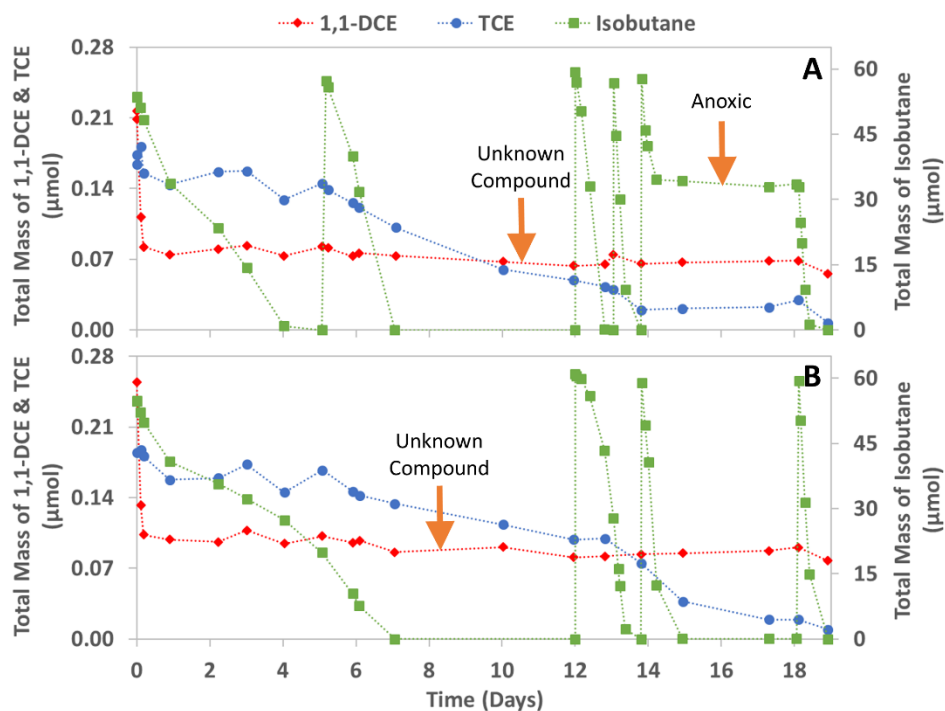


Figure 4.27. Total mass of isobutane, 1,1-DCE, and TCE over time set 3, bottles 1 (A) and 2 (B) bioaugmented with 0.5 mg 21198. The residual 1,1-DCE was hypothesized to be an unknown compound that coelutes with 1,1-DCE (further discussed below)

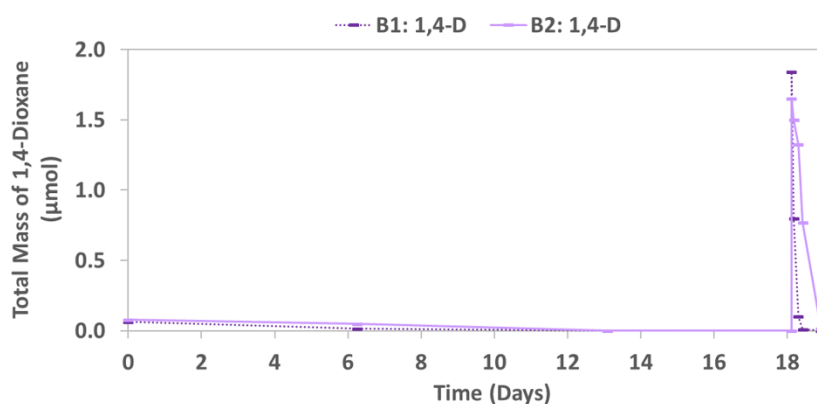


Figure 4.28. Total mass of 1,4-dioxane in set 3, bottles 1 and 2 bioaugmented with 0.5 mg 21198.

The total mass of 1,1-DCE decreased from 0.2 to 0.25 μmol to 0.07 to 0.08 μmol . It is hypothesized that the remaining 0.07 to 0.08 μmol was not 1,1-DCE but rather an unknown compound that coelutes with 1,1-DCE and was not able to be degraded by 21198. Based on the 1,1-DCE transformation capacity

obtained for isobutane-grown 21198 and reported in Section 4.1.5 (0.66 μmol 1,1-DCE per mg TSS), 0.5 mg of 21198 should have been able to fully transform the initial mass of 1,1-DCE present in the microcosms. GC analyses were performed for chloroform, carbon tetrachloride, vinyl chloride, and t-DCE to compare retention times with that of 1,1-DCE. None of the retention times for these compounds matched that of 1,1-DCE, suggesting they are not the unknown compound. Multiple GC-MS analyses were conducted to try and identify this compound. These analyses were unsuccessful, likely because the concentration of the mystery compound is below the limits of detection on the GC-MS.

Isobutane, TCE, and 1,4-dioxane were added to the active microcosms 1 and 2 on day 26. Isobutane and 1,4-dioxane were transformed within one day, while TCE was more slowly degraded over six days (data not shown). As shown in Figure 4.29, 1,1-DCE was re-added to the system on day 33, along with another spike of isobutane, TCE, and 1,4-dioxane. 1,1-DCE was transformed very rapidly (within 1 to 2 hours), followed by isobutane uptake and 1,4-dioxane degradation within one day. TCE was more slowly transformed over six days.

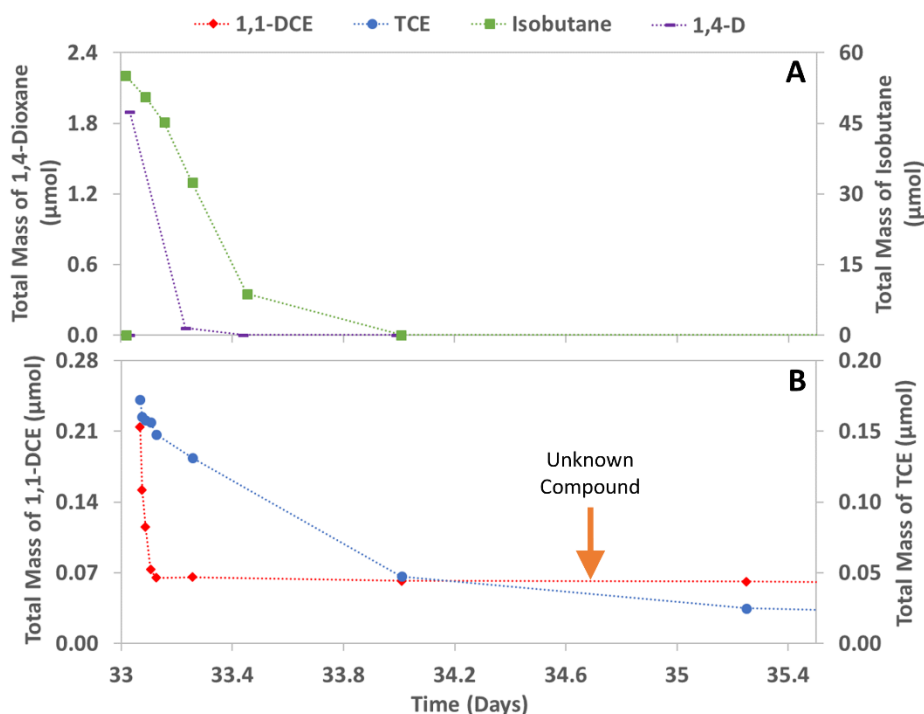


Figure 4.29. Total mass of 1,4-dioxane and isobutane (A), and 1,1-DCE and TCE (B) over time in one microcosm bioaugmented with 0.5 mg of isobutane-grown 21198 (set 3, bottle 1). This depicts an early spike of isobutane and COCs added to this microcosm on day 33.

Three subsequent additions of isobutane, TCE, 1,1-DCE, and 1,4-dioxane were made between days 40 and 75, with gradual increases in TCE concentrations, culminating in a liquid concentration of 4.4 to 4.6

mg/L. The final spike of primary substrate and COCs on day 75 is depicted in Figure 4.30. Rapid 1,1-DCE transformation continued to be observed, followed by concurrent isobutane uptake and 1,4-dioxane degradation. TCE was able to be slowly degraded by the established microbial community. The final measured concentration of TCE was approximately 1.1 mg/L (an approximately 75% overall reduction).

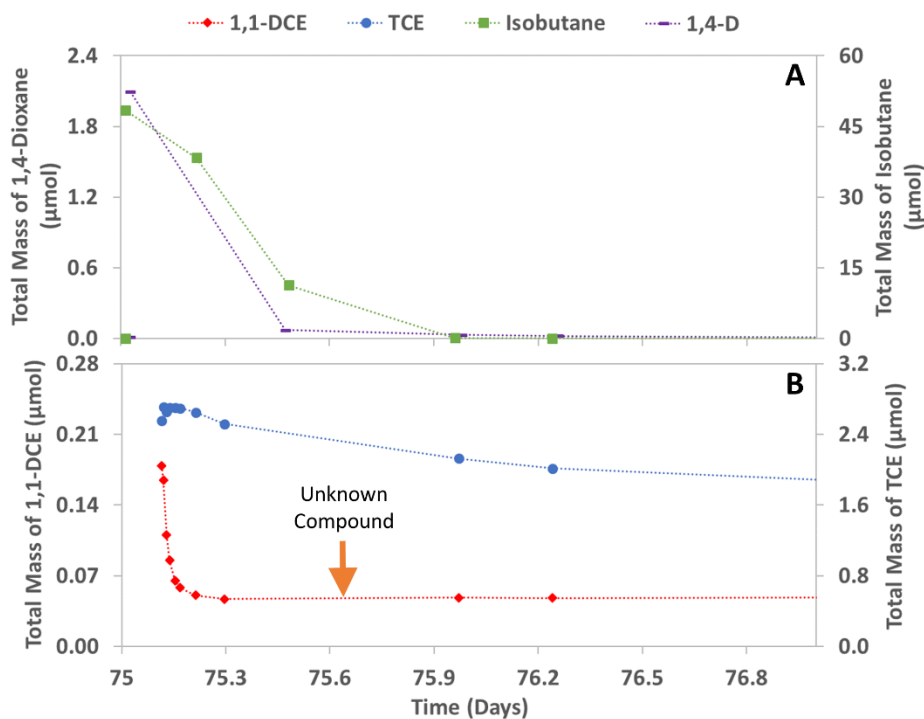


Figure 4.30. Total mass of 1,4-dioxane and isobutane (A), and 1,1-DCE and TCE (B) over time in one microcosm bioaugmented with 0.5 mg of isobutane-grown 21198 (set 3, bottle 1). This depicts the final spike of isobutane and COCs added to this microcosm on day 75 after gradual increases in TCE concentration.

As with the set 2 microcosms, TCE was added to the acetylene control bottles 3 and 4 at a comparable concentration to the last TCE spike in bottles 1 and 2 in order to verify that the observed decrease in TCE concentration in bottles 1 and 2 was due to biological activity. Over the span of 10 days, the TCE concentrations in bottles 3 and 4 decreased by approximately 25%, while the concentrations in the active bottles 1 and 2 decreased by approximately 50% (Figure 4.31). This suggests that while there is some TCE concentration decrease likely due to sorption to sediment and/or the rubber septa, there is also a biological component to the decrease.

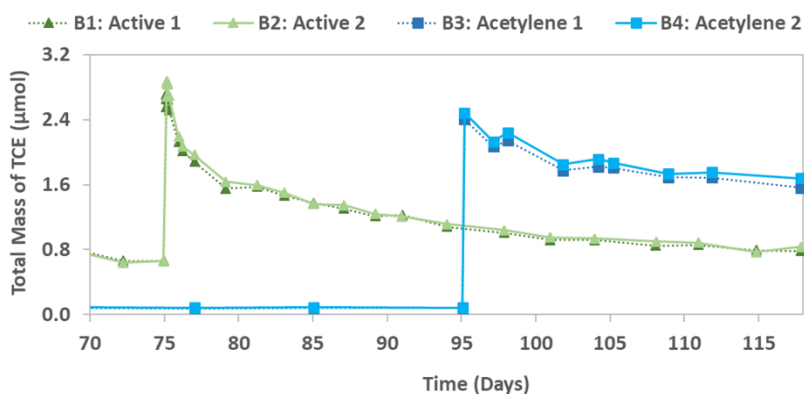


Figure 4.31. Comparison of total mass of TCE over time in microcosms bioaugmented with 0.5 mg of 21198. Active and acetylene control microcosms that were initially sparged to remove CAHs (set 3, bottles 3-6). TCE was added to the acetylene control bottles on day 102 in order to compare the change in total mass over time to the change observed in the active bottles.

Set 4 was comprised of four microcosms that were bioaugmented with 0.7 mg of 21198. Microcosms 1 and 2 were described as “active”, while microcosms 3 and 4 were acetylene controls. All microcosms had nutrients added to the system. Figure 4.32 depicts data from the long-term incubation of groundwater with isobutane in the presence of CAHs and bioaugmented with 0.7 mg of isobutane-grown 21198. The initial hypothesis regarding the residual mass of 1,1-DCE remaining in the set 3 microcosms was that not enough biomass was added to fully transform the 1,1-DCE, despite the transformation capacity determined in pure culture tests. The set 4 microcosms were bioaugmented with a greater initial biomass in order to fully transform the present mass of 1,1-DCE. As described in greater detail later in this section, 1,1-DCE transformation was observed immediately and rapidly, followed by isobutane uptake, 1,4-dioxane transformation, and slow TCE transformation. Subsequent respikes of isobutane, 1,4-dioxane, and CAHs were performed over 115 days of incubation, with gradually increasing concentrations of 1,1-DCE.

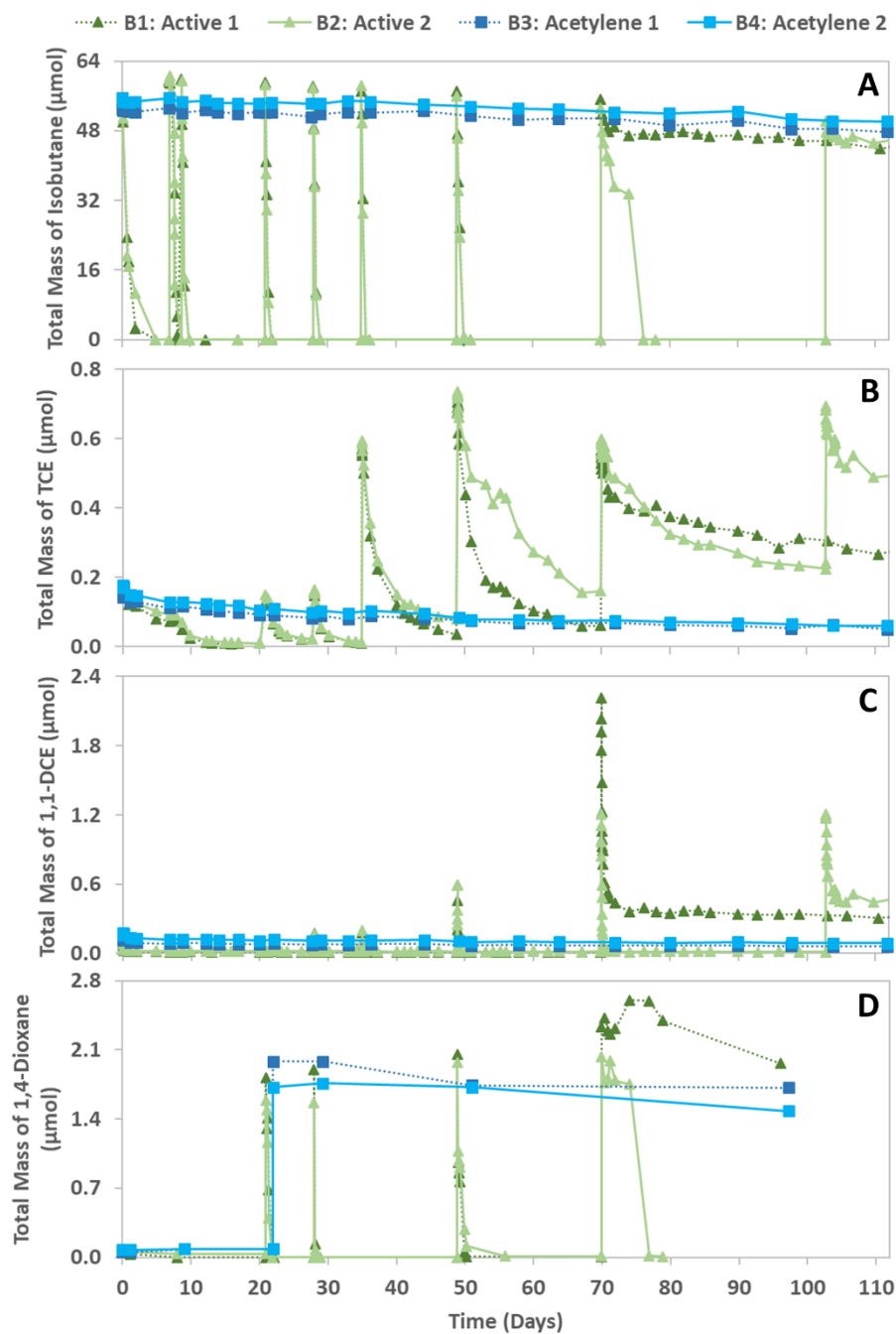


Figure 4.32. Total mass of isobutane (A), TCE (B), 1,1-DCE (C), and 1,4-dioxane (D) over time in microcosms bioaugmented with 0.7 mg of 21198 (set 4). Nutrients were added to all microcosms on day 0. Bottles 3 and 4 were acetylene controls. Bottles 1 and 2 were respiked with isobutane, TCE, 1,4-dioxane, and gradually increasing concentrations of 1,1-DCE over 115 days of incubation.

As shown in Figure 4.33, 1,1-DCE was immediately transformed within one hour. The total mass of 1,1-DCE decreased from approximately 0.1 μmol to approximately 0.015 μmol . The recurring presence of residual mass of 1,1-DCE supported the hypothesis that the residual was another unknown compound that was coeluting with 1,1-DCE and unable to be degraded by 21198. Isobutane was consumed at a

faster rate with greater initial biomass. Complete isobutane uptake was observed within two to five days. TCE was slowly transformed over 15 days with the addition of three spikes of isobutane. Though minimal 1,4-dioxane was initially present in the groundwater, the concentration decreased from approximately 115 to 130 $\mu\text{g/L}$ to below the detection limit over the first 2 spikes of isobutane (data not shown).

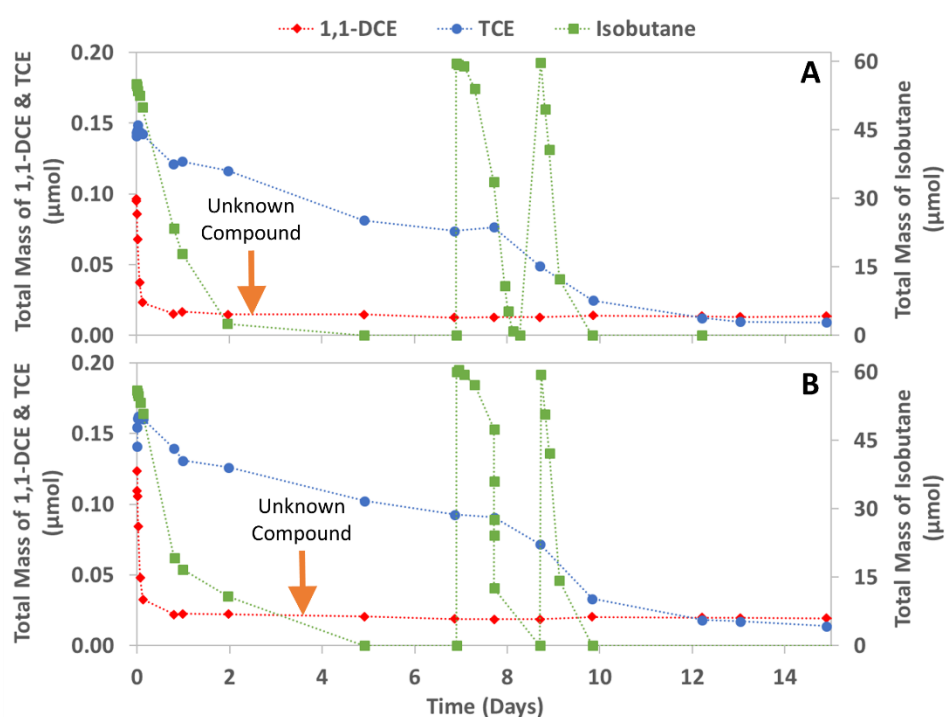


Figure 4.33. Total mass of isobutane, 1,1-DCE, and TCE over time in set 4, bottles 1 (A) and 2 (B) bioaugmented with 0.7 mg 21198.

Isobutane, TCE, and 1,4-dioxane were added to bottles 1 and 2 on day 21. Isobutane and 1,4-dioxane were transformed within one day, while TCE was more slowly degraded over seven days (data not shown). As shown in Figure 4.34, 1,1-DCE was re-added to the system on day 28, along with another spike of isobutane, TCE, and 1,4-dioxane. 1,1-DCE was transformed very rapidly (within 1 to 2 hours), followed by isobutane uptake and 1,4-dioxane degradation within one day. TCE was more slowly transformed over seven days.

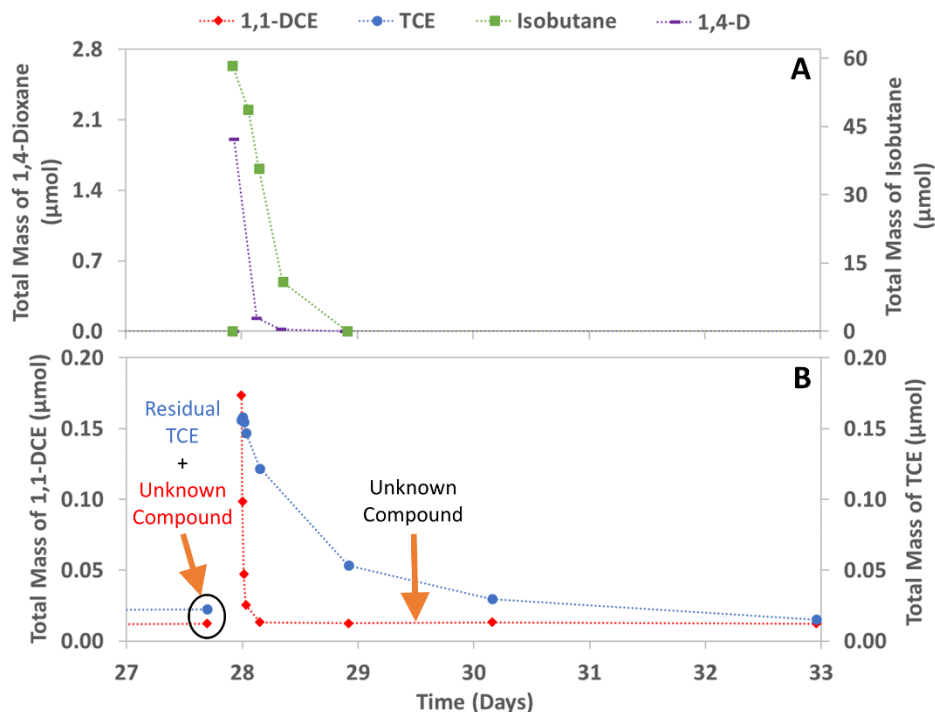


Figure 4.34. Total mass of 1,4-dioxane and isobutane (A), and 1,1-DCE and TCE (B) over time in one microcosm bioaugmented with 0.7 mg of isobutane-grown 21198 (set 4, bottle 1). This depicts an early spike of isobutane and COCs added to this microcosm on day 28.

Three subsequent additions of isobutane, TCE, 1,1-DCE, and 1,4-dioxane were made to bottle 1 between days 35 and 70, with gradual increases in 1,1-DCE concentration, culminating in a liquid concentration of 1.5 mg/L. The final spike of primary substrate and COCs on day 70 is depicted in Figure 4.35. 1,1-DCE transformation occurred more slowly and completely stalled at a concentration of approximately 200 $\mu\text{g/L}$ (0.3 μmol total mass). Isobutane uptake and 1,4-dioxane and TCE degradation were minimally observed. The total mass of 1,1-DCE transformed was approximately 1.9 μmol . The biomass present in the system was likely exhausted by the transformation of this quantity of 1,1-DCE.

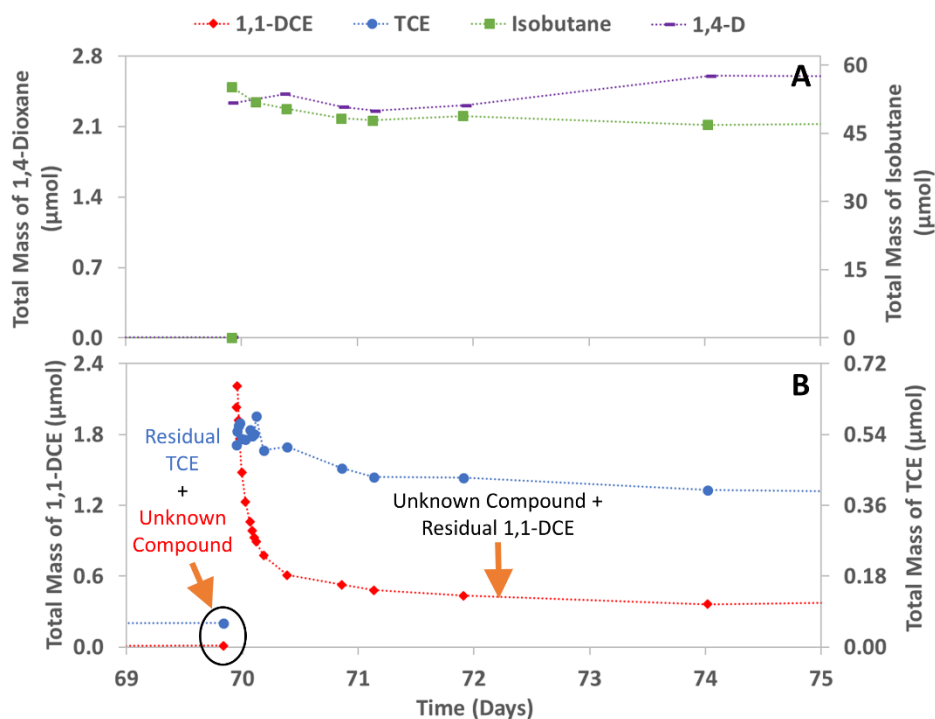


Figure 4.35. Total mass of 1,4-dioxane and isobutane (A), and 1,1-DCE and TCE (B) over time in one microcosm bioaugmented with 0.7 mg of isobutane-grown 21198 (set 4, bottle 1). This depicts the final spike of isobutane and COCs added to this microcosm on day 70 after gradual increases in 1,1-DCE concentration. The presence of the unknown compound cannot be visualized due to the scale of the plot. 1,1-DCE was not able to be fully transformed.

Three subsequent additions of isobutane, TCE, 1,1-DCE, and 1,4-dioxane were made to bottle 2 between days 35 and 70, with gradual increases in 1,1-DCE concentration, culminating in a liquid concentration of 0.97 mg/L. The second-to-last spike of primary substrate and COCs on day 70 is depicted in Figure 4.36. 1,1-DCE transformation occurred more slowly. Minimal isobutane uptake and 1,4-dioxane degradation were observed over four days following the respire. Between days 74 and 76, complete isobutane uptake and 1,4-dioxane transformation resumed, followed by slow TCE transformation. The system was able to moderately recover following the exposure to a high concentration of 1,1-DCE.

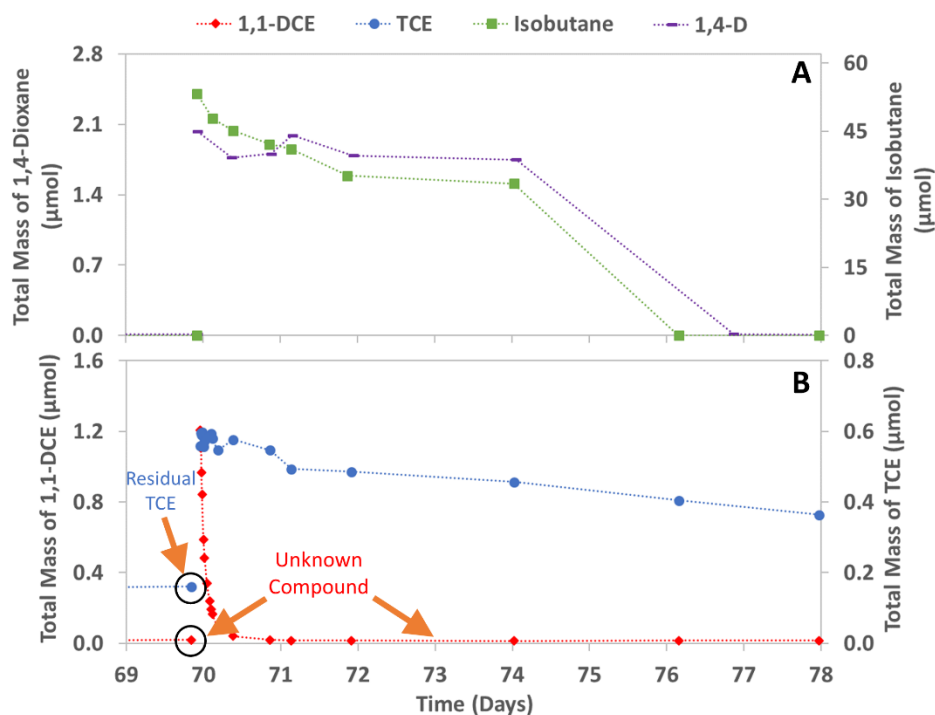


Figure 4.36. Total mass of 1,4-dioxane and isobutane (A), and 1,1-DCE and TCE (B) over time in one microcosm bioaugmented with 0.7 mg of isobutane-grown 21198 (set 4, bottle 2). This depicts a spike of isobutane and COCs added to this microcosm on day 70 after gradual increases in 1,1-DCE concentration. The presence of the unknown compound cannot be visualized due to the scale of the plot.

Cometabolism of 1,1-DCE was achieved by the bioaugmented culture and resulted in the rapid initial decrease of 1,1-DCE prior to isobutane utilization. This outcome was consistent with pure culture rate test results utilizing isobutane-grown 21198 that showed rapid transformation of 1,1-DCE but with a low transformation capacity. Based on the quantity of biomass added to the system and the calculated transformation capacity, 0.5 and 0.7 mg of 21198 should have been able to transform 0.33 and 0.46 μmol of 1,1-DCE, respectively. At a slow rate, TCE was also moderately transformed. Isobutane uptake exhibited a shorter lag time using a bioaugmented system, and 1,4-dioxane transformation occurred at a similar rate to isobutane uptake. These results were also consistent with pure culture rate test results with 21198. In summary, bioaugmentation with isobutane-grown 21198 was shown to successfully transform 1,1-DCE and promote sustained cometabolism over 115 days.

4.2.4 Isobutane competitive inhibition

As illustrated in the previous sections, 1,1-DCE toxicity and inhibition resulted in difficulty to stimulate native microbial communities to perform cometabolism. The experimental approach described in this section was conducted in an attempt to competitively inhibit the transformation of 1,1-DCE via the

addition of a high concentration of isobutane. Isobutane was initially added to two native microcosms established in the presence of CAHs at a liquid concentration of 6.6 and 6.7 mg/L (set 5, bottles 3 and 4), approximately ten times greater than the isobutane liquid concentrations in other microcosms. As shown in Figure 4.37, isobutane uptake was not observed over the course of 22 days. This suggests that a high concentration of isobutane cannot competitively inhibit the transformation of 1,1-DCE and preferentially uptake isobutane.

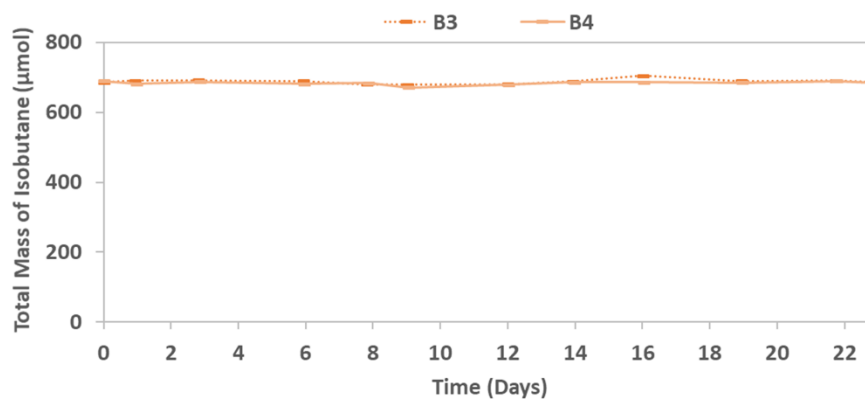


Figure 4.37. Total mass of isobutane over time in two native microcosms established in the presence of CAHs with approximately ten times greater starting mass of isobutane than other microcosms.

4.2.5 Isobutane and isobutanol

As shown in Figure 2.3, isobutanol is the product of isobutane transformation by SCAM. The purpose of this approach was to determine if isobutane-utilizers could be stimulated in the presence of isobutane and CAHs via the direct addition of the isobutane metabolite, isobutanol.

After approximately 20 days of incubation without isobutane uptake in the presence of CAHs and 1,4-dioxane, isobutanol was added to two native microcosms (set 5, bottles 5 and 6). Six additions of approximately 30 to 45 µmol of isobutanol were added to the microcosms over a span of 60 days (Figure 4.38A). Subsequent oxygen consumption and carbon dioxide production were observed, indicating that isobutanol-utilizers were present and active in the system (Figure 4.38B). The total mass of oxygen consumed was approximately 570 µmol, and the total mass of isobutanol consumed was approximately 220 µmol. Based on the stoichiometry from the redox reaction of isobutanol and oxygen, approximately 95 µmol of isobutanol would need to be consumed to produce the observed oxygen consumption. The discrepancy between the quantity of oxygen consumed for the amount of isobutanol utilized could be explained by isobutanol being used for the production of new cell mass rather than complete oxidation.

Isobutane uptake was not observed over 82 days of incubation following the first addition of isobutanol (Figure 4.38A), and minimal 1,1-DCE and TCE degradation occurred (Figure 4.38C). These results indicate that direct isobutanol-utilizers cannot necessarily utilize isobutane, and that isobutane-utilizers cannot be stimulated via the addition of isobutanol.

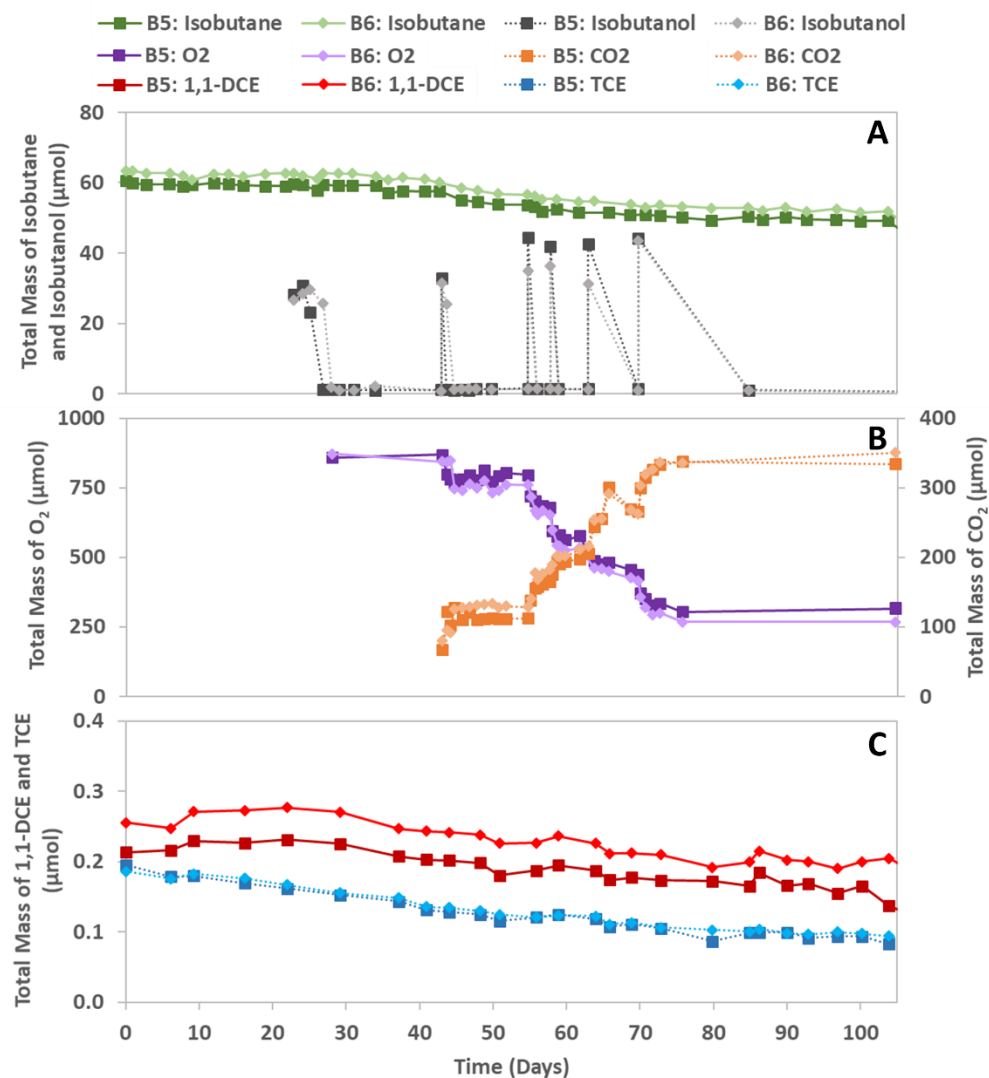


Figure 4.38. Total mass of isobutane and isobutanol (A), O_2 and CO_2 (B), and 1,1-DCE and TCE (C) in isobutanol-amended microcosms initially in the presence of isobutane. Isobutanol was initially added to microcosms on day 23.

An additional set of isobutanol-amended microcosms was established initially in the presence of CAHs and in the absence of isobutane. The purpose of this approach was to prevent the activation of the isobutane-induced monooxygenase enzyme responsible for the transformation of 1,1-DCE into the toxic epoxide and to stimulate an isobutanol-utilizing microbial community prior to the addition of isobutane. It was hypothesized that a healthy isobutanol-enriched culture could exhibit monooxygenase induction

following isobutane exposure. To investigate this hypothesis, three additions of 20 to 45 μmol of isobutanol were made to four microcosms in the presence of CAHs and in the absence of isobutane over the first 12 days of incubation (Figure 4.39A).

Subsequent oxygen consumption and carbon dioxide production were observed, indicating that isobutanol-utilizers were present in the system (Figure 4.39B). Approximately 60 μmol of isobutane were added to the microcosms on day 17. Isobutane uptake was not observed over 42 days of incubation (Figure 4.39A). Minimal 1,1-DCE and TCE degradation was observed (Figure 4.39C). Three additions of isobutanol were made between days 30 and 39. Corresponding oxygen consumption and carbon dioxide production were observed. This indicates that isobutanol-utilizers were not negatively impacted by the potential isobutane-induced monooxygenase production and subsequent 1,1-DCE epoxide formation. These results suggest that direct isobutanol-utilizers cannot necessarily utilize isobutane, and that isobutane-utilizers cannot be stimulated via the addition of isobutanol.

The total mass of oxygen consumed was approximately 790 μmol , and the total mass of isobutanol consumed was approximately 190 μmol . Based on the stoichiometry from the redox reaction of isobutanol and oxygen, approximately 130 μmol of isobutanol would need to be consumed to produce the observed oxygen consumption. The discrepancy between the quantity of oxygen consumed for the amount of isobutanol utilized could be explained by isobutanol being used for the production of new cell mass rather than complete oxidation.

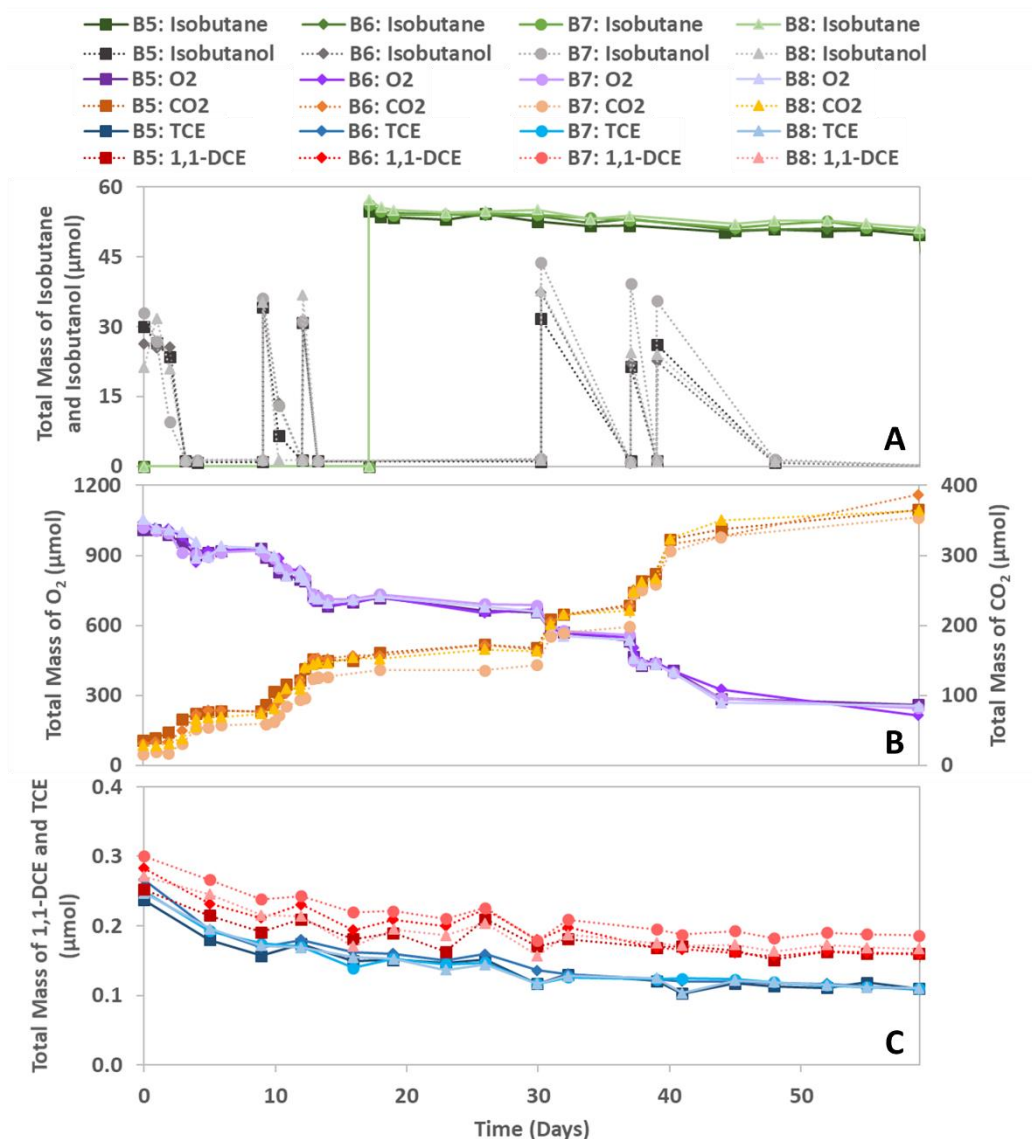


Figure 4.39. Total mass of isobutane and isobutanol (A), O₂ and CO₂ (B), and 1,1-DCE and TCE (C) in isobutanol-amended microcosms initially in the absence of isobutane. Isobutanol was initially added to microcosms on day 0.

4.2.6 Isobutene in the presence of CAHs

Due to the 1,1-DCE toxicity and inhibition, a different primary growth substrate was desired that would potentially better perform cometabolic transformations of CAHs. Preliminary work conducted by Rich suggested that a model isobutene-utilizer, ELW1, could transform TCE better than the model isobutane-utilizer, 21198 (Rich, 2015). To explore the use of isobutene as a primary growth substrate, eight microcosms were established in the presence of CAHs (set 6). All microcosms had nutrients added. Microcosms 7 and 8 were propyne controls. Isobutene uptake was not observed in microcosms 3 or 4 over 25 days or in microcosms 5 or 6 over 33 days of incubation in the presence of CAHs and 1,4-dioxane (Figure 4.40). Microcosms 3 and 4 were subsequently sparged (further discussed in Appendix D), and

microcosms 5 and 6 were bioaugmented with isobutene-grown ELW1 (further discussed in Section 4.2.8).

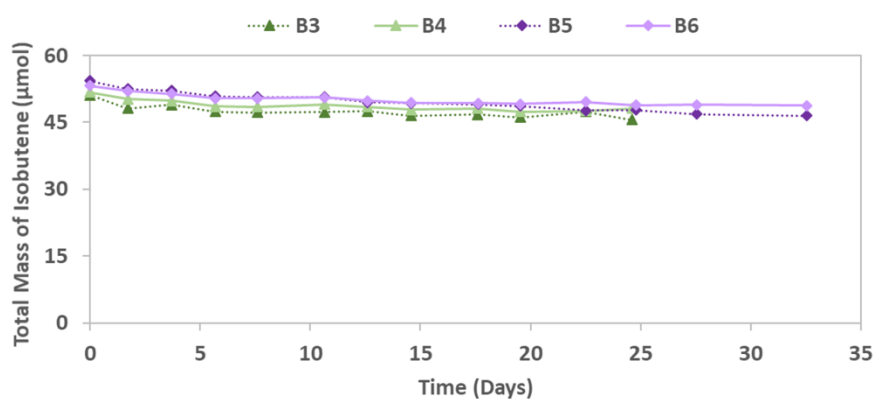


Figure 4.40. Total mass of isobutene over time in native isobutene microcosms established in the presence of CAHs (set 6, bottles 3 through 6). Microcosms 3 and 4 were sparged to remove CAHs on day 25, and microcosms 5 and 6 were bioaugmented with 0.9 mg of isobutene-grown ELW1 on day 33.

Isobutene uptake was observed in one native isobutene microcosm established in the presence of CAHs (set 6, bottle 1) after 52 days of incubation in the presence of CAHs (Figure 4.41). The long lag phase suggests either native isobutene-utilizers exist in low quantities in the subsurface at NAS North Island and/or exhibit slow growth rates. It took approximately 8 days for complete isobutene uptake (50 μmol). CAH transformation was strongly inhibited by the presence of isobutene. Rapid 1,1-DCE degradation was observed once the liquid concentration of isobutene was below 500 $\mu\text{g/L}$. Slower TCE degradation followed the transformation of 1,1-DCE. These results are consistent with those observed in pure culture studies with isobutene-grown ELW1 (Figure 4.12).

Three subsequent additions of isobutene, 1,1-DCE, and TCE showed a similar response, with increasing rates of isobutene uptake and TCE transformation with the second and third respire. As shown in Figure 4.42A/C, the degradation rates of isobutene and TCE approximately doubled for the second and third spike of primary substrate and CAHs. The rate of 1,1-DCE transformation greatly increased between the first and second spikes, but decreased slightly between the second, third, and fourth spikes (Figure 4.42B). 1,4-dioxane has been minimally transformed over the course of the four respikes of isobutene and CAHs (Figure 4.43).

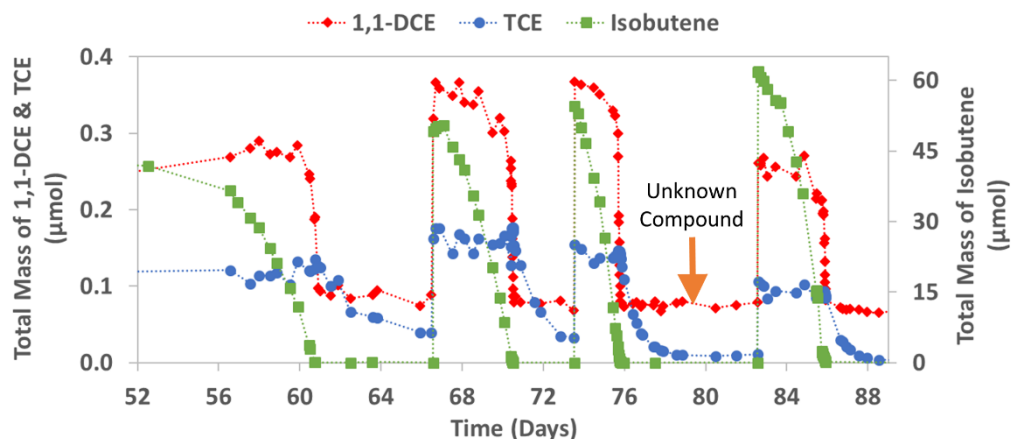


Figure 4.41. Total mass of isobutene, 1,1-DCE, and TCE over time in the native isobutene microcosm established in the presence of CAHs and 1,4-dioxane (set 6, bottle 1). The residual mass of 1,1-DCE remaining after the transformation is likely the unknown compound discussed in Section 4.2.3.

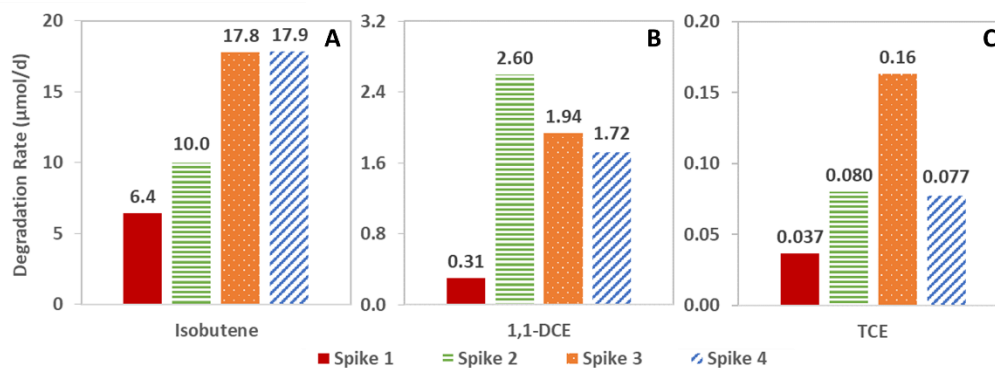


Figure 4.42. Comparison of degradation rates of isobutene (A), 1,1-DCE (B), and TCE (C) in the native isobutene microcosm established in the presence of CAHs over four spikes of primary substrate and CAHs (set 6, bottle 1).

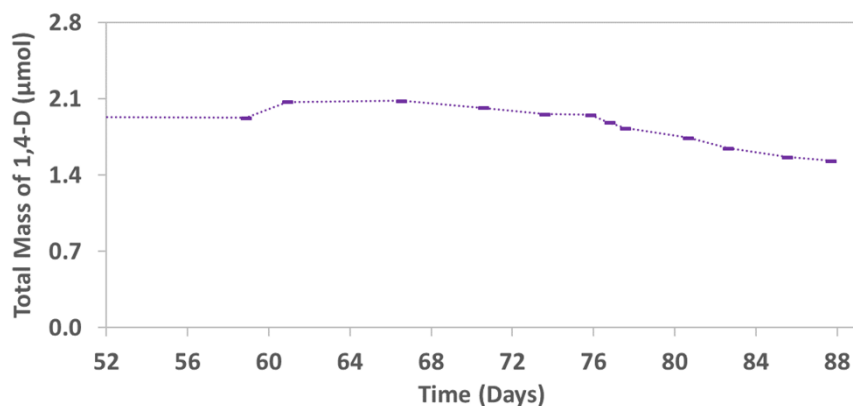


Figure 4.43. Total mass of 1,4-dioxane over time in the native isobutene microcosm established in the presence of CAHs and 1,4-dioxane (set 6, bottle 1).

Isobutene uptake was also observed in a second native isobutene microcosm established in the presence of CAHs (set 6, bottle 2) after 89 days of incubation in the presence of CAHs (Figure 4.44). The

rate of isobutene uptake was much slower than the initial observed rate in bottle 1. As with bottle 1, CAH transformation was strongly inhibited by isobutene. 1,1-DCE was not fully transformed, and TCE was not transformed.

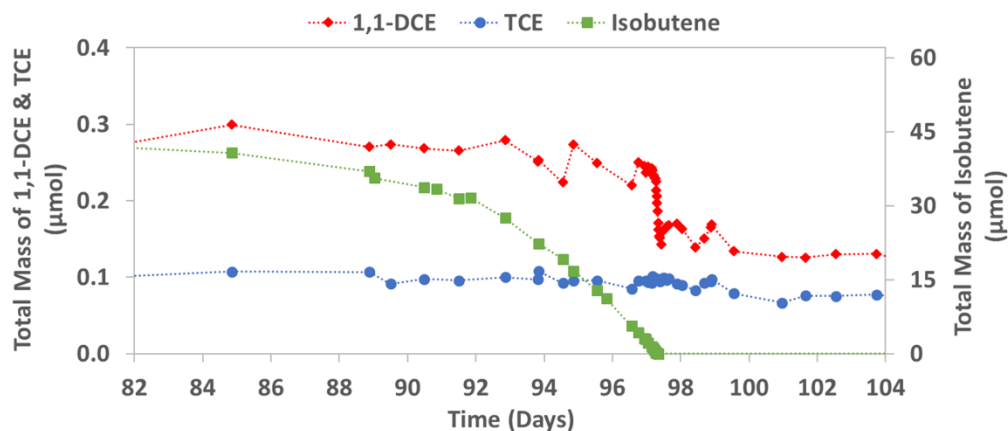


Figure 4.44. Total mass of isobutene, 1,1-DCE, and TCE over time in a second native isobutene microcosm established in the presence of CAHs (set 6, bottle 2).

The strong inhibition of 1,1-DCE transformation by the presence of isobutene is advantageous because a microbial population can be established during primary substrate utilization prior to the transformation of 1,1-DCE to the toxic epoxide. The complete transformation of TCE is also significant when compared to isobutene-enriched systems that minimally transformed TCE.

4.2.7 Isobutene bioaugmentation with ELW1

After 33 days of incubation without observable isobutene uptake, two native isobutene microcosms established in the presence of CAHs (set 6, bottles 5 and 6) were bioaugmented with 0.9 mg of isobutene-grown ELW1 (cultured as described in Sections 3.3.1 and 3.3.2). The biomass inoculum quantity was chosen based on the 1,1-DCE transformation capacity reported in Section 4.1.5 (0.30 µmol/mg TSS). Sufficient biomass was desired to be able to fully transform the 1,1-DCE present in the microcosms. 0.9 mg of ELW1 should have been able to transform 0.27 µmol of 1,1-DCE, the approximate starting mass of 1,1-DCE in bottles 5 and 6.

The total mass of isobutene, 1,1-DCE, and TCE over time are presented in Figure 4.45). CAH transformation was strongly inhibited by the presence of isobutene, as was observed in the native microcosm. Rapid 1,1-DCE transformation was observed after isobutene uptake, and slower TCE transformation followed. Slow 1,4-dioxane degradation was observed in both microcosms between days 33 and 67 (Figure 4.46).

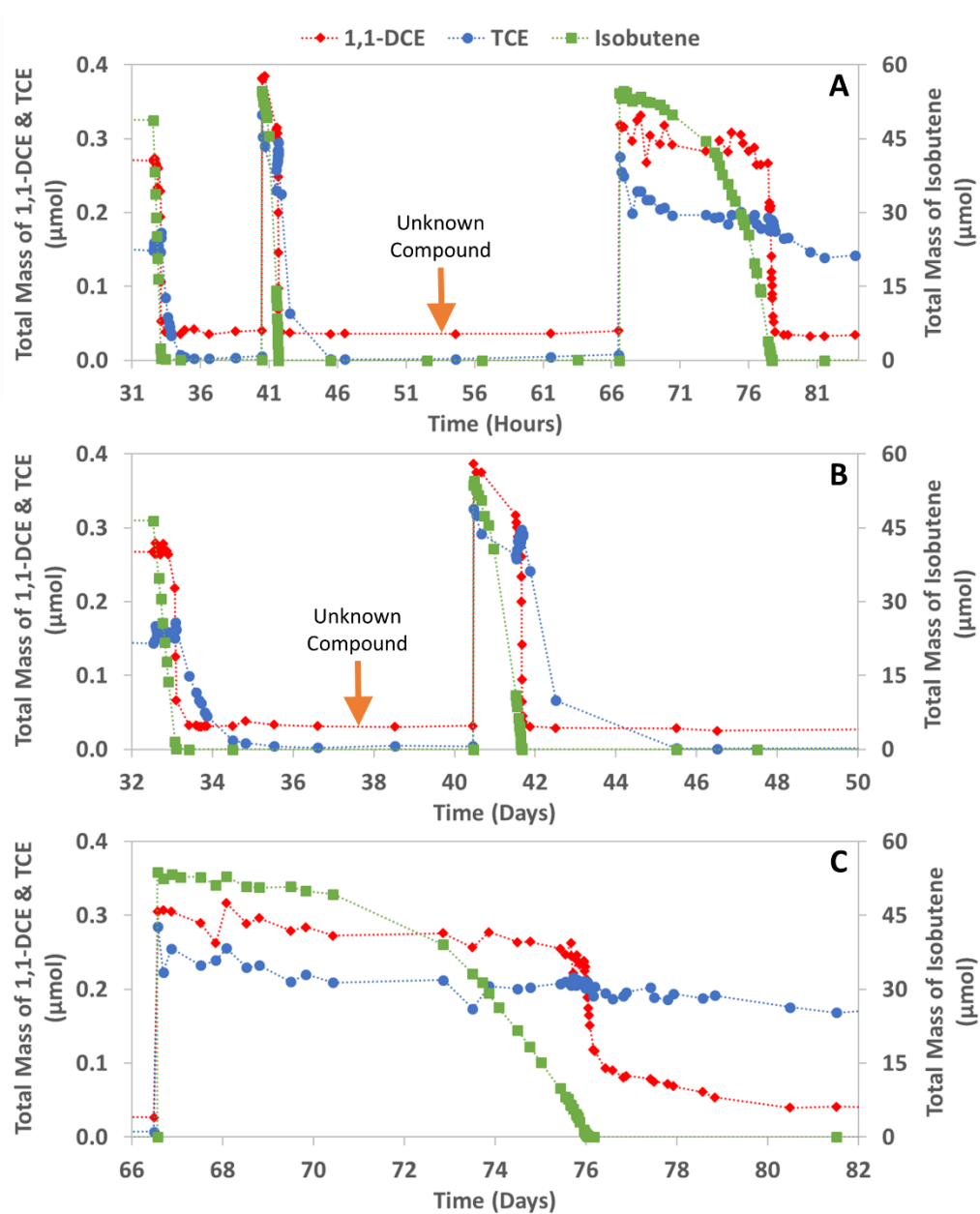


Figure 4.45. Total mass of isobutene, 1,1-DCE, and TCE over time in ELW1 bioaugmented microcosm 5 (A). The first and second spikes spanning 16 days (A) and the third spike spanning 16 days (B) are shown to observe the inhibition of CAH transformations by the presence of isobutene.

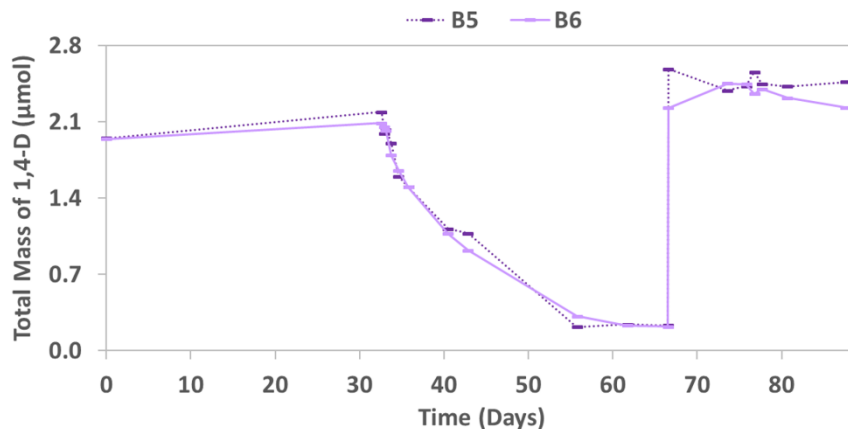


Figure 4.46. Total mass of 1,4-dioxane over time in native isobutene microcosms established in the presence of CAHs and bioaugmented with 0.9 mg of isobutene-grown ELW1 on day 33 (set 6, bottles 5 and 6).

The initial rate of isobutene uptake was much greater than that of the active native microcosm discussed in Section 4.2.6. The rate of isobutene uptake significantly decreased with subsequent spikes, and the rates of 1,1-DCE and TCE transformation between the second and third spikes decreased by 87% and 99%, respectively (Figure 4.47A-C). The dramatic differences in results from the native microcosm and the bioaugmented microcosms suggest that a different and more robust microbial community had been enriched from the native aquifer. Microbial analyses are currently being conducted by Dr. Michael Hyman from North Carolina State University to attempt to isolate the microorganism that was stimulated in the native isobutene microcosm.

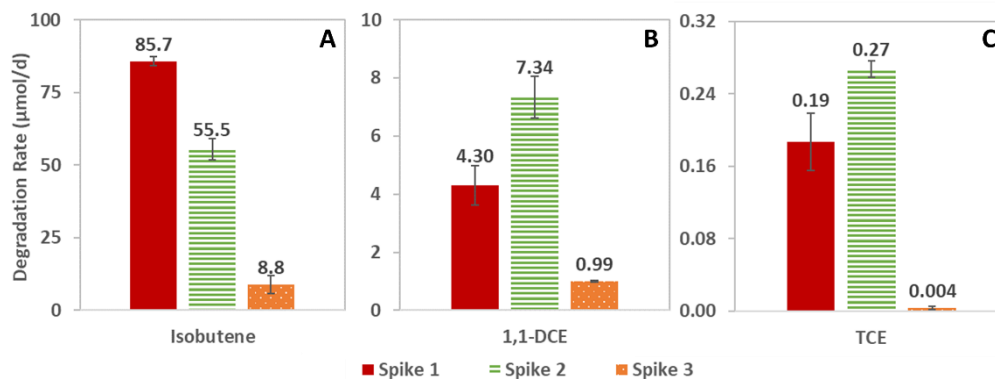


Figure 4.47. Comparison of degradation rates of isobutene (A), 1,1-DCE (B), and TCE (C) in ELW1 bioaugmented microcosms over three spikes of primary substrate and CAHs. Error bars indicate the standard deviation of a two sample average.

4.2.8 Nutrient assessment

In order to assess the importance of nutrient addition to the microcosm system, media addition was omitted from two microcosms established with isobutane in the absence of CAHs (set 2, bottles 1 and 2), and media was added to two microcosms established with isobutane in the absence of CAHs (set 2,

bottles 3 and 4). After approximately 12 days of incubation in the absence of CAHs, isobutane uptake was observed in bottles 2 through 4 (Figure 4.48). Isobutane uptake was not observed in bottle 1. Isobutane uptake in bottle 2 that did not have nutrients initially added stalled around day 20, and 0.2 mL of media was subsequently added to bottles 1 and 2 on day 24. This quantity of media corresponds to a concentration of approximately 620 $\mu\text{mol N/L}$ and 240 $\mu\text{mol P/L}$. Isobutane uptake in bottle 2 resumed, and the system was able to consume an additional spike of isobutane at a faster rate. Twenty days after media was added to bottle 1, isobutane uptake was observed.

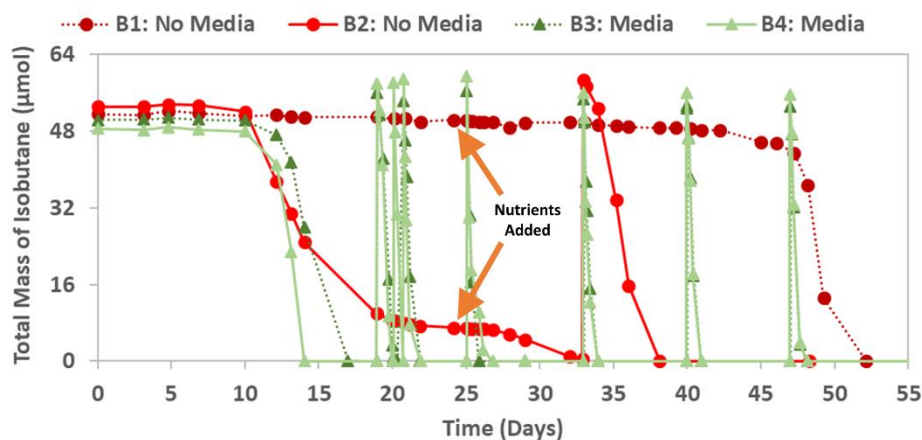


Figure 4.48. Liquid concentration of isobutane over time in microcosms initially sparged to remove CAHs (set 2). Microcosms 3 and 4 received nutrients on day zero, while microcosms 1 and 2 received nutrients on day 24.

The importance of nutrients to the success of bioremediation installations has been widely studied. Brockman et al. examined the effect nitrogen and phosphorous addition on in situ bioremediation of TCE (Brockman et al., 1995). The addition of nitrogen and phosphorous was found to increase the biomass count by an order of magnitude and increased the TCE biodegradative potential by three orders of magnitude. Palumbo and Scarborough also found that the addition of nitrogen and phosphorous increased methanotrophic populations by a factor of six and increased TCE mineralization (Palumbo and Scarborough, 1995). The findings of previous investigations and the microcosm results from this study indicate that nutrient addition is likely important to the stimulation of native microbes at the NAS North Island, though minimal aquifer solids were present in the system.

5.0 CONCLUSIONS

Pure-culture rate tests utilizing isobutane, ethane, and propane-grown 21198 and isobutene-grown ELW1 were conducted to assess these cultures' abilities to cometabolize CAHs and 1,4-dioxane in both single-compound and mixture analyses. Microcosm studies were also conducted using aquifer solids and groundwater from NAS North Island in San Diego, California to determine the potential for cometabolic stimulation of native microbial communities utilizing isobutane and isobutene as primary growth substrates. The main conclusions drawn from pure-culture studies are presented in Section 5.1, and the highlights from microcosms studies are described in Section 5.2.

5.1 Rate Test Studies

- For single-compound rate tests with 21198, isobutane-grown 21198 generally demonstrated faster rates of transformation than ethane and propane-grown 21198, though the rates of TCE transformation were similar for all substrates. More chlorinated compounds (TCE and 1,1,1-TCA) exhibited slower rates of transformation than less chlorinated compounds (c-DCE, 1,1-DCE, and 1,2-DCA). For all substrates the rates of transformation were ranked as follows: 1,1-DCE > 1,2-DCA > c-DCE > 1,1,1-TCA > TCE.
- ELW1 transformed TCE approximately twice as fast as 21198 grown on the substrates tested, though 21198 grown on all substrates transformed 1,4-dioxane much more readily than ELW1.
- Rate tests performed with mixtures of contaminants demonstrated similar results to single-compound tests. Transformation rates were generally fastest for isobutane-grown 21198, followed by ethane-grown 21198 and then propane-grown 21198. Isobutene-grown ELW1 was not able to readily transform 1,4-dioxane, 1,2-DCA, or 1,1,1-TCA, but was much more effective at transforming TCE.

5.2 Microcosm Studies

- Native isobutane-utilizers could not be stimulated in the presence of CAHs and 1,4-dioxane. It was hypothesized that the likely formation of the 1,1-DCE epoxide via activation of monooxygenase enzymes by isobutane was toxic and inhibitory to biostimulation of the native microbial community.
- Native isobutane-utilizers were able to be stimulated in the absence of CAHs. When 1,1-DCE and TCE were removed from solution via sparging, isobutane uptake was observed after 12 to 69 days

of incubation. Effective long-term cometabolic treatment of groundwater for the removal of CAHs and 1,4-dioxane was achieved, though slow TCE transformation was a process limitation.

- Bioaugmentation with isobutane-grown 21198 was a successful mechanism to achieve rapid 1,1-DCE transformation, moderate 1,4-dioxane transformation, and slow TCE transformation. Bioaugmentation effectively promoted long-term cometabolic treatment of groundwater for the removal of CAHs and 1,4-dioxane, though 1,1-DCE toxicity and slow TCE transformations remained as process limitations, as observed in the native system. The rapid transformation of 1,1-DCE, effective transformation of 1,4-dioxane, and slow TCE transformation were consistent with results observed with pure-culture studies of isobutane-grown 21198.
- Native isobutane-utilizers could not be stimulated via the addition of a high concentration of isobutane to competitively inhibit the transformation of 1,1-DCE.
- Native isobutane-utilizers could not be stimulated via the addition of isobutanol. Isobutanol consumption was observed in the presence of CAHs, but isobutane uptake was not observed. These results indicated that native isobutanol-utilizers were likely not isobutane-utilizers.
- Native isobutene-utilizers were able to be stimulated in the presence of CAHs and 1,4-dioxane. Isobutene strongly inhibited the transformation of CAHs. Once the liquid concentration of isobutene reached below 500 $\mu\text{g/L}$, rapid 1,1-DCE transformation was observed, followed by slower, but eventually complete, TCE degradation. 1,4-dioxane was minimally transformed by the native isobutene-utilizers. The dimensionless Henry's constant of isobutene (8.7) is much lower than that of isobutane (49.3); consequently, the initial liquid concentration of isobutene in the microcosms was much higher ($\sim 3,000 \mu\text{g/L}$) than that of isobutane ($\sim 600 \mu\text{g/L}$). The higher liquid concentration of the isobutene could have resulted in greater bioavailability and contributed to the strong inhibition of isobutene on the transformation of CAHs.
- Bioaugmentation with isobutene-grown ELW1 is a successful mechanism to achieve contaminant degradation. As observed in the native microcosm systems, isobutene strongly inhibited the transformation of CAHs. Once the liquid concentration of isobutene reached below 500 $\mu\text{g/L}$, rapid 1,1-DCE transformation was observed, followed by slower, but eventually complete, TCE degradation. 1,4-dioxane was slowly transformed in the bioaugmented system. Rates of isobutene uptake and CAH transformations were drastically reduced with successive additions of primary substrate and COCs, which strained the long-term viability of the bioaugmented system. The strong inhibition of CAH transformation by isobutene and the rapid transformation of 1,1-

DCE, minimal transformation of 1,4-dioxane, and slow TCE transformation were consistent with results observed with pure-culture studies of isobutene-grown 21198.

- The addition of inorganic nutrients was important for the stimulation of native isobutane utilizers, though the lack of substantial aquifer solids could have contributed to the necessity of nutrient additions.

6.0 FUTURE WORK

Future studies should be conducted with a greater initial mass of aquifer solids. Aquifer cores were not provided for the experimental studies described in this thesis. Experimentation was solely conducted using groundwater that contained trace amounts of sediment. The limited quantity of aquifer solids present for the experimentation described in this thesis could explain the importance of nutrient addition and the extended lag times observed in the native sparged isobutane microcosms and the native isobutene microcosms. Future studies should also focus on the potential use of other primary substrates such as methane and propane to determine their ability for potential concurrent transformation of 1,4-dioxane and CAHs. Future studies should also be performed in columns, rather than microcosms, to more accurately reflect natural transient subsurface conditions.

An objective of this study was to evaluate the potential use of a dual-substrate approach in which multiple primary substrates would be used to effectively transform contaminant mixtures. Based on the results presented in this thesis, further microcosm studies should be conducted utilizing isobutene first to promote the complete transformation of 1,1-DCE and TCE and then introducing isobutane to stimulate the transformation of 1,4-dioxane.

Numerical models for the cometabolism of primary substrates, 1,4-dioxane, and CAHs should also be developed for both pure-culture and microcosm results to be able to better understand and predict field-scale application and success. This would include a more detailed study of the inhibition kinetics of primary substrates and COCs and determination of kinetic parameters such as maximum transformation rates and half-saturation constants.

Microbial analyses should also be performed to compare the microbial communities established in the native and bioaugmented microcosms. A more detailed analysis should be conducted on the native isobutene microcosm to isolate the microorganism that was stimulated and enriched. If the microorganism is found to be different from ELW1, pure culture rate tests and microcosm bioaugmentation should be performed to evaluate its potential for field application.

7.0 REFERENCES

- Adams, G.O., Fufeyin, P.T., Okoro, S.E., and Ehinomen, I. (2015). Bioremediation, Biostimulation and Bioaugmentation: A Review. *International Journal of Environmental Bioremediation & Biodegradation* 3, 28–39.
- Adamson, D.T., Mahendra, S., Walker, K.L., Rauch, S.R., Sengupta, S., and Newell, C.J. (2014). A Multisite Survey To Identify the Scale of the 1,4-Dioxane Problem at Contaminated Groundwater Sites. *Environmental Science & Technology Letters* 1, 254–258.
- Agency for Toxic Substances and Disease Registry (2012). Toxicological Profile for 1,4-Dioxane.
- Alvarez-Cohen, L., and Speitel, G.E. (2001). Kinetics of aerobic cometabolism of chlorinated solvents. *Biodegradation* 12, 105–126.
- Anderson, J.E., and McCarty, P.L. (1996). Effect of Three Chlorinated Ethenes on Growth Rates for a Methanotrophic Mixed Culture. *Environmental Science & Technology* 30, 3517–3524.
- Anderson, R.H., Anderson, J.K., and Bower, P.A. (2012). Co-occurrence of 1,4-dioxane with trichloroethylene in chlorinated solvent groundwater plumes at US Air Force installations: Fact or fiction. *Integrated Environmental Assessment and Management* 8, 731–737.
- Aptim Federal Services, LLC (2018). Site Characterization Work Plan, ESTCP Project ER-201733, Evaluation of a Novel Multiple Primary Substrate (MPS) Cometabolic Biosparging Technology for In Situ Bioremediation of 1,4-Dioxane and Chlorinated Solvents in Groundwater, Operable Unit 11, Naval Air Station North Island, Coronado, California.
- Ayala, M., and Torres, E. (2004). Enzymatic activation of alkanes: constraints and prospective. *Applied Catalysis A: General* 272, 1–13.
- Aziz, C.E., Georgiou, G., and Speitel, G.E. (1999). Cometabolism of Chlorinated Solvents and Binary Chlorinated Solvent Mixtures Using *M. trichosporium* OB3b PP358. *Biotechnology and Bioengineering* 65, 100–107.
- Babu, J.P., and Brown, L.R. (1984). New Type of Oxygenase Involved in the Metabolism of Propane and Isobutane. *Applied and Environmental Microbiology* 48, 260–264.
- Balasubramanian, R., and Rosenzweig, A.C. (2007). Structural and Mechanistic Insights into Methane Oxidation by Particulate Methane Monooxygenase. *Accounts of Chemical Research* 40, 573–580.
- Battelle, and Accord Engineering, Inc. (2017). Draft Annual Evaluation Groundwater Monitoring Program Report for Calendar Year 2016, Naval Air Station North Island, Coronado, California.
- Bell, Philp, Aw, and Christofi (1998). The genus *Rhodococcus*. *Journal of Applied Microbiology* 85, 195–210.
- Bennett, P., Hyman, M., Smith, C., El Mugammar, H., Chu, M.-Y., Nickelsen, M., and Aravena, R. (2018). Enrichment with Carbon-13 and Deuterium during Monooxygenase-Mediated Biodegradation of 1,4-Dioxane. *Environmental Science & Technology Letters* 5, 148–153.
- Bradley, P.M. (2003). History and Ecology of Chloroethene Biodegradation: A Review. *Bioremediation Journal* 7, 81–109.
- Brockman, F.J., Payne, W., Workman, D.J., Soong, A., Manley, S., and Hazen, T.C. (1995). Effect of gaseous nitrogen and phosphorus injection on in situ bioremediation of a trichloroethylene-contaminated site. *Journal of Hazardous Materials* 41, 287–298.

- Burrows, K.J., Cornish, A., Scott, D., and Higgins, I.J. (1984). Substrate Specificities of the Soluble and Particulate Methane Mono-oxygenases of *Methylosinus trichosporium* OB3b. *Microbiology* 130, 3327–3333.
- Chang, H.-L., and Alvarez-Cohen, L. (1995). Transformation capacities of chlorinated organics by mixed cultures enriched on methane, propane, toluene, or phenol. *Biotechnology and Bioengineering* 45, 440–449.
- Chang, H.-L., and Alvarez-Cohen, L. (1996). Biodegradation of Individual and Multiple Chlorinated Aliphatic Hydrocarbons by Methane-Oxidizing Cultures. *Applied and Environmental Microbiology* 62, 3371–3377.
- Commander, Navy Installations Command Naval Air Station North Island.
- Deng, D., Li, F., Wu, C., and Li, M. (2018). Synchronic Biotransformation of 1,4-Dioxane and 1,1-Dichloroethylene by a Gram-Negative Propanotroph *Azoarcus* sp. DD4. *Environmental Science & Technology Letters* 5, 526–532.
- Doherty, R.E. (2000). A History of the Production and Use of Carbon Tetrachloride, Tetrachloroethylene, Trichloroethylene and 1,1,1-Trichloroethane in the United States: Part 2--Trichloroethylene and 1,1,1-Trichloroethane. *Environmental Forensics* 1, 83–93.
- Dolan, M.E., and McCarty, P.L. (1995). Methanotrophic Chloroethene Transformation Capacities And 1,1-dichloroethene Transformation Product Toxicity. *Environmental Science & Technology* 29, 2741–2747.
- Dolinová, I., Štrojsová, M., Černík, M., Němeček, J., Macháčková, J., and Ševců, A. (2017). Microbial degradation of chloroethenes: a review. *Environmental Science and Pollution Research* 24, 13262–13283.
- Doughty, D.M., Sayavedra-Soto, L.A., Arp, D.J., and Bottomley, P.J. (2005). Effects of Dichloroethene Isomers on the Induction and Activity of Butane Monooxygenase in the Alkane-Oxidizing Bacterium “*Pseudomonas butanovora*.” *Appl. Environ. Microbiol.* 71, 6054–6059.
- Frasconi, D., Zanaroli, G., and Danko, A.S. (2015). In situ aerobic cometabolism of chlorinated solvents: A review. *Journal of Hazardous Materials* 283, 382–399.
- Freedman, D.L., and Herz, S.D. (1996). Use of ethylene and ethane as primary substrates for aerobic cometabolism of vinyl chloride. *Water Environment Research* 68, 320–328.
- van der Geize, R., and Dijkhuizen, L. (2004). Harnessing the catabolic diversity of rhodococci for environmental and biotechnological applications. *Current Opinion in Microbiology* 7, 255–261.
- Hamamura, N., Page, C., Long, T., Semprini, L., and Arp, D.J. (1997). Chloroform Cometabolism by Butane-Grown CF8, *Pseudomonas butanovora*, and *Mycobacterium vaccae* JOB5 and Methane-Grown *Methylosinus trichosporium* OB3b. *Applied and Environmental Microbiology* 63, 3607–3613.
- Hatzinger, P.B., Banerjee, R., Rezes, R., Streger, S.H., McClay, K., and Schaefer, C.E. (2017). Potential for cometabolic biodegradation of 1,4-dioxane in aquifers with methane or ethane as primary substrates. *Biodegradation* 28, 453–468.
- Hou, C.T., Patel, R., Laskin, A.I., Barnabe, N., and Barist, I. (1983). Production of methyl ketones from secondary alcohols by cell suspensions of C2 to C4 n-Alkane-Grown Bacteria. *Applied and Environmental Microbiology* 46, 178–184.

- Hyman, M. (2013). Biodegradation of gasoline ether oxygenates. *Current Opinion in Biotechnology* 24, 443–450.
- Hyman, M. Activity-Based Protein Profiling for Detection of SCAM in 21198 Grown on Various Substrates.
- Jahng, D., and Wood, T.K. (1994). Trichloroethylene and Chloroform Degradation by a Recombinant Pseudomonad Expressing Soluble Methane Monooxygenase from *Methylosinus trichosporium* OB3B. *Applied and Environmental Microbiology* 60, 2473–2482.
- Jeffers, P.M., Ward, L.M., Woytowitch, L.M., and Wolfe, N.L. (1989). Homogeneous hydrolysis rate constants for selected chlorinated methanes, ethanes, ethenes, and propanes. *Environmental Science & Technology* 23, 965–969.
- Jitnuyanont, P., Sayavedra-Soto, L.A., and Semprini, L. (2001). Bioaugmentation of butane-utilizing microorganisms to promote cometabolism of 1,1,1-trichloroethane in groundwater microcosms. 12.
- Kim, Y., Semprini, L., and Arp, D.J. (1997). Aerobic Cometabolism of Chloroform and 1,1,1-Trichloroethane by Butane-Grown Microorganisms. 1, 135–148.
- Kim, Y., Arp, D.J., and Semprini, L. (2000). Chlorinated Solvent Cometabolism by Butane-Grown Mixed Culture. *Journal of Environmental Engineering* 126, 934–942.
- Kim, Y., Arp, D.J., and Semprini, L. (2002). Kinetic and inhibition studies for the aerobic cometabolism of 1,1,1-trichloroethane, 1,1-dichloroethylene, and 1,1-dichloroethane by a butane-grown mixed culture. *Biotechnology and Bioengineering* 80, 498–508.
- Kottegoda, S., Waligora, E., and Hyman, M. (2015). Metabolism of 2-Methylpropene (Isobutylene) by the Aerobic Bacterium *Mycobacterium* sp. Strain ELW1. *Applied and Environmental Microbiology* 81, 1966–1976.
- Mackay, D., and Shiu, W.Y. (1981). A critical review of Henry's law constants for chemicals of environmental interest. *Journal of Physical and Chemical Reference Data* 10, 1175–1199.
- MacMichael, G.J., and Brown, L.R. (1987). Role of Carbon Dioxide in Catabolism of Propane by "Nocardia paraffinicum" (*Rhodococcus rhodochrous*). *Applied and Environmental Microbiology* 53, 65–69.
- Mahendra, S., and Alvarez-Cohen, L. (2006). Kinetics of 1,4-Dioxane Biodegradation by Monooxygenase-Expressing Bacteria. *Environmental Science & Technology* 40, 5435–5442.
- Malachowsky, K.J., Phelps, T.J., Teboli, A.B., Minnikin, D.E., and White, D.C. (1994). Aerobic Mineralization of Trichloroethylene, Vinyl Chloride, and Aromatic Compounds by *Rhodococcus* Species. *Applied and Environmental Microbiology* 60, 542–548.
- Mandelbaum, R.T., Shati, M.R., and Ronen, D. (1997). In situ microcosms in aquifer bioremediation studies. *FEMS Microbiology Reviews* 20, 489–502.
- Martinkova, L., Uhnakova, B., Patek, M., Nesvera, J., and Kren, V. (2009). Biodegradation potential of the genus *Rhodococcus*. *Environment International* 35, 162–177.
- Mohr, T. (2001). Solvent Stabilizers White Paper (San Jose, California).
- Mohr, T., Stickney, J., and DiGuseppi, W. (2010). *Environmental Investigation and Remediation: 1,4-Dioxane and other Solvent Stabilizers* (CRC Press).

- Oldenhuis, R., Oedzes, J.Y., van der Waarde, J.J., and Janssen, D.B. (1991). Kinetics of Chlorinated Hydrocarbon Degradation by *Methylophilus trichosporium* OB3b and Toxicity of Trichloroethylene. *Applied and Environmental Microbiology* 57, 7–14.
- Palumbo, A.V., and Scarborough, S.P. (1995). Influence of Nitrogen and Phosphorus on the In Situ Bioremediation of Trichloroethylene. *Applied Biochemistry and Biotechnology* 51/52, 635–647.
- Rich, S. (2015). Kinetic Analysis of the Aerobic Degradation of Chlorinated Ethenes by the *Mycobacterium* ELW-1 and Chlorinated Ethanes and Ethenes by *Rhodococcus rhodochrous* ATCC 21198. Honors B.S. Thesis. Oregon State University.
- Rolston, H. (2017). Experimental Demonstration and Modeling of Aerobic Cometabolism of 1,4-Dioxane by Isobutane-Utilizing Microorganisms in Aquifer Microcosms. M.S. Thesis. Oregon State University.
- Rui, L., Kwon, Y.M., Reardon, K.F., and Wood, T.K. (2004). Metabolic pathway engineering to enhance aerobic degradation of chlorinated ethenes and to reduce their toxicity by cloning a novel glutathione S-transferase, an evolved toluene o-monooxygenase, and gamma-glutamylcysteine synthetase. *Environmental Microbiology* 6, 491–500.
- Schrlau, J.E., Kramer, A.L., Chlebowski, A., Truong, L., Tanguay, R.L., Simonich, S.L.M., and Semprini, L. (2017). Formation of Developmentally Toxic Phenanthrene Metabolite Mixtures by *Mycobacterium* sp. ELW1. *Environmental Science & Technology* 51, 8569–8578.
- Semprini, L., Dolan, M.E., Mathias, M.A., Hopkins, G.D., and McCarty, P.L. (2007a). Bioaugmentation of butane-utilizing microorganisms for the in situ cometabolic treatment of 1,1-dichloroethene, 1,1-dichloroethane, and 1,1,1-trichloroethane. *European Journal of Soil Biology* 43, 322–327.
- Semprini, L., Dolan, M.E., Mathias, M.A., Hopkins, G.D., and McCarty, P.L. (2007b). Laboratory, field, and modeling studies of bioaugmentation of butane-utilizing microorganisms for the in situ cometabolic treatment of 1,1-dichloroethene, 1,1-dichloroethane, and 1,1,1-trichloroethane. *Advances in Water Resources* 30, 1528–1546.
- Semprini, L., Dolan, M.E., Hopkins, G.D., and McCarty, P.L. (2009). Bioaugmentation with butane-utilizing microorganisms to promote in situ cometabolic treatment of 1,1,1-trichloroethane and 1,1-dichloroethene. *Journal of Contaminant Hydrology* 103, 157–167.
- Tanaka, K., Kimura, K., and Yamamoto, M. (1973). Process for Producing Cells of Microorganisms (Machida).
- Thankitkul, S. (2016). Kinetic Analysis and Modeling Cometabolic Transformation of CAHs by *Rhodococcus* ATCC 21198 (Oregon State University).
- Tovanabootr, A., and Semprini, L. (1998). Comparison of TCE Transformation Abilities of Methane- and Propane-Utilizing Microorganisms. *Bioremediation Journal* 2, 105–124.
- Tsien, H.-C., Brusseau, G.A., Hanson, R.S., and Wackett, L.P. (1989). Biodegradation of Trichloroethylene by *Methylophilus trichosporium* OB3b. *Applied and Environmental Microbiology* 55, 3155–3161.
- US EPA (1992). Handbook of RCRA Ground-Water Monitoring Constituents: Chemical & Physical Properties.
- US EPA (1995). National Primary Drinking Water Regulations: cis- and trans-1,2-Dichloroethylene.
- US EPA (2006). Treatment technologies for 1,4-Dioxane: Fundamentals and field applications (Office of Solid Waste and Emergency Response).

US EPA (2016). The Third Unregulated Contaminant Monitoring Rule (UCMR 3): Fact Sheet for Assessment Monitoring (List 1 Contaminants).

US EPA (2017a). Risk Assessment for Carcinogenic Effects.

US EPA (2017b). Technical Fact Sheet – 1,4-Dioxane.

Verce, M.F., and Freedman, D.L. (2000). Modeling the kinetics of vinyl chloride cometabolism by an ethane-grown *Pseudomonas* sp. *Biotechnology and Bioengineering* *71*, 274–285.

Vogel, T. (1987). Rate of abiotic formation of 1,1-dichloroethylene from 1,1,1-trichloroethane in groundwater. *Journal of Contaminant Hydrology* *1*, 299–308.

(2010). *In situ remediation of chlorinated solvent plumes* (New York: Springer).

8.0 APPENDICES

A. Recipe for mineral salts media (growth media)

Mineral salts medial trace element solution:

Compound	Mass added to 500 mL nano-pure H₂O (g)
EDTA	25
ZnSO ₄ ·7H ₂ O	11
CaCl ₂	2.27
MnCl ₂ ·4H ₂ O	2.53
FeSO ₄ ·7H ₂ O	2.5
(NH ₄) ₆ Mo ₇ O ₂₄ ·4H ₂ O	0.55
CuSO ₄ ·5H ₂ O	0.753
CoCl ₂ ·6H ₂ O	0.855

1. Adjust pH to 6.0 with KOH
2. Store in refrigerator

Solution 1 (concentrated by 10x):

Compound	Quantity added to 1,000 mL nano-pure H₂O
NH ₄ Cl	20 g
MgCl ₂ ·6H ₂ O	0.75 g
(NH ₄) ₂ SO ₄	1.0 g
Trace element soln.	2.0 mL

Solution 2 (concentrated by 100x):

Compound	Mass added to 1,000 mL nano-pure H₂O (g)
K ₂ HPO ₄	155
NaH ₂ PO ₄	85

1. Autoclave Solution 1 and Solution 2 separately
2. Mix 1X concentration by dilution with autoclaved nano-pure water

B. Heterotrophic and minimal media plates

Heterotrophic growth plates:

Compound	Mass added to 1,000 mL nano-pure H₂O (g)
Tryptic soy	3
Glucose	10
Agar	15

1. Autoclave solution
2. Store at 4°C prior to use
3. Wrap in parafilm after streaking and store at 30°C

Minimal media plates:

Compound	Quantity added to 890 mL nano-pure H₂O
Agar	15 g
Solution 1	100 mL
Solution 2	10 mL

1. Autoclave agar and nano-pure water
2. Add Solution 1 and Solution 2 once the agar mixture is cool to the touch
3. Store at 4°C prior to use

C. Pure Culture Rate Test Results

C.1 Isobutane-grown 21198 Pure Culture Rate Test Results

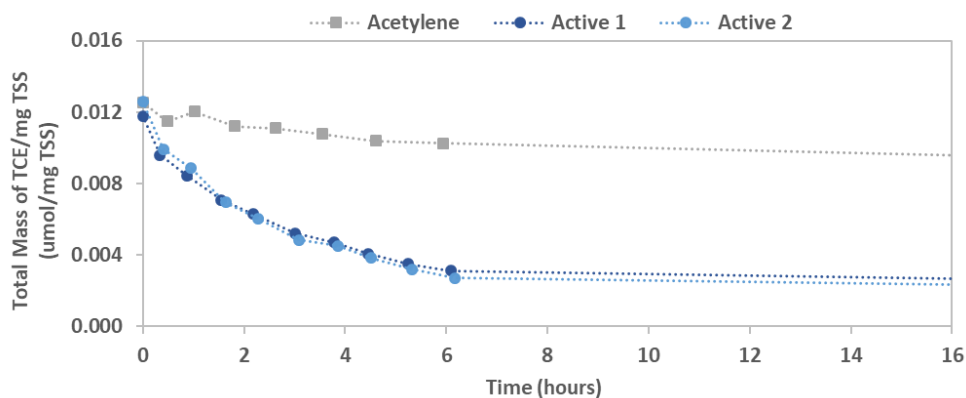


Figure A.1. Total mass of TCE per mg TSS over time for isobutane-grown 21198.

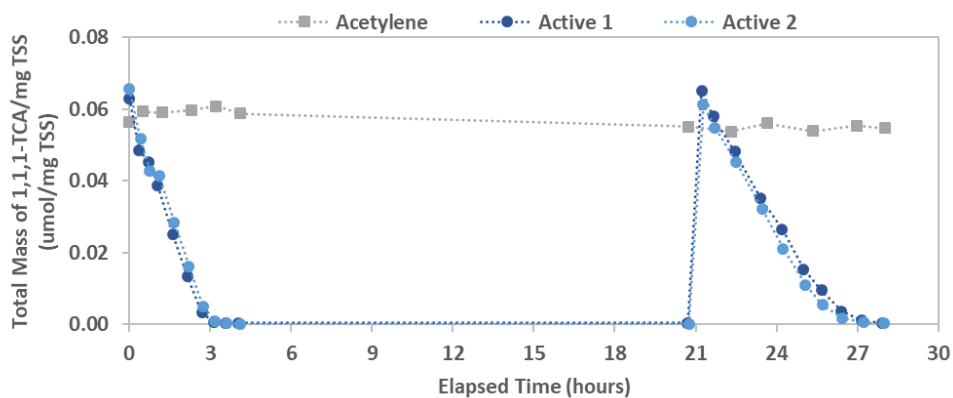


Figure A.2. Total mass of 1,1,1-TCA per mg TSS over time for isobutane-grown 21198.

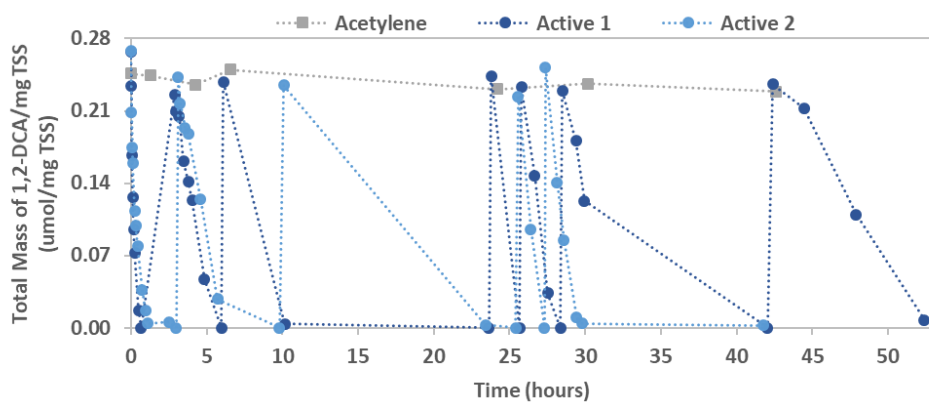


Figure A.3. Total mass of 1,2-DCA per mg TSS over time for isobutane-grown 21198.

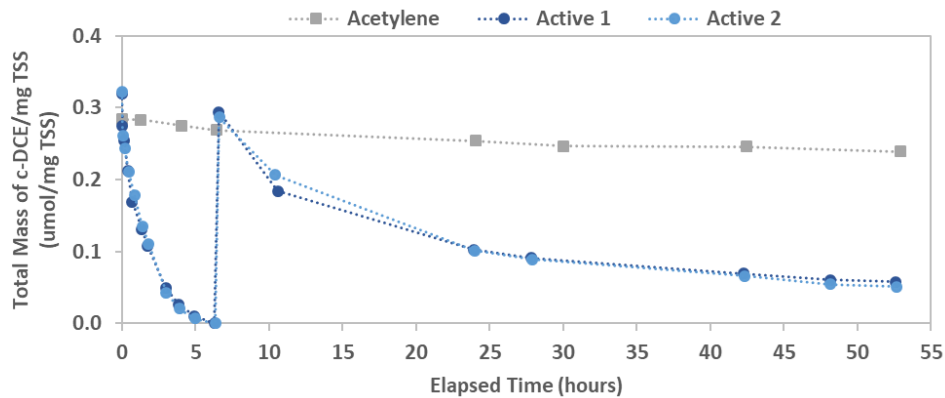


Figure A.4. Total mass of *c*-DCE per mg TSS over time for isobutane-grown 21198.

C.2 Ethane-grown 21198 Pure Culture Rate Test Results

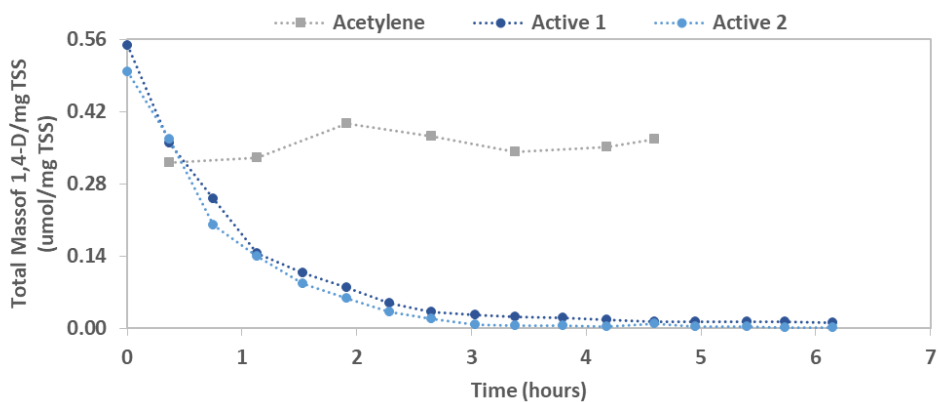


Figure A.5. Total mass of 1,4-dioxane per mg TSS over time for ethane-grown 21198.

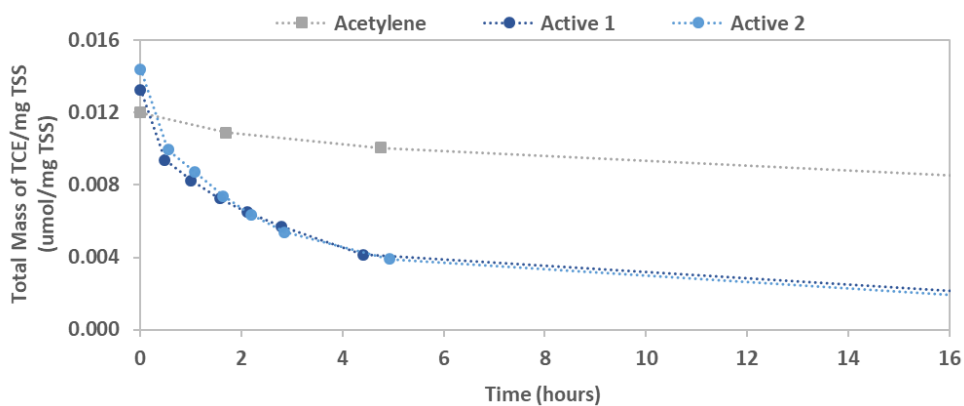


Figure A.6. Total mass of TCE per mg TSS over time for ethane-grown 21198.

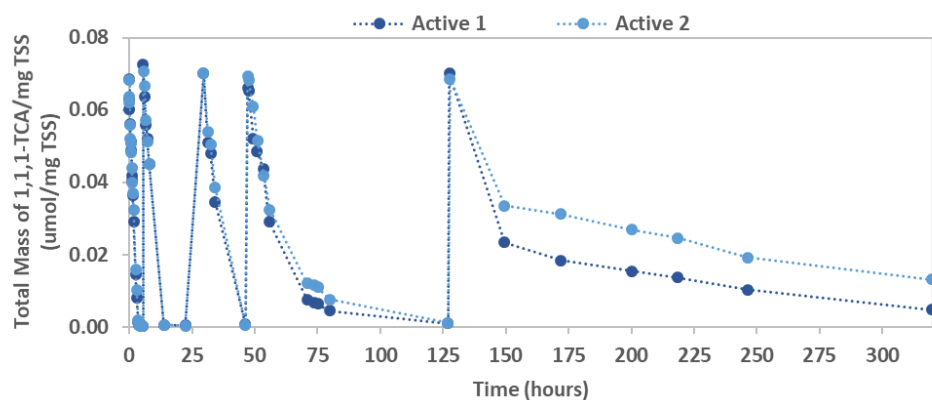


Figure A.7. Total mass of 1,1,1-TCA per mg TSS over time for ethane-grown 21198.

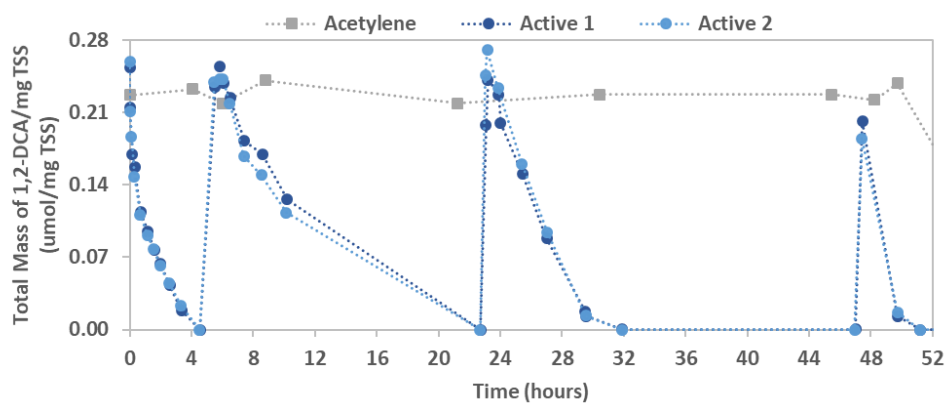


Figure A.8. Total mass of 1,2-DCA per mg TSS over time for ethane-grown 21198.

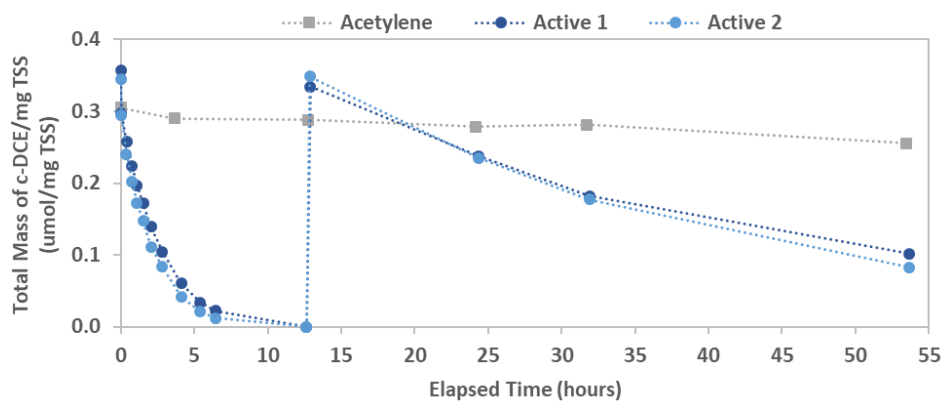


Figure A.9. Total mass of c-DCE per mg TSS over time for ethane-grown 21198.

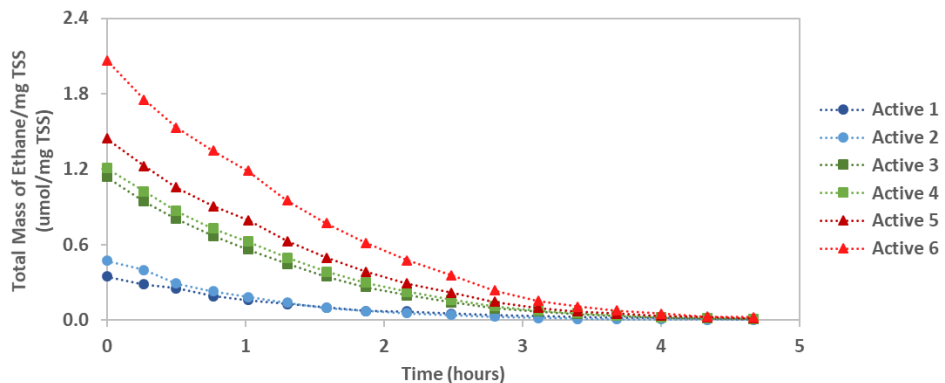


Figure A.10. Total mass of ethane per mg TSS over time for ethane-grown 21198.

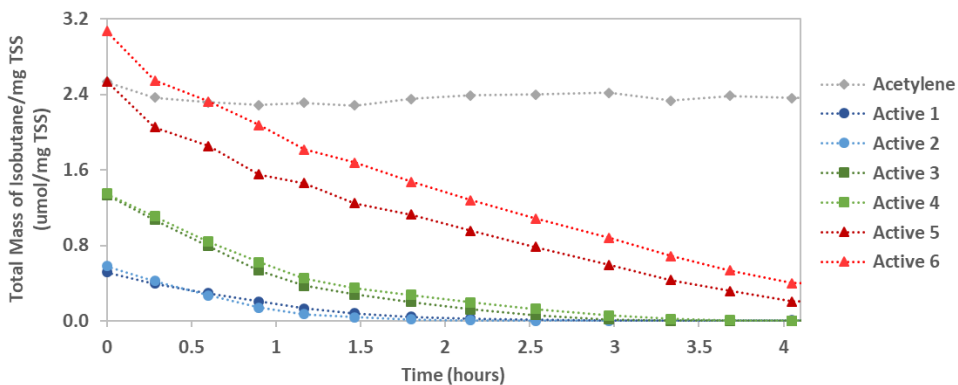


Figure A.11. Total mass of isobutane per mg TSS over time for ethane-grown 21198.

C.3 Propane-grown 21198 Pure Culture Rate Test Results

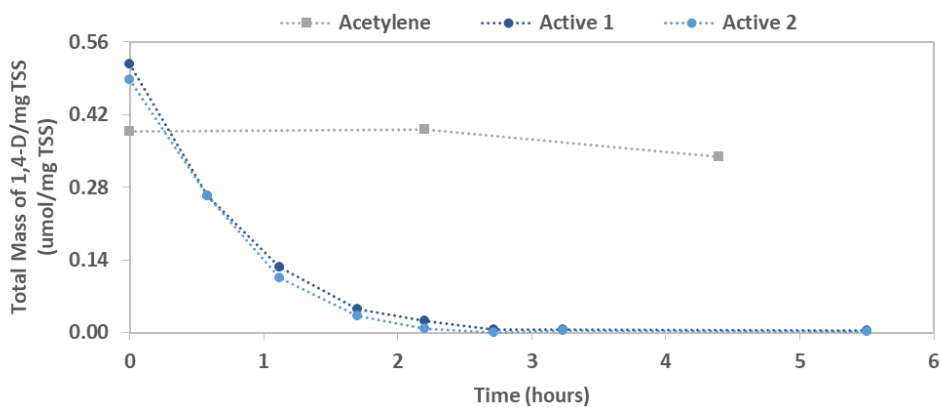


Figure A.12. Total mass of 1,4-dioxane per mg TSS over time for propane-grown 21198.

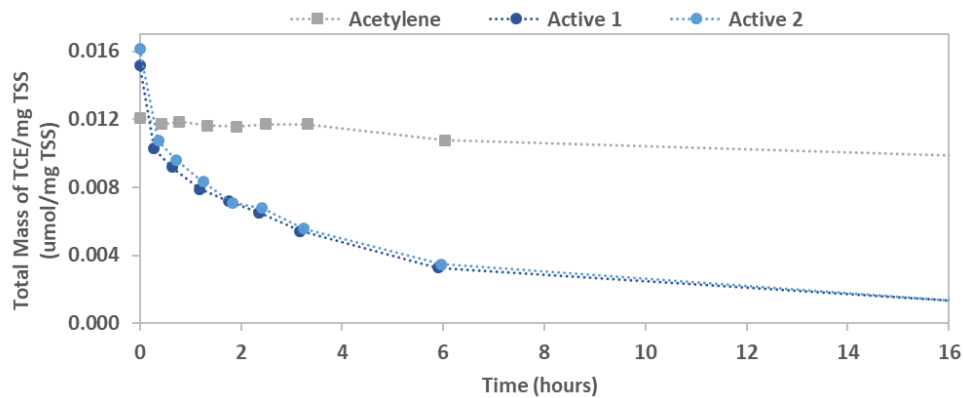


Figure A.13. Total mass of TCE per mg TSS over time for propane-grown 21198.

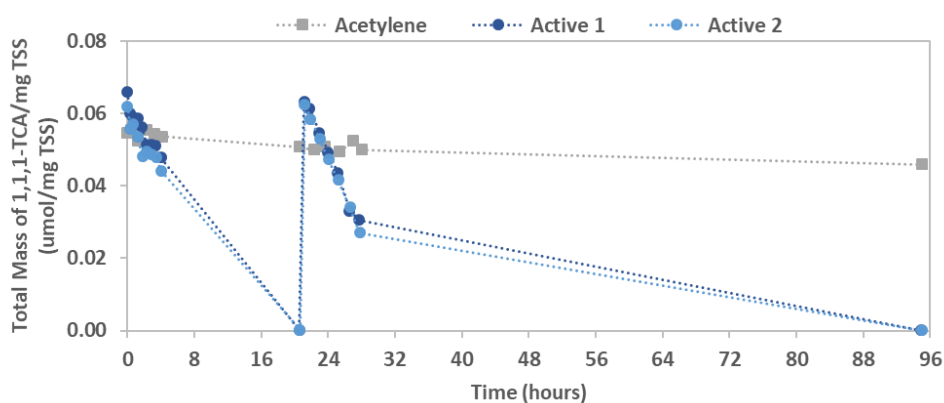


Figure A.14. Total mass of 1,1,1-TCA per mg TSS over time for propane-grown 21198.

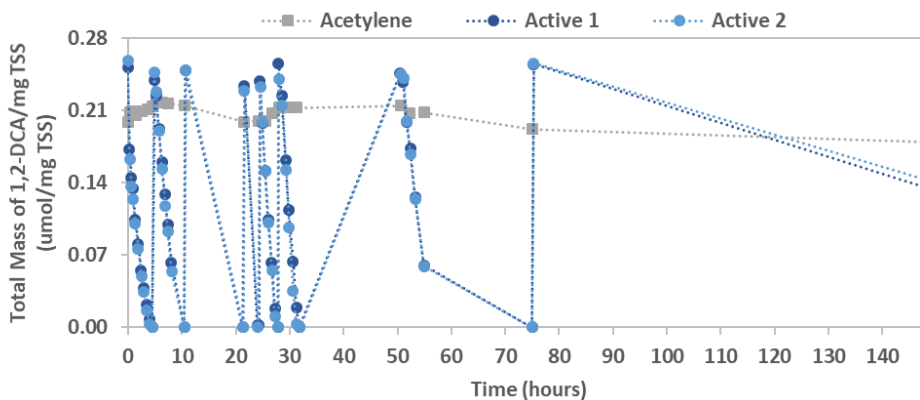


Figure A.15. Total mass of 1,2-DCA per mg TSS over time for propane-grown 21198.

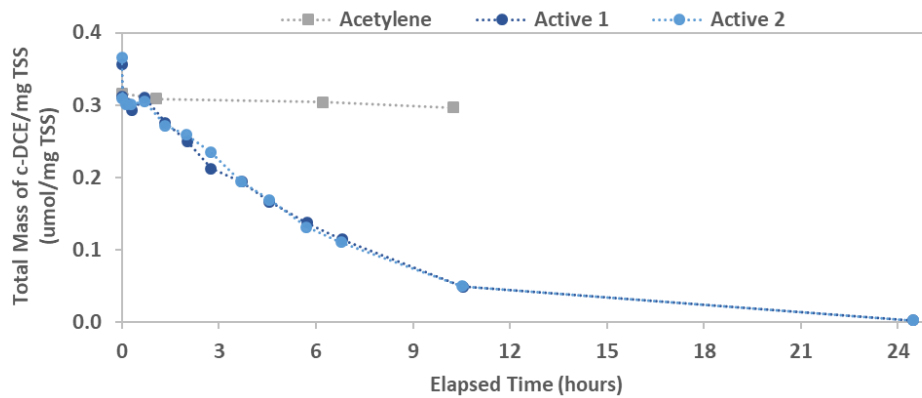


Figure A.16. Total mass of c-DCE per mg TSS over time for propane-grown 21198.

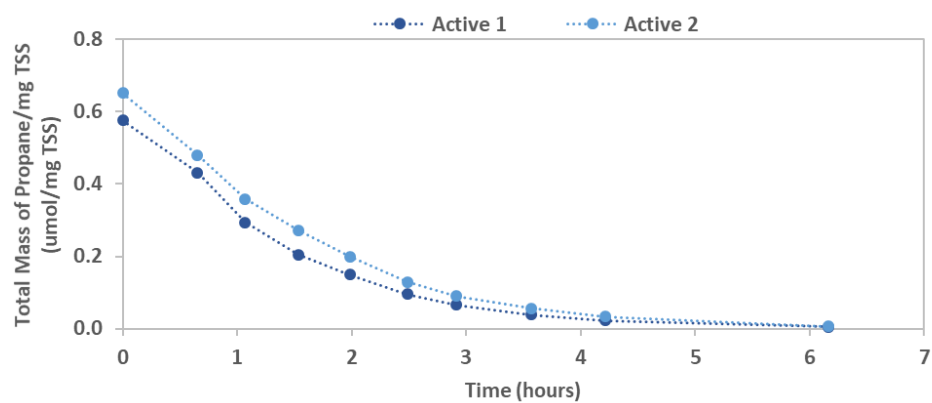


Figure A.17. Total mass of propane per mg TSS over time for propane-grown 21198.

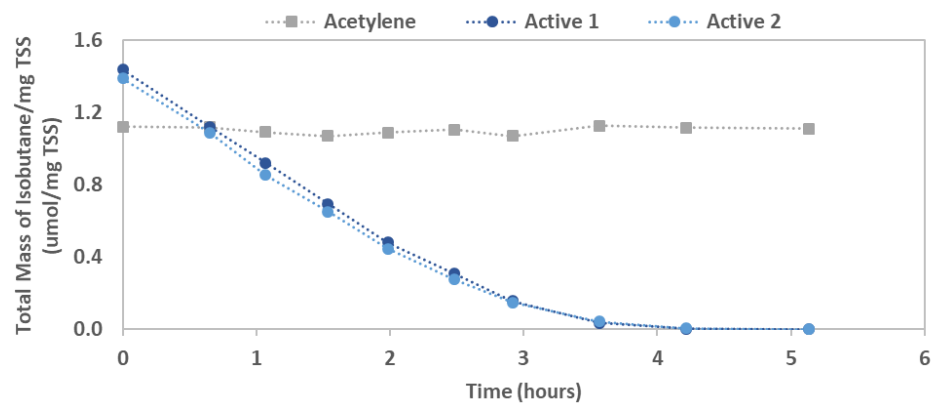


Figure A.18. Total mass of isobutane per mg TSS over time for propane-grown 21198.

C.4 Propane-grown 21198 Pure Culture Rate Test Results

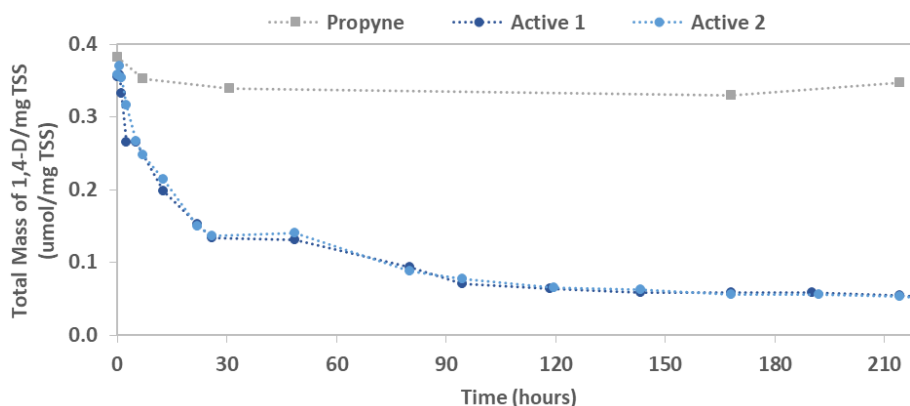


Figure A.19. Total mass of 1,4-dioxane per mg TSS over time for isobutene-grown ELW1.

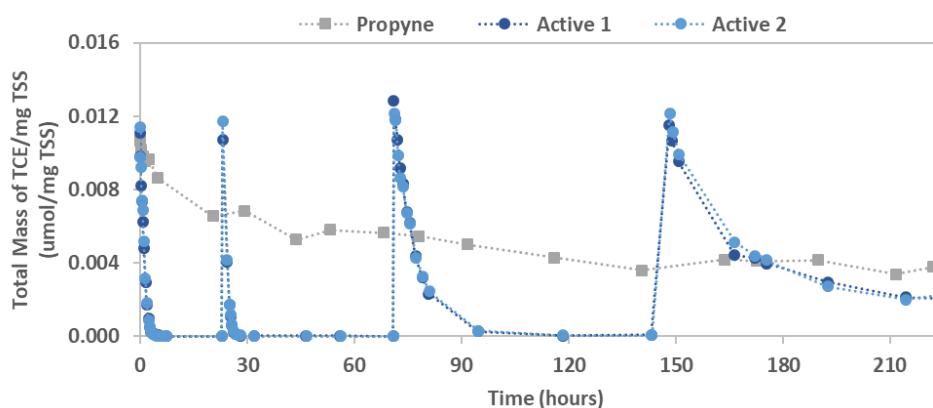


Figure A.20. Total mass of TCE per mg TSS over time for isobutene-grown ELW1.

D. Isobutene in the absence of CAHs

After 25 days of isobutene exposure in the presence of CAHs, native microcosms initially established in the presence of CAHs and isobutene (set 6 bottles 3 and 4) were sparged with nitrogen to remove 1,1-DCE and TCE from solution. Isobutene uptake was not observed in the relative absence of CAHs after 50 days of isobutene incubation that followed initial concurrent CAH/isobutene exposure (Figure A.21). A small residual of CAHs remained in these bottles at liquid concentrations of approximately 10 $\mu\text{g/L}$ (1,1-DCE) and 40 $\mu\text{g/L}$ (TCE) due to desorption from sediments. Isobutene uptake was also not observed after 60 days of isobutene exposure in the absence of CAHs (Figure A.22). The absence of microbial activity can likely be attributed to a low prevalence of isobutene-utilizing bacteria in the natural system and/or a very slow growth rate of isobutene-utilizers.

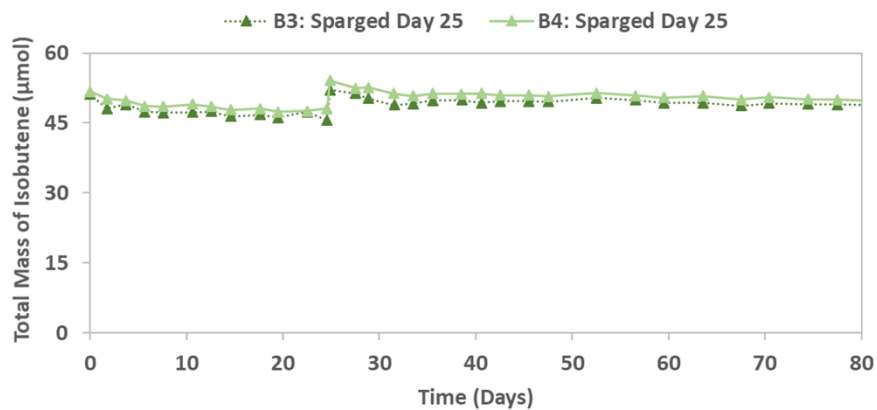


Figure A.21. Total mass of isobutene over time in native microcosms initially established in the presence of CAHs (set 6, bottles 3 and 4). CAHs were sparged from solution on day 25, and isobutene was re-added to the headspace.

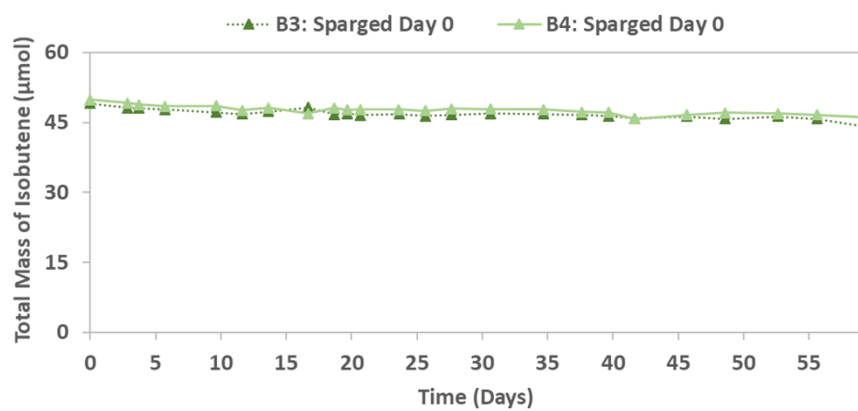


Figure A.22. Total mass of isobutene over time in native microcosms established in the absence of CAHs (set 7, bottles 3 and 4). CAHs were sparged from solution on day 0 when isobutene was initially added to the headspace.